Quantifying the Impacts of Flash Flooding on Dominica’s Material Stocks in Buildings:
A GIS-based methodological framework for Small Island States

by

Tianyu Ren

A thesis
presented to the University of Waterloo
in the fulfillment of the
thesis requirement for the degree of
Master of Science
in
Geography

Waterloo, Ontario, Canada, 2023

Author’s Declaration

I hereby declare I am the sole author of this thesis. This is a true copy of the thesis, including any required final revisions, as accepted by my examiners.

I understand that my thesis may be made electronically available to the public.

Abstract

Economic growth is usually accompanied by extensive extraction of natural resources, especially in developing countries. From a "material-stock-flow-service" perspective, the substantial part (e.g., construction materials) of the extracted natural resources as inflows to a society get accumulated in the built environment as "material stocks" (MS). Depending on the end-use types of their containers, MS provide essential services to a society such as housing, education and transportation. When an environmental hazard strikes, MS lose their functionality due to the destruction of the physical structure of their carriers, resulting in extra construction waste that then must be cleared for recovery. To make a society more resilient to environmental hazards, which is especially important in small island states with limited natural and human resources, the knowledge of exposure of MS to hazard risk is critical.

This research focuses on the quantity and spatial distribution of MS in buildings in the context of intense rainfall-triggered flash flooding in Dominica, a small island state in the Caribbean region. A Geographical Information System (GIS)-based stock-driven methodology is used to quantify four typical types of construction materials: concrete, aggregates, timber, and steel. To quantify exposed MS in buildings to flash flooding, an event-based flood model is used to generate flood inundation extents at the national scale. To investigate the degrees to which the exposed households are susceptible to the impacts of environmental hazards, this research also designs a resident survey to collect social factors contributing to household vulnerability to hazards. For 2020, the total MS in the building sector is estimated at 6,574 kt, equivalent to 91 t per capita, given Dominica's population of the year. In terms of the distributions of MS in different material categories, concrete accounts for 86% of the total MS in buildings, followed by aggregate at 7%, timber at 4% and steel at 3%. Examining the exposure of MS in buildings to flash flooding, it is found that flood events of larger magnitudes would result in more MS contained in the exposed buildings. For flash flood events with 5-year, 10-year, and 20-year return periods, the numbers of exposed buildings are 2,781, 3,030, and 3,274, respectively, which contain 17%, 18%, and 19% of the total MS in buildings in Dominica. This research demonstrates how to link the results of material stock accounting to flash flood modelling, approaching the concept of socio-economic metabolism from an environmental hazard risk perspective. Knowledge of the quantity and spatial distribution of the exposed MS in buildings can assist local governments in making cost-effective mitigation plans before a hazard event. Although the designed survey was not implemented due to

travel restrictions, it is a valuable instrument to collect the information about household vulnerability to environmental hazards, which can help hazard response agencies with more-efficient rescue operations during a hazardous event.

Keywords: Small Island States, material stocks, Geographical Information Systems (GIS), flood modelling, material stock accounting, Dominica

Acknowledgements

It is without any doubt that I would not complete this milestone if it was not for the valuable people who have been providing me with their support and care throughout this journey. Appreciation and deepest gratitude are extended to these people without whom this thesis would not be possible.

First and foremost, I would like to express my sincerest gratitude to my thesis supervisor, Dr. Su-Yin Tan, for your continuous support, smiles, and dedication to get me through the frustrating moments during the COVID-19 pandemic. You are more than an instructor with expertise and the ability to see the academic potential in me, more importantly, you are a mentor who provided me with invaluable insights and guidance that helped me move on smoothly to the next stage of my life.

Also, I would like to thank Dr. Erin O'Connell and Dr. Quinn Lewis, without whom my committee would not have been complete. The distance and time difference between us never interfered with your ability to provide me with the invaluable feedback and insights on my thesis, which gets me to think beyond my research scope, for this I am eternally grateful.

To my friends of the Applied Geomatics Research Laboratory, although we didn’t really have much time spent together in the lab, I really miss those online coffee chats and the meal we had after Kristen’s thesis defence. I would like to thank Samantha for her support on the development of the survey instrument in this study.

To my father, mother, and my grandparents, I would not have made it this far in my life if it was not for your everlasting love and support, both financial and emotional. The happy childhood you gave me helped me remember where I was from, whenever I felt lost or nearly lost faith in myself.

Last but not least, I would like to thank my roommates and my friends in Waterloo, who accompanied me through part of this journey and were always by my side. I feel so lucky that I met Jinghan, as she gave me the courage and strength to face whatever challenges that we might encounter in the future.

Table of Contents

List of Figures

List of Tables

1 Thesis Introduction

1.1 Decoupling and Socio-economic Metabolism

Economic growth, often accompanied by population growth, the desire for higher levels of consumption, and rapid industrialization especially in developing countries and regions, has resulted in more extensive extraction and use of natural resources both locally and globally (Krausmann et al., 2016). A ten-fold increase has been observed in global raw material extraction from 1900 to 2010, with the built environment being the most crucial sector for material extraction growing from 18% to 55% (Krausmann et al., 2017b). After being extracted, these raw materials get accumulated in buildings, infrastructures, and durable goods in a society as in-use material stocks (MS) that provide essential services like housing, transportation, education, and communication (Krausmann et al., 2017a; Pauliuk & Müller, 2014). Currently, the increase in global material extraction is not equally distributed across the world, with developing countries in Asia contributing to most of the growth over western industrialized countries since 2000 (Schaffartzik et al., 2014). For example, the increase in material extraction from 1980 to 2006 is 352.76% in Indonesia but is only 5.42% in Japan (York et al., 2011). In terms of different end-use carriers where materials get accumulated, the growth in extracted materials is also not equally distributed within a society. For residential buildings only, the global growth of accumulated materials from 2020 to 2050 is predicted to be 50% (Deetman et al., 2020).

However, the world's resources are finite, while the expansion of economic activities is generally required by the improvement of human well-being, which inevitably leads to more materials extracted from nature (IRP, 2011). As the scarcity of natural resources is expected to evolve in the future, decoupling has become one of the main themes in the field of industrial ecology. Decoupling aims to reduce the amount of resource required for economic growth and to delink economic growth from environmental deterioration (Fischer-Kowalski et al., 2011; IRP, 2011). Accordingly, as is shown in Figure 1.1, there are two aspects of the term "decoupling": resource decoupling and impact decoupling. While the former aims to ease over-exploitation of natural resources by enlarging the difference between resource usage and economic activity (usually measured as gross domestic production or GDP), the latter is considered equally significant because profound environmental impacts (e.g., pollution, harm of biodiversity, and climate change and cascading hazards like flooding and sea-level rise,) caused by the expansion of consumption are leading to economic loss and casualty (IRP, 2011). To achieve a decent level of both resource decoupling and impact decoupling, one solution is to limit virgin material extraction and utilize recycled materials from demolition and hazard waste to ideally form a closed-loop resource cycle (Symmes et al., 2020).

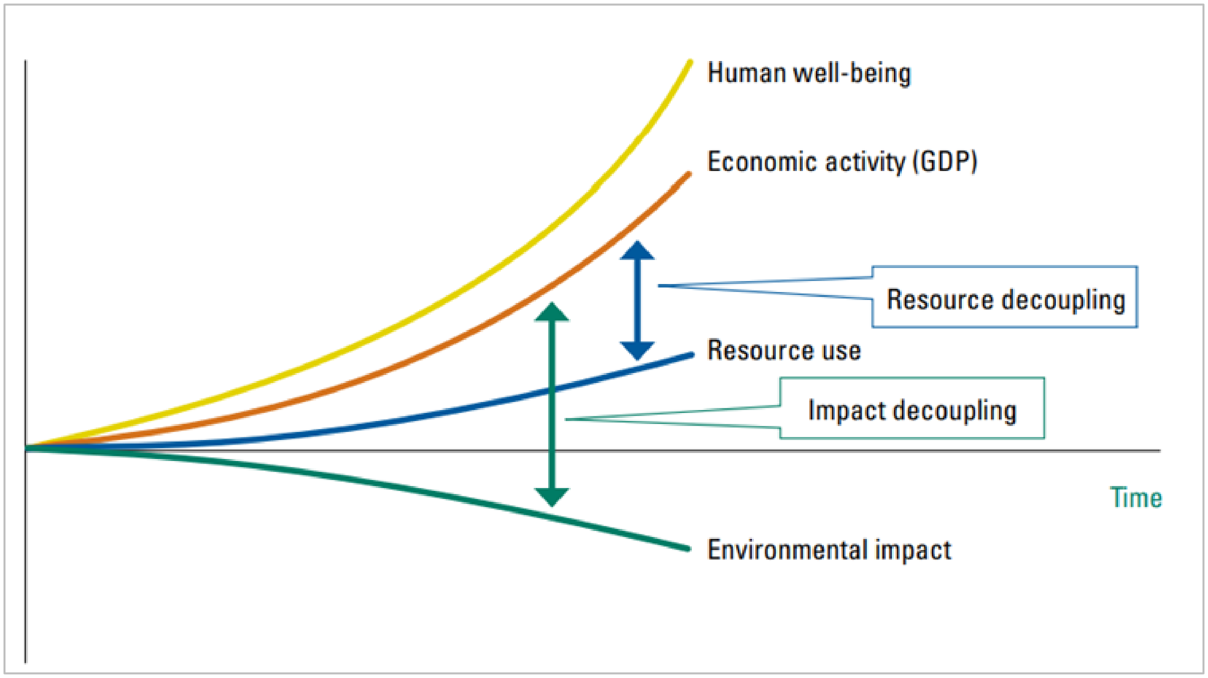

Figure 1.1: *The two aspects of the term "decoupling": resource decoupling and impact decoupling, adopted from IRP (2011).*

To monitor the level of resource decoupling achieved in a society, socio-economic metabolism is defined as the flows of materials and energy between a social system and nature, which enables holistic investigation of the underlying biophysical factors influencing these flows (Fischer-Kowalski & Haberl, 1998; Pauluik & Hertwich, 2015). The flow perspective of social metabolism is vital because although material stocks are fundamental for the direct provision of service, material and energy flows are also required to establish, energize, maintain, and update in-use MS (Fishman et al., 2014). In other words, while the state of a society can be indicated by in-use stocks accumulated within its boundary, the change of that society can only be measured by flows (Meadows, 1998). How socio-economic metabolism fits in sustainability science can be explained in Figure 1.2, which demonstrates the 'means and end' framework developed by Meadows (1998) using the building sector as an example. At the bottom of the 'means and end' triangle is the ultimate means or natural capital, which in the case of the building sector includes earth materials like sand, wood, and stone. With the help of science and technology, raw materials turn into processed materials for the constructions of buildings (intermediate means or built capital), which provides the services required in a society (intermediate ends or human/social capital). Most socioeconomic metabolism studies focus on the transformation from the ultimate means to the intermediate ends in the triangle and investigate the quantity of raw materials accumulated in different types of built capital such as residential buildings (Condeixa et al., 2017; Ortlepp et al., 2018; Wiedenhofer et al., 2015), non-domestic buildings (Deetman et al., 2020, Ortlepp et al., 2016), transport sector (Gassner et al., 2021) and infrastructures (Pailiuk et al., 2014).

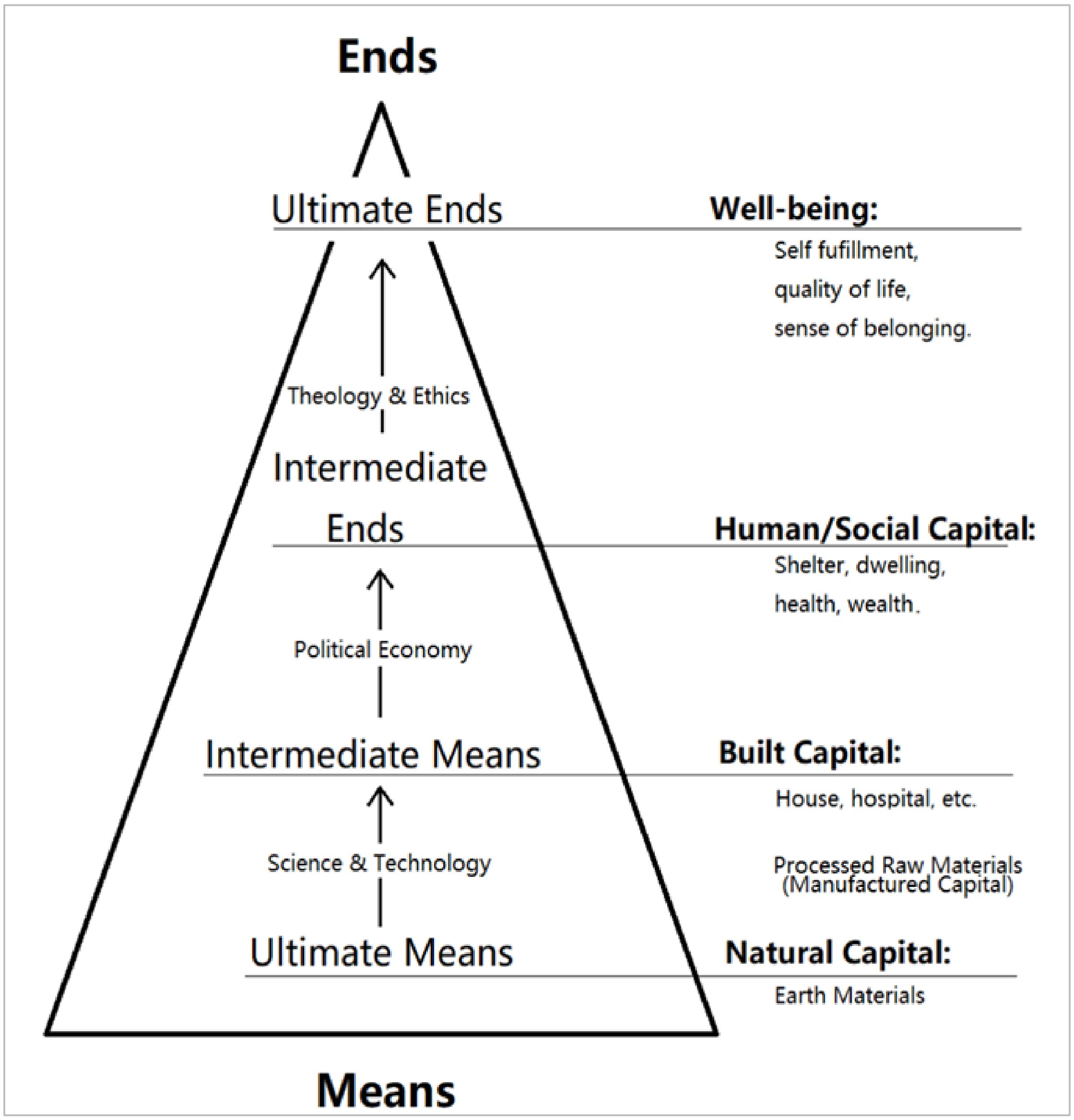

Figure 1.2: *The integrating framework of the "Daly Pyramid" that relates natural wealth and ultimate human well-being, modified from Meadows (1998).*

One of the goals of socio-economic metabolism studies is to assess the material efficiency in a society, which is conventionally defined as economic growth (usually measured as GDP) contributed by per unit of material use (Fishman et al., 2014). Assessment of material efficiency can be operationalized from a new perspective by using the material stock-flow-service (SFS) nexus approach developed by Haberl et al. (2017) in Figure 1.3. The SFS-nexus links socio-economic metabolism with the provision of services and the well-being of a society (Kalt et al., 2021). Material flow alone is not sufficient for service provision; instead, they alter the patterns of MS (e.g., types of function and spatial distribution) that respond to the need of a society (Pauliuk & Müller, 2014). This service-based approach for material efficiency measurement offers more complementary insights beyond mainstream economic measurements (Haberl et al., 2017). Material efficiency can be further quantified by economic data-based indicators associating both stocks and flows to the services they provide. One example of these indicators is the Material Productivity developed by Tanikawa et al (2021) for Japan. Material Productivity is an integrated framework developed by linking six individual indicators, each of which has a corresponding role and position in the "Daly Pyramid" in Figure 1.2. Despite different methodologies used in socio-economic metabolism studies, understanding the patterns of in-use MS, flow dynamics, and associated services is fundamental.

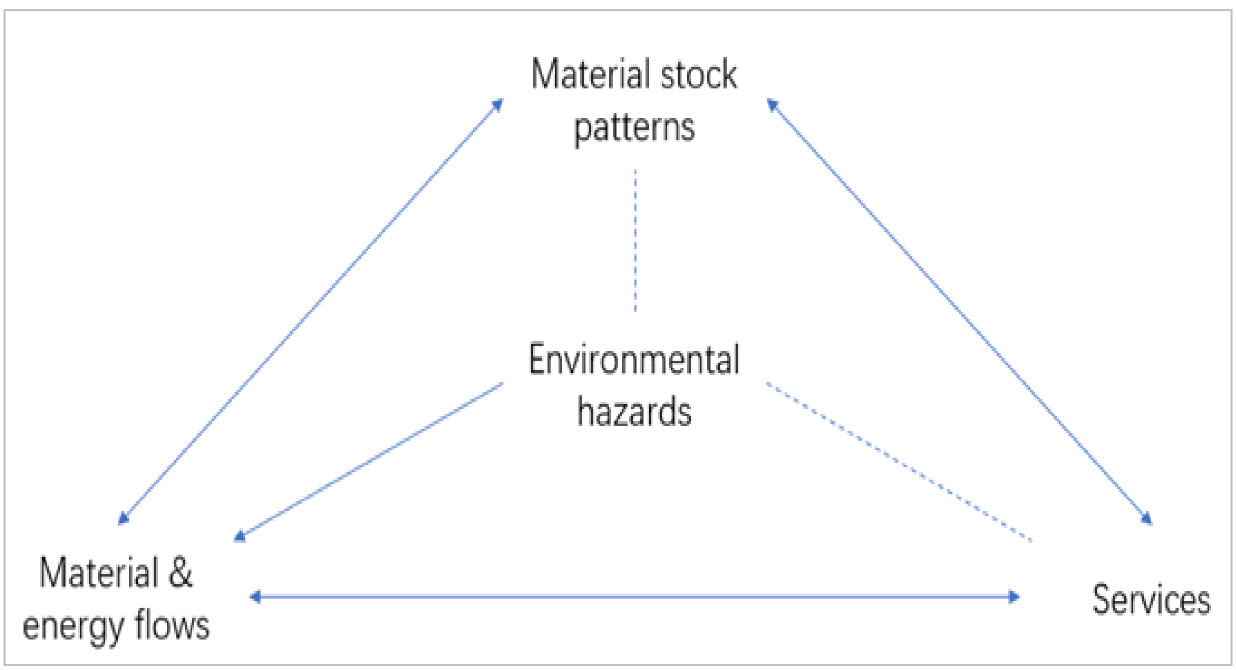

Figure 1.3: *The material stock-flow-service nexus approach incorporating the impact of environmental hazards, modified from Haberl et al. (2017).*

1.2 The Role of Environmental Hazards

Over the last decade, many regions worldwide have been affected by a large number of environmental hazard events. Amongst all kinds of environmental hazards, climate-related hazards (e.g., tropical cyclones and storms) and subsequently triggered hydrological hazards (e.g., flooding and landslides) are more destructive, especially in coastal areas. According to the Emergency Events Database (EM-DAT), 2,882 hydrological and climate-related hazard events occurred from 2010 to 2019 worldwide, which caused 0.17 million casualties and a total economic loss of US$0.68 billion (EM-DAT, 2023).

While social metabolism studies reveal long-term patterns of economic growth from a material and energy perspective, the impacts of environmental hazards are more immediate. Environmental hazard is an example of ecosystem “dis-services” which force a society to alter its current patterns of socio-economic metabolism to protect itself (Singh, Fischer-Kowalski & Chertow, 2020). As is shown in Figure 1.3, environmental hazards cause sudden changes to the input and output of both material and energy throughput. For example, despite various average building lifespans in different areas (e.g., 34 years for residential buildings in Japan and 100 years in Brazil) caused by different proportions of short-lived buildings, environmental hazards can completely change the demolition rate of facilities and infrastructures in a given year (Condeixa et al., 2017; Daigo et al., 2017; Miatto, Schandl, & Tanikawa, 2017). When environmental hazards strike, in-use MS are first affected due to the destruction of the physical structure of their carriers, resulting in lost MS, defined as MS that lose their social function (Tanikawa, Managi, & Lwin, 2014). Following this change in in-use MS pattern, the corresponding absence of services previously provided by lost MS will function as a driver for the increase in subsequent material flows (Müller, 2006). After a hazard event, either new input of materials or the recycling of lost MS is required to restore the essential services. The latter is recommended to achieve a higher resource efficiency and create job opportunities, which is particularly beneficial in developing countries (Brown, Milke & Seville, 2011). However, Deetman et al. (2020) argue that even under ordinary urban mining circumstances without the influence of environmental hazards, the growing demand for construction materials is not sufficiently covered by recycled materials from regular demolition. Nevertheless, demolition waste management and recycling are the initial steps for recovering from a hazard (Moriguchi & Hashimoto, 2016), and understanding the location and composition of potential disaster waste is imperative to maximizing the quantity of recycled materials following a hazard event (Tabata et al., 2016).

1.3 Vulnerability of Small Island States to Environmental Hazards

1.3.1 Common Factors Contributing to Vulnerability to Environmental Hazards

The impact of environmental hazards has a place-specific nature. The same environmental hazard event can cause various degrees of damage to different places due to their unique combinations of social and physical characteristics (Cutter et al., 2008). As a result, the impact of environmental hazard is disproportionately distributed across the world with small island developing states (SIDS) as the most vulnerable group (UNCTAD, 1997). SIDS is conventionally defined as a group of islands and coastal countries or territories facilitated by the United Nations (UN) to promote partnerships for addressing common needs (Shultz et al., 2016). Recently, there are conflicting perspectives on the use of the term SIDS regarding the ambiguous meaning of "developing", so this research is adopting the terminology of "small island states" instead. Every island state has its own features, but compared to continental nations with greater landmass, some common factors that put small island states at risk include: 1) physical remoteness that results in delayed and high-cost external aids when hazards strike (Pelling & Uitto, 2001; Shultz et al., 2016); 2) scarcity of natural, human, and financial resources that results in a heavy dependence on imports of food and fossil fuels (Chertow et al., 2012; Krausman et al., 2014); 3) limited scope of economic diversification with tourism as the key sector, while a significant proportion of tourism activities occur in hazardous coastal areas (UNDP, 2016; Becken et al., 2014); 4) climate change-related risks such as intensified rainfall patterns, sea-level rise, and more frequent extreme weather events (Hagedoorn et al., 2019), which are aggravated by rapid global economic growth as material production currently contributes to almost a quarter of greenhouse gas emissions (Pauliuk et al., 2021). Apart from these factors originated from the small island states themselves, from a humanitarian aid perspective, Singh, Ficher-Kowalski & Haas (2018) argued that a small island nation's limited resource base may not be sufficient to generate enough income to sustain a more industrialized consumption pattern enforced by external help. Considering Sustainable Development Goals 11.5 and 13.1 indicated in the 2030 Agenda for Sustainable Development, making cities and human settlements inclusive, safe, resilient, and sustainable to combat climate-related natural hazards is one of the main concerns in the short term (UN, 2022). When the differences in vulnerability are examined within small island states, it is also found that island states in different regions of the world are susceptible to environmental hazards to different extents due to their different economical and demographical characteristics (Pelling & Uitto, 2001). Nevertheless, because of the vulnerable nature of small island states, many researchers in the field of hazard risk management are paying more attention to the vulnerability assessments of these island nations to environmental hazards.

When resource scarcity is examined in more detail, it is found that small island states are more limited in domestic resource bases with few locally occurring resource types, and most construction materials are unsustainably extracted from beaches and coastal reefs (Babinard et al., 2014; Krausmann et al., 2014). Such resource scarcity is exacerbated by economic development, which is often accompanied by rapid housing and infrastructure improvements to accommodate the increased demand in tourism (Babinard et al., 2014; Becken et al., 2014). Therefore, small island states depend heavily on imports of construction materials. In addition, small island states are at the frontline of global climate change facing sea-level rise and more frequent and stronger storms that threaten the "long-term existence of whole island nations" (Petzold & Magnan, 2019). For example, after Hurricane Maria in 2017, the monetary need to recover the housing and other infrastructure sectors in Dominica was estimated at 235% of its GDP in 2018 (Government of the Commonwealth of Dominica, 2017). Thus, there is an urgent need for a better understand of material stocks and associated services in small island states, which helps them achieve more-sustainable resource use patterns in the reality of limited funding (Haberl et al., 2017).

1.3.2 Flooding in the Context of Small Island States

Small island states are frequently impacted by climate-related hazards, resulting in significant property loss and casualties. Conventional climate-related hazards include sea-level rise, subsequent coastal erosion and saltwater intrusion that threaten freshwater resources (Holding et al., 2016). Apart from these types of hazards, the changed pattern of extreme weather events in terms of their frequency and intensity is another research focus in recent years, especially in the Caribbean region (Robinson, 2020). The increase in the number of more intense tropical cyclones and hurricanes (tropical storms with a sustained wind speed over 63 km/h) and associated high precipitation has been observed as the global hydrological cycle intensifies with anthropogenic global warming (IPCC, 2019; Huntington, 2006; Nunez, 2023). During hurricanes, devastating storm surges can occur, leading to an abnormal rise of sea water that threatens population in costal areas, and evacuations in such extreme events are primarily due to storm surge (World Meteorological Organization, 2023). The cascading impacts of intense rainfall like flooding are equally devastating. In general, there are two types of flooding: flash flooding and river flooding. Flash flooding is defined as intense flow of water triggered by short and extreme precipitation activating substantial surface runoff that exceeds the capacity of river channels, whereas river flooding is associated with multiple rainfall events spanning days or months (Borga et al., 2014; Charlton, 2007; Doswell III et al., 1996). In island states in the Caribbean region, the rugged and steep terrain resulted from their volcanic origin also contributes to relatively intense precipitation during extreme weather events, which cannot be captured by rainfall forecast models at the global scale (Nugent & Rios-Berrios, 2018). Therefore, investigating the impact of environmental hazards for individual islands is necessary for site-specific results, which can provide more-accurate flood characteristic information to hazard response agencies for more-effective mitigation planning.

One of the tools for flood risk estimation is physics-based flood inundation modelling. In physics-based flood inundation modelling, the evolution of a flood event caused by extreme rainfall is simulated based on a continuum representation of the study area as detailed as possible. Such models also require a comprehensive understanding of the physics of hydrological processes to calculate surface flows (Wheater, 2002). Generally required input datasets for the physical properties of the study area include topography, river channel dimension, land use and soil physical characteristics (Bout et al., 2018). Expected outputs of flood inundation models are usually flood extent, maximum flood height, maximum flow velocity, flood start time and flood duration (Yan et al., 2015). The flood properties mentioned above are essential for identifying the locations exposed to various levels of flood risk (e.g., to what extent and how quickly these exposed locations are impacted). Such information can provide an objective basis for policymakers to initiate proactive emergency preparedness plans before flooding occurs or optimize priority settings in evacuation actions during a flood event for a better emergency response (Jetten, 2016).

1.4 Research Objectives

Most studies about material stocks and flows focus on static material stock accounting which captures a ‘snapshot’ of the quantity of certain types of materials accumulated in a social system or using historical flow data to forecast the future stocks. Although an environmental hazard causes sudden unexpected outflows of materials which alters the pattern of in-use MS, few studies have prospectively approached MS exposure to the impact of such events. To bridge this research gap, this thesis presents a methodological framework for integrating the results of material stock accounting with hazard exposure. Using the impact of flash flooding on the building sector in Dominica (a small island state in the Caribbean region) as a case study, this thesis also attempts to incorporate household-level vulnerability factors to assess the susceptibility of households exposed to different flooding scenarios.

This study is the first attempt to perform a material stock analysis in Dominica at the national level and to examine the impacts of flash flooding through flood modelling. This research builds on two previous studies, one was conducted in Grenada by Symmes et al. (2020) and the other was conducted in Dominica by Jetten (2016). The former provides a methodological framework for material stock accounting in small island states in the Caribbean region, and the latter provides the primary workflow of flood inundation modelling. This study also paves the way to examining household-level vulnerability to environmental hazards once hazard exposure has been revealed. The main research questions that guide this study are:

1. What, and where are the concentrations of material stocks in buildings in Dominica?
2. What are the quantity and spatial distribution of material stocks in buildings in Dominica exposed to potential intense rainfall triggered flash flooding?
3. What are the commonly used variables for social factors of vulnerability to environmental hazards that can be applied at the household level in Dominica?

To answer these questions, the research objectives of this study are as follows:

1. Conduct a material stock accounting analysis for buildings in Dominica for 2020 and map the quantity of material stocks.
2. Develop a flash flood model with updated river channel dimension and building footprint datasets, identifying building stocks exposed to flash flooding in Dominica.
3. Identify social factors to define vulnerability to environmental hazards in Dominica based on the literature and design a corresponding household survey for collecting primary data.

1.5 Study Area

The Commonwealth of Dominica (Dominica in short) is one of the member states of the Organization of Eastern Caribbean States. It is a small island state located in the Eastern Caribbean (shown in Figure 1.4). Dominica is a single-island nation, whose population is 71,991 in 2020 with its per capita GDP of US$11,000 (The World Bank, 2020). The landmass of Dominica spans about 750 km^2 (CREAD, 2020), so its population density is about 96 people per square km. There are ten parishes in Dominica, and the capital city Roseau is in the parish of St. George on the west coast of the island. About 30% of the population in Dominica live in St. George parish, and 25% of the buildings on the island are also in St. George (Central Statistics Office of Dominica, 2011). Due to Dominica's mountainous inland topography, buildings are also not evenly distributed across the island, with 13% of the buildings within 100 m from the coastline.

Agriculture was the most significant contributor to Dominica's economic growth in the 1970s. However, agriculture and other primary sector activities have gone through a drastic shrink over the past few decades, with their contribution declining from 35% in 1977 to 12% in 2021 (Eastern Caribbean Central Bank, 2021). Accordingly, such decline has been gradually compensated by the rise of the service sector. Like other small island states in the Caribbean region, Dominica greatly depends on the travel and tourism sector. In 2019, travel and tourism contributed to 36.9% of Dominica's GDP and 38.7% of its total employment, and the international visitors contributed 56.4% of the country's total exports (WTTC, 2020). However, hotels and population are mostly clustered along the coast (Government of the Commonwealth of Dominica, N.D.), resulting in most of the country's socio-economic activities occurring in low-lying coastal areas vulnerable to climate change-related impacts like sea-level rise (Parry, 2007).

In terms of environmental hazards, destructive tropical cyclones can be expected during late summer (Central Intelligence Agency, 2020). Table 1.1 lists the country-level statistics of the major environmental hazard events that have struck Dominica since 2000. On September 18, 2017, Dominica was hit by Hurricane Maria and was exposed to extraordinary winds and intense rainfall, which provoked landslides and flash flooding. Hurricane Maria caused US$1.3 billion of damage and loss, which accounts for 226% of Dominica's GDP in 2016 (The Government of the Commonwealth of Dominica, 2017). In this hazard event, the housing sector in Dominica was heavily impacted, with 15% of houses destroyed and 75% suffering different levels of damage (The Government of the Commonwealth of Dominica, 2017). As for the tourism sector, 39% of hotel rooms were heavily damaged and were not recoverable within a year, which caused US$91 million economic loss and the unemployment of hotel staff and other support personnel in the tourism sector (The Government of the Commonwealth of Dominica, 2017).

Table 1.1: *Basic statistics of the impact of the major environmental hazards that struck Dominica since 2000, source: EM-DAT (2022).*

Hazard Type	**Event Name**	**Month/Year**	**Associated Hazard**	**Number of Deaths**	**Number of Injured**	**Affected Population**	**Total Damages (Thousand US$)**
Earthquake	-	Nov. 2004	-	-	-	100	-
Tropical Cyclone	Hurricane “Dean”	Aug. 2007	Flooding	2	30	7,500	20,000
Tropical Cyclone	Tropical Storm Orphelia	Sep. 2011	Flooding	-	-	144	-
Tropical Cyclone	Hurricane “Erika”	Aug. 2015	Flooding, Landslide	30	20	28,000	482,810
Tropical Cyclone	Hurricane “Maria”	Sep. 2017	Flooding, Landslide	64	100	71,293	1,456,000

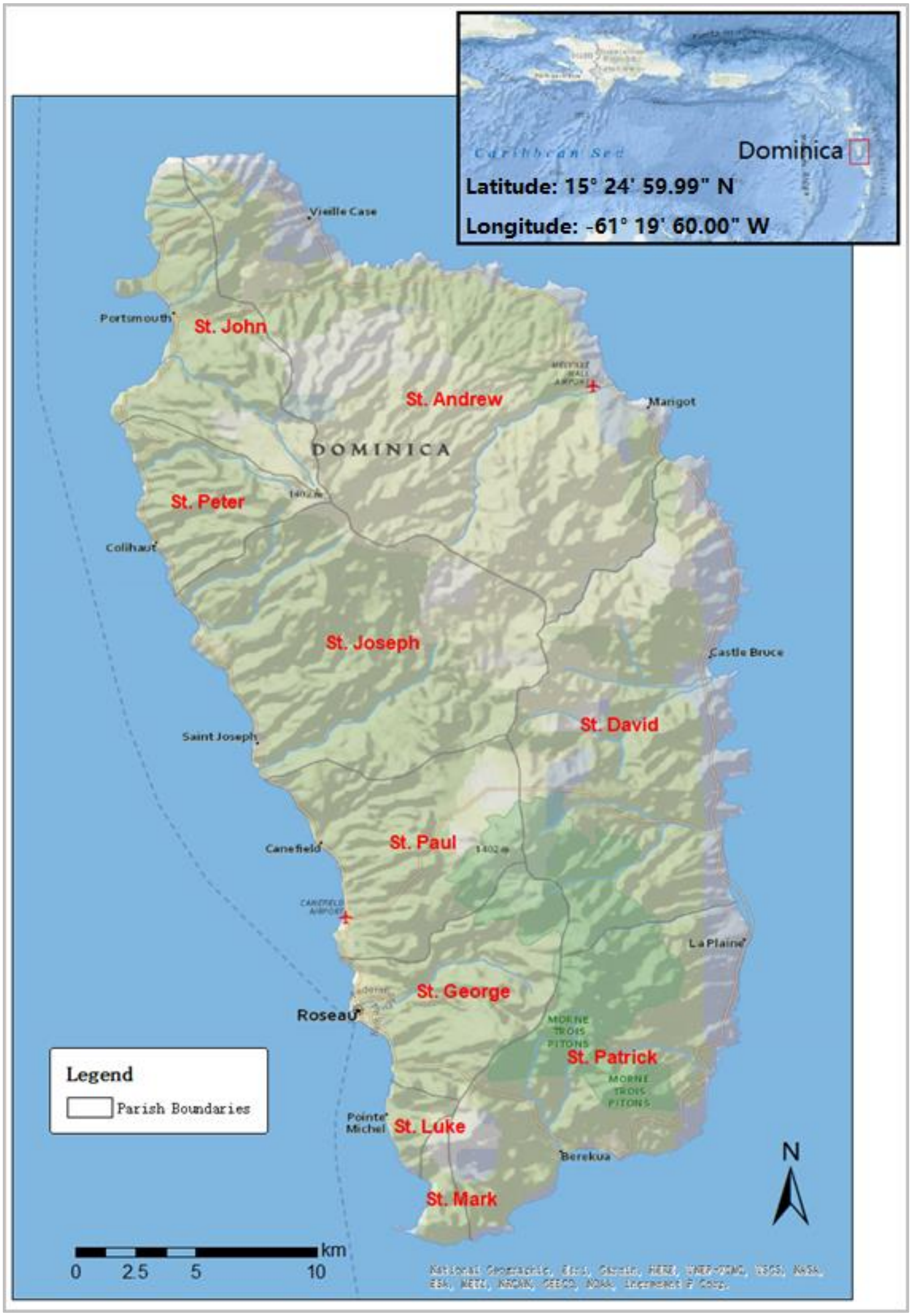

Figure 1.4: *Map of the island of Dominica showing its location in the Caribbean Sea and its parish boundaries.*

1.6 Thesis Structure

The built environment is currently the most crucial sector for raw material extraction, so better understanding the composition of its MS is important for sustainable development planning. This work focuses on the quantity and the spatial distribution of MS in buildings in Dominica, while investigating the potential impact of intensive rainfall triggered flash flooding on these stocks. This thesis follows a manuscript style and has five sections. Section 1 is an introduction to fundamental concepts of socio-economic metabolism in the context of small island states, and the role of environmental hazards in relevant metabolic processes. Section 2 is a literature review presenting a theoretical background of the relationship between material stocks and environmental hazards, frequently used flood modelling methodologies, followed by common physical and social factors of vulnerability to environmental hazards. Section 3 starts with a methodological framework which shows an overview of the workflow of this research, followed by more detailed explanations of the approaches used for the material stock accounting of Dominica's buildings, the flash flood modelling, as well as the design and application of a resident survey instrument for the collecting primary data of household vulnerability to environmental hazards. Following the methodology section, Section 4 presents the results of MSA and flood modelling in maps and tables. To expand on the results, Section 5 interprets the findings, compares the results with those of previous studies, and summarizes key conclusions of the thesis.

2 Literature Review

The role of environmental hazards in socioeconomic metabolism is illustrated in Figure 1.3. In the short term of post-recovery efforts, environmental hazards cause an unexpected increase in MS outflow, which must be compensated by either inflow or recycled waste to restore associated services (Tanikawa, Managi, & Lwin, 2014). Small island states have more recovery constraints due to limited natural and human resources than developed countries with giant landmasses. As is shown in Figure 2.1, there was a sudden turning point where Dominica's import of buildings cement started increasing dramatically, partly due to the impact of Hurricane Maria in 2017 (Central Statistics Office of Dominica, 2020). The increase continued until 2019, which agrees with the estimation by the government of Dominica that the recovery may take one or two years (The Government of the Commonwealth of Dominica, 2017). A pre-disaster analysis is an effective way to mitigate such impacts and determining where the materials are located is the first step. This literature review section contains three parts and begins with material stock accounting studies and approaches. This literature review also covers flood modelling studies and techniques, indicator-based vulnerability assessment studies and practices, and how the methods work in the field of hazard management.

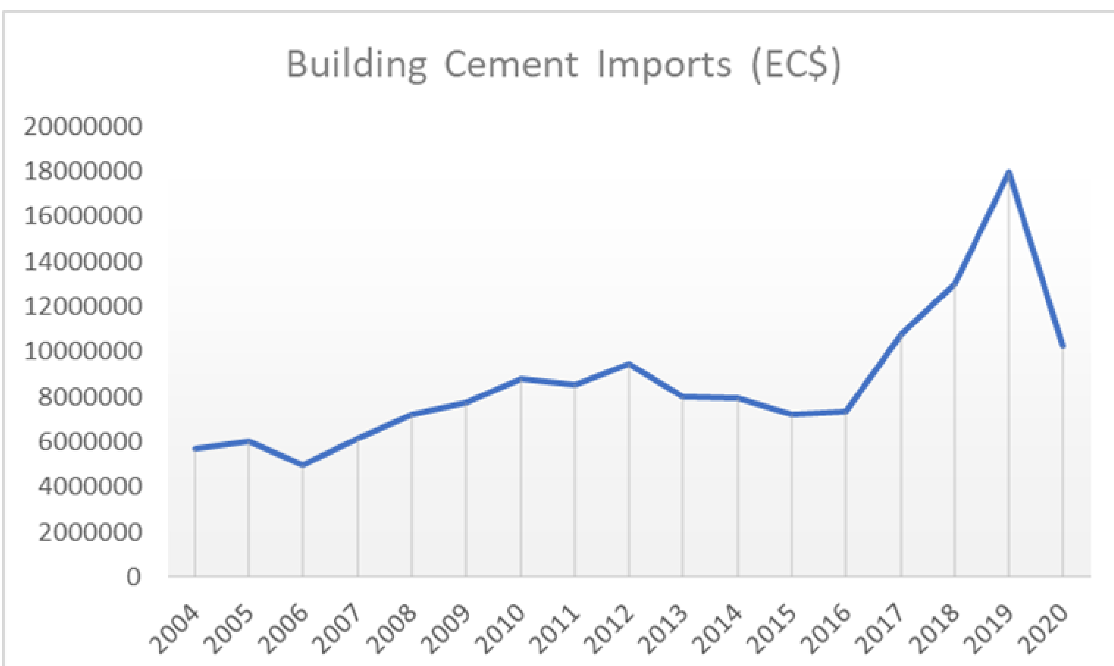

Figure 2.1: *The trend of Dominica's building cement imports (in EC$) from 2004 to 2020 (Central Statistics Office of Dominica, 2020).*

2.1 Existing Material Stock Analysis Approaches in Previous Research

Material stock analysis has a relatively long history which can be traced back to the 1980s. In Europe, knowledge about material stocks was once gathered from traditional housing surveys (Wilhelmsen, 1982; O'Dell, 1988). More recent studies on material stock analysis conducted since the late 1990s were different in spatial and temporal scales, as well as their main purposes (e.g., from merely city planning to resource efficiency assessment) (Augiseau & Barles, 2017). Despite these evolvements of scale and purpose, classical material stocks analysis approaches used in previous studies or projects can be categorized into two major types: bottom-up stock analysis and top-down stock analysis (Tanikawa et al., 2015; Augiseau & Barles, 2017).

The bottom-up approach, also known as a static approach or stock-driven approach, divides MS into categories, based on which different material ratios or intensities can be applied (Augiseau & Barles, 2017). This approach is good at revealing the "inner structure" of MS as it investigates different elements both qualitatively and quantitatively (Lichtensteiger & Baccini, 2008). Also, bottom-up approaches make it possible to investigate the spatial distribution of certain types of MS (Symmes et al., 2020), since the basic analytical unit of these approaches is usually individual buildings that can be divided into groups sharing a common material intensity (MI). Due to its static nature, the results of a bottom-up approach are fixed points on the timeline as "snapshots" of MS (Tanikawa et al., 2015). Bottom-up approaches are very popular among studies of different space and time scales when data sources for MI of the study areas are available. In a local scale study of the urban area of Vienna, Obernosterer et al. (1998) used a bottom-up approach to estimate the MS of all constructions in 1997 and argued that material stock analysis is a good complement to conventional environmental and resource management tools as it provides a holistic base for the prediction of future stocks. For regional scale studies, Tanikawa et al. (2014) used a bottom-up approach to estimate the amount of lost MS in 47 prefectures in Japan due to buildings and roads destroyed by the 2011 Great East Japan Earthquake and Tsunami. Compared with ordinary bottom-up approaches, the approach used by Tanikawa et al. (2014) took the underground foundation and roads and the upper structures of buildings into consideration (by involving the effects of atriums and setbacks when calculating gross floor area). For national scale studies, Wiedenhofer et al. (2015) used a bottom-up approach to account for the amount of nonmetallic mineral stock in residential buildings and transportation networks in 25 European Union members. In this study, residential buildings were categorized into 72 types, roads into four types, and railways into two types. Each type has its responding MI for each type of material, and the approach was made dynamic by utilizing data from different time steps (Wiedenhofer et al., 2015).

Another popular type of MS accounting approach is the top-down approach. The top-down approach uses long-period data of annual net additions to MS, which is derived from inflows and outflows by calculating the difference between these values (Augiseau & Barles, 2017). This type of accounting approach is similar to the dynamic MS flow analysis driven by stock demand models, but the former utilizes direct material flow values, either from statistical official construction and demolition data or from estimations of average lifespans and current conditions (Tanikawa et al., 2015; Augiseau & Barles, 2017). Compared with bottom-up approaches, top-down MS accounting approaches are more popular in studies of national scale, especially in developed countries, since statistical data is more available and detailed. Fishman et al. (2014) utilized long-term data sources for annual inflow of 60 material groups. With the estimated lifespan of building and infrastructure, these data sources made it feasible to calculate the MS from the 1870s to 2005 in both Japan and the United States (Fishman et al., 2014). Müller (2006) used a similar MS accounting framework, but the approach took population and lifestyle into the calculation to investigate how these factors affect MS in the residential building sector. The framework was calibrated by historical data, and then used to predict MS in the near future before 2100 (Müller, 2006).

There are also other MS accounting approaches. Remote sensing-based approaches have been used in more recent studies which reveal geographical distributions of MS by correlated human activity intensities (Tanikawa et al., 2015). For example, Liang et al. (2017) utilized night-time satellite imagery to estimate distribution of steel stocks based on light intensity at the prefectural level of Japan. At a continental scale, Peled & Fishman (2021) estimated total material stocks of Europe using radiance values from nighttime lights data derived from satellite imagery. This novel type of approach can ease the scarcity of material stock data, and provides spatial comparability and the possibility of more regular updates, because satellite data can be acquired regularly for relatively large spatial extent (Peled & Fishman, 2021). Apart from its fundamental role in novel material stock analysis approaches, remote sensing technique is also beneficial for traditional bottom-up MS accounting approaches. For example, LiDAR datasets can help to improve the accuracy of MS accounting by allowing more accurate gross floor area calculation when building heights are not available (Symmes et al., 2020). In addition to different spatial and time scales, there is also research investigating MS in terms of their physical containers rather than low-level material categories like timber, steel, aggregate, etc. For example, Aroa et al. (2019) estimated MS of residential buildings in Singapore at the component level (e.g., doors and windows), because materials cannot always be isolated from their physical (natural) state and components are usually more cost-efficient secondary resources in material circularity.

2.2 Material Stocks and Environmental Hazard

From a spatial scale point of view, material stocks have been investigated at different levels, including urban (Pauliuk et al., 2014), national (Fishman et al., 2014), regional (Wiedenhofer et al., 2015), and the global scale (Deetman et al., 2020). Nevertheless, studies on MS often focus on a single sector or a particular type of material. For example, Venkatesh et al. (2009) used an integrated life cycle-MF analysis approach to predict the amount of input material to the wastewater pipeline sector in the city of Oslo in Norway. For the transportation sector, Wang et al. (2016) examined the high-speed rail network in China regarding the cumulative steel and cement consumption at the national level. Kalt et al. (2021) quantified the composition of primary bulk materials accumulated in the global electricity infrastructure sector. As a result, MS studies of various spatial scales provide different levels of details: insights of urban metabolism like scenario-based predictions on future flows can help urban planning specialists anticipate the need for rehabilitation and maintenance hotspots (Pauliuk et al., 2014), which is incorporated into modern smart city initiatives (Gassner et al., 2021); while MS studies at the national level in combination with standard economic indicators can help reveal the efficiency of resource use of a country (Matthews et al., 2000).

The linkage between MS and environmental hazards is underexplored. Still, there is an agreement that MS and associated concepts are significant in hazard risk management for three reasons: 1) MS provides direct socioeconomic services, and some services are crucial when environmental hazards strike (e.g., medical services and shelters) (Pauliuk & Müller, 2014); 2) material stocks accounting (MSA) provides the possibility of quantitatively evaluating lost materials due to hazard events and the quantities required for reconstruction (Tanikawa et al., 2014); and 3) results of material flow analysis indicate a society’s sustainability by revealing its capability of reproducing MS, especially from outputs after hazard events (Wiedenhofer et al., 2016). There is also a consensus that areas with a higher composition of critical services are more prone to destruction due to the vulnerability inherent in the material-intensive lifestyle (Tanikawa et al., 2014). Compared with developed countries, rural areas of developing countries are more vulnerable to seismic hazards and high winds during hurricanes because of the higher composition of traditional and low-quality building materials (e.g., straw and clay) (Cuny, 2017; Endlhardt et al., 2019). Reasons for the limited studies relating MS to environmental hazards include the lack of detailed information about individual buildings' damage due to the significant effort required to collect it (Wahab & Tiong, 2016). Such information is usually collected through surveys, making it practical only for studies of small scale (Englhardt et al., 2019). Among the limited studies, Thieken et al. (2008) included building quality and use type in a model for estimating direct monetary losses due to flooding in Germany. Englhardt et al. (2019) developed a framework to define the vulnerability of buildings to flooding based on their construction type and material, in which four vulnerability classes are identified with a unique vulnerability curve showing the relationship between water depth and the amount of damage.

An environmental hazard event is also a common incident in which MS is converted to waste, even long before the ends of expected lifespans (Tabata et al., 2018). Waste is generated either as debris or damaged consumer goods (e.g., furniture and appliances). Traditional quick treatments for disaster waste include incineration and landfill (Tabata et al., 2018). Although such quick treatments can help accelerate the reconstruction of affected areas by clearing up transformation lines and restoring the space to rebuild, they may not be cost-effective. In small island states that rely on imports of construction materials, these quick treatments can even lead to overexploitation of natural resources because waste is a reliable source of secondary materials for reconstruction (Tabata et al., 2017). One example of recycling hazard waste is that 81% of disaster waste and 99% of tsunami debris were recycled after the 2011 Great East Japan Earthquakes (Japan Ministry of Environment (JMOE), 2017).

2.3 Flood Risk Assessment

According to the action of the Sendai Framework for Disaster Risk Reduction 2015-2030 (UNDRR, 2015), understanding hazard risk is essential for reducing current hazard risk and preventing potential threats in the future. As for flood risk management, systematic efforts trace back to the 1970s (Teng et al., 2017). However, it is since the 1980s that simulation-based models have gained more popularity than empirical methods that rely on historical data and statistics of previous hazard events (Galasso et al., 2021). In addition to these two types of models, regressionbased models are applied in data-scarce developing areas, using information from another data-rich basin with similar geological characteristics (Galasso et al., 2014). Despite the variety of modelling methodologies, there is a consensus that flooding is one of the most challenging types of hazards to model for: 1) its multi-stage complexity from precipitation to inundation; 2) high data requirement (details of rainfall, soil type, land cover, topography etc.); 3) limitations on computational feasibility in simulation-based models that result in the compromise of temporal efficiency (European Commission, 2016). The rest of this section reviews the state-of-the-art flood modelling techniques, focusing on hydrodynamic models.

2.3.1 Empirical Methods

Flood investigation approaches can be divided into two major groups: empirical methods and hydrodynamic models (Teng et al., 2017). Studies employing empirical methods utilize flood-related observations like geologic evidence from prehistoric floods that reveals ancient flood generation mechanisms and magnitudes (O'Connor & Costa, 2004). Also valuable are observations that depict flow path alteration from aerial and satellite imageries (Kastridis et al., 2020), flood depth from in-situ watermarks (Mathew et al., 2021), and post-flood interviews of eyewitnesses that help reconstruct the temporal evolvement of the event (Marchi et al., 2009). Although such empirical observations are commonly considered accurate, Teng et al. (2017) argue that the limitations of empirical approaches include: the high cost of financial and human resources in post-flood data collection in large watersheds, lack of prediction functions but only static snapshots of past events, as well as potential artificial errors during the data collection and processing phases.

2.3.2 Hydrodynamic Models

Also known as simulation-based models, hydrodynamic models generally use multiple input datasets describing the watershed under investigation to mathematically emulate the impact of certain flood events. In terms of varying degrees of physical complexity involved in the simulation processes, hydrodynamic models can be further grouped into one-dimensional (1D), two-dimensional (2D), and three-dimensional (3D) models (Teng et al., 2017).

In general, water flow can be grouped into three types when it comes to flood modelling: overland flow, channel flow, and flooding, as is shown in Figure 2.2. Overland flow is triggered by intense precipitation or snowmelt and runs into river channels, and flooding is initiated when channel flow reaches the maximum capacity (Bout et al., 2018). In 1D models, floodplain flow is simplified as flow parallel to the centerline of the main river channel, so any point of a given cross-section shares the same averaged velocity. Such simplification results in low computing power requirement, and 1D models are considered sufficient when knowledge in other dimensions is not required in a project, or the flow being modelled is indeed one dimensional (e.g., artificial confined channel flow) (Teng et al., 2017). For example, Anju et al. (2021) used the 1D MIKE HYDRO River model to simulate water levels of the Pamba river during the flood season in 2010. Comparing the recorded and the simulated water levels, they found that the observed values agree with the simulated values, with the correlation coefficient reaching 0.94 (Anju et al., 2021).

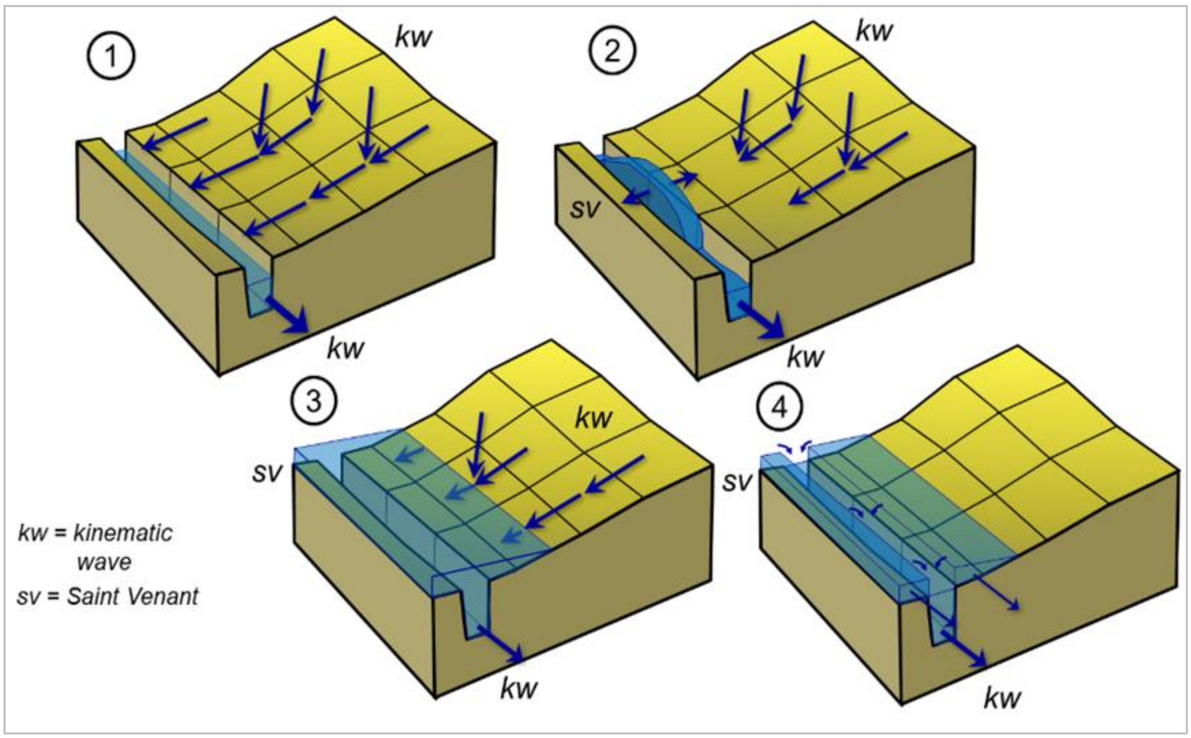

Figure 2.2: *Illustrations of overland flow (1), channel flow (2), flooding (3) and flood recession (4), adopted from Jetten (2016).*

Since the 2000s, 2D flood models have become widely used to map flood extent for the advances in high-resolution data availability, mathematical solutions to physical equations, as well as computational power (Tayefi et al., 2007). Compared with 1D models, 2D flood models incorporate an additional dimension to express the floodplain as a collection of planes but assume shallow water depth (Teng et al., 2017). Therefore, 2D models can ease the impact of the complexity of topographic features like small objects in urban areas and artificial obstacles in rural areas (Tayefi et al., 2007). However, the quality of topography data is critical for the accuracy of the 2D modelling results. According to Yu & Lane (2006), flood inundation extent and timing of inundation is relatively sensitive to even minor fluctuations in model resolution in the context of fluvial flood modelling. In a national flash flood modelling project, Jetten (2016) also argues that the simulation of a flood hazard can be considerably altered by a better digital elevation model (DEM) that represents the topography better by matching the visually interpreted river network from satellite imageries.

Compared with 2D models, 3D flood models are more physically complex since velocities are not considered vertically identical. This added dimension is crucial in circumstances that the vertical component of the flow velocity is not negligible: when the topology of the modelled floodplain goes through abrupt changes frequently (Casulli & Stelling, 1998), or when a catastrophic flood occurs because of dam collapse, tsunamis, and levee breaks (Teng et al., 2017). This vertical characteristic of 3D models also enables the simulation of suspended-sediment transport analysis, a significant factor in flood hazard mitigation actions (Jia et al., 2014). The dam failure modelling study by Prakash et al. (2014) used the 3D smoothed particle hydrodynamics (SPH) model, incorporating potential vertical turbulence and vortices caused by the presence of dam wall fragments. In terms of inundation time and water level of the downstream area, the simulated event agrees with the observed data of the historical dam failure (Prakash et al., 2014). Although 3D flood models can capture the three-dimensional nature of flooding, especially in the early stage of flood generation, one drawback of 3D models is the high requirement of computing power. 3D models, or even 2D models, were once considered unviable to simulate areas over 1000 km2 at a resolution less than 10 m (Teng et al., 2017). However, this situation has been improved by recent advances in algorithms to solve hydrodynamic equations and high-efficient supercomputers. For example, Zhang et al. (2021) reproduced a flood event along the 280 km reach in the Three Gorges Reservoir using a 3D flood model and found that the 3D model can accurately predict the impact of flooding at a relatively big scale.

2.4 Vulnerability Assessment to Environmental Hazard

2.4.1 General Definition of Vulnerability

In the context of environmental hazards, risk can be defined as a combination of three components: hazard (intensity, extent, duration), exposure (land and population exposed), and vulnerability (social factors that affect the susceptibility of the exposed land and people) (UNISDR, 2015). The first two components are more site-specific and cannot be easily eliminated in the short term. Different parts of the world are exposed to varying combinations of environmental hazards. For example, tropical regions such as the Caribbean are frequently affected by tropical storms and hurricanes (Smith et al., 2009), while South America and Central Asia often experience debris flows due to more frequent tectonic activity and concentrated precipitation (Kelfoun et al., 2008). According to IPCC, vulnerability is defined as the degree to which a social system is prone to and is uncapable to cope with negative effects (McCarthy et al., 2006). Vulnerability, as the third component of hazard risk discussed earlier, can be further considered as a combination of factors from multiple dimensions: physical, social, institutional, economic, and environmental (Fuchs, 2009). Institutional, economic, and environmental vulnerability are often investigated at a larger scale (e.g., in a regional scale), whereas physical and even social vulnerability can be estimated at the building level (Papathoma-Köhle et al., 2019).

2.4.2 Physical Factors of Vulnerability to Environmental Hazard

Despite the interconnected multiple dimensions of vulnerability to environmental hazards, physical factors of vulnerability is identified as a primer (Mazzorana et al., 2014), and is defined as the physical elements of the built environment affecting the degree of loss by a hazard (Fuchs, 2009). Regarding physical factors of vulnerability, three approaches are summarized by Papathoma-Köhle et al. (2017): 1) vulnerability matrices; 2) vulnerability curves; and 3) vulnerability indicators. Supported by the knowledge of historical hazards, the first two approaches investigate the relationship between hazard intensity level (e.g., water levels in the context of flooding) and the degree of damage. As a result, they may not be applicable in areas where detailed hazard records are absent. Although initially used to examine social factors of environmental hazard vulnerability, approaches utilizing vulnerability indicators are also prevalent in research focusing on physical vulnerability. Vulnerability indicators are composed of variables indicating a system's capacity to offer information of the "susceptibility, coping capacity and resilience" to a hazard event (Birkmann, 2006). This indicator-based approach is flexible and can be adjusted to the needs of a specific area with the following general procedures: 1) selecting relevant indicators that are considered typical in the affected area; 2) identifying a weighting scheme to combine the selected indicators; and 3) aggregating all indicators to a vulnerability index to show the overall vulnerability (e.g., by weighted linear combination) (Kappes, Papathoma-Köhle & Keiler, 2012).

One example that uses physical vulnerability indicators is by Papathoma-Köhle et al. (2007), in which a Geographic Information System (GIS) database was generated to store physical factors that would affect the vulnerability of buildings to landslides. The selected indicators included construction materials, surrounding conditions (existence of walls), up-hill side conditions (walls or windows), and the number of floors. (Papathoma-Köhle et al., 2007). In the context of small island states in the Caribbean region, where tropical storms causing high winds can be expected during late summer, some common variables of physical vulnerability factors are presence or absence of foundation pillars, hurricane straps, and bracing in the building corners (Canevari-Luzardo et al., 2017). For physical vulnerability to flash flooding, some building specific variables are identified as number of floors, presence of basement, height of lowest opening, building age, and wall material (masonry or non-masonry) (Granger et al., 1999; Menoni et al., 2006; Kappes, Papathoma-Köhle & Keiler, 2012).

2.4.3 Social Factors of Vulnerability to Environmental Hazard

Compared with physical factors, social factors of vulnerability to environmental hazards are often regarded as inherent human system properties independent from the environmental hazards themselves and hazard exposure (Holand et al., 2011). According to Wisner et al. (2004), social factors of vulnerability can be defined as the characteristics and conditions of an individual or a group of people which influence their capacity of predicting, resisting, and recovering from hazard events, which can also be considered as a broad definition of social resilience (Cutter et al., 2008). Social factors of vulnerability are discussed less frequently in the literature due to the difficulty in its quantification (Cutter et al., 2003). When investigating social aspects of vulnerability to environmental hazards, the most commonly used approach is also based on indicators.

A wide range of social variables would impact vulnerability to environmental hazards. Some common concepts of vulnerability reflected by social variables are age, socioeconomic status, gender, education, and special needs. To expand on these vulnerability concepts, both sides of the age spectrum result in limited mobility for evacuation (Cutter et al., 2000), and burden of care in hazard aftermath (Morrow, 1999); Income level is usually the best indicator for the ability to absorb losses due to hazard events through insurance and other means (Chen et al., 2013; Cutter et al., 2000); Women is recognized as a social group with higher levels of vulnerability due to family care responsibilities, traditional gender roles and gender discrimination (Forhergill, 1996);

A higher level of education results in a better understanding of hazard warning and recovery information (Center & John, 2000; Tierney, 2006), and a better chance to survive hazard events (Frankenberg et al., 2013); People with disabilities are disproportionately affected and more likely to require transportation, medical care or assistance with their daily activities during and after hazard events (Cutter et al., 2003; Flanagan et al, 2011; Morrow, 1999).

With the recognition of the influence of social factors on disaster management, policymakers are incorporating social vulnerability into policy making (Spielman et al., 2019). One critical study in the literature for social factors of vulnerability to environmental hazards was conducted by Cutter et al. (2003). The impact of the study is beyond the academic literature and has been applied worldwide by practitioners in place-based vulnerability assessments (e.g., Flanagan et al., 2011; U.S. Environmental Projection Agency, 2015). This study used a robust social vulnerability assessment framework consisting of 42 variables to derive the Social Vulnerability Index (SoVI). SoVI is a comprehensive index that involves a wide range of factors, such as access to resources (e.g., medical, information), access to political power and social capital. The SoVI was initially developed for the United States but has proven applicable in other cultural contexts. For example, Chen et al. (2013) applied the methodology in China's Yangtze River Delta region. They found that it could capture most social factors (e.g., per capita disposable income, median age, number of beds in health care institutions per thousand population) of the study area. Some studies tried to improve the framework by Cutter et al. (2003) rather than replicating the same methodology in a new context. For example, Holand & Lujala (2013) demonstrated three types of index accommodations for the better adaption of the SoVI approach in a non-US context by investigating the correlation between the replicated and the adapted indexes. Such studies can guide the future application of the SoVI methodology to be better adapted to a new context.

In a study by Borden et al. (2007), social factors of vulnerability were divided into two groups from a new perspective: socioeconomic vulnerability factors and built environment vulnerability factors. The former is at the individual level about education, employment, gender, etc. The latter is more emphasized at the household level about surrounding environmental factors, such as distance to the nearest hospital and population density. Inspired by this idea of distinguishing socioeconomic factors and built environment factors, Holand et al. (2011) quantitatively assessed social vulnerability to environmental hazards in Norway. They found that by separately investigating socioeconomic and built environment factors, it is possible to prevent minor high-score indices from masking other significant factors.

2.5 Research Gaps

This literature review section has covered existing material stock analysis approaches, the relationships between MS and environmental hazards, methodologies for flood risk investigation, and indicator-based vulnerability assessment to environmental hazards. Most previous studies that focused on the impacts of environmental hazards on MS were conducted from a post-disaster perspective, which aid governments in identifying areas requiring rebuild and managing waste flows (Fu et al., 2021). A few studies have estimated future MS losses in the contexts of climate-change related hazards such as high winds during extreme weather events and coastal flooding, using qualitative damage assessments of historical hazard events and sea-level rise scenarios (Symmes et al., 2020; Bradshaw et al., 2020). However, few studies have focused on the exposure of MS to flash flooding through physics-based models that involve fluvial geomorphology and hydrodynamics. Thus, the benefits of integrating the results of material stock analysis and more detailed hazard risk assessment remain unexplored.

In combination with hazard characteristics (e.g., intensity, extent, and duration) and hazard exposures, hazard vulnerabilities define hazard risks (UNISDR, 2015). Although vulnerability is the only element of hazard risk that can be eliminated in the short term, most studies considered only social or physical factors of vulnerability to environmental hazards. One reason for this separation of social and physical factors could be the difference between the spatial scales to which these two types of factors are suitable for, respectively. For example, some physical factors such as the up-hill side condition (wall or windows) or the height of lowest opening (Papathoma-Köhle et al., 2007) are more sensible at the household level, while some social factors are more meaningful at a more aggregated level, such as the median age of residents in a community and the per capita number of community hospitals (Cutter et al., 2013). However, in small island states with a lower population density, estimating vulnerability at the island level with parish as the analytical unit may not be detailed enough to reveal where vulnerable population are located. Therefore, further one direction for vulnerability assessment in the context of small island states is involving both social and physical factors at the household level.

3 Methodology

3.1 The Methodological Framework

This section describes the methodologies used to address the research questions mentioned in Section 1.4. To link the findings, a methodological framework consisting of three major parts in response to the three previously described research questions is shown in Figure 3.1. The framework begins with an island-level material stock accounting (MSA) to estimate MS in buildings, which is aimed to form the basis of a further flood risk analysis. Following the MSA, a flood model is used to simulate flash flooding events of different return periods. The major output of flood modelling is a collection of flood extent maps for flash flood events with different magnitudes. If examined together with the estimated MS in buildings, these flood extent maps can be used to locate high concentrations of MS in buildings exposed to flash flooding.

Once hazard exposure levels are revealed, the last part of the framework examines flood risk from a social vulnerability perspective in the context of small island states. This part of the framework has two steps. First, relevant variables are collected from the literature, tailored for the area under investigation, and a household survey is designed to collect these selected variables. Next, data reductionist techniques (e.g., principal components analysis and composite index development) are used to combine these variables into an index for each building to indicate its degree of vulnerability by incorporating social factors of vulnerability to flooding, which can be further used to identify vulnerable households exposed to potential flash flood hazard events. In this study, only the first step was completed due to the constraints on travel during the COVID-19 pandemic, which hindered a field work to implement the household survey for data collection.

This study is the first attempt to investigate MS from an environmental hazard perspective in Dominica. The proposed methodological framework was partially tested, excluding the vulnerability assessment part (highlighted by the dashed box in Figure 3.1) due to limited access to secondary data and the constraints on primary data collection during this research. A stock-driven approach that was employed for MSA is described in Section 3.2, followed by a flood modelling approach explained in Section 3.3. If the whole methodological framework is applied, this study could help the government locating clusters of potential hazard demolition waste and help a hazard mitigation agency or municipality to identify vulnerable households at risk and accordingly prioritize evacuation and recovery actions during and after a flood event, respectively.

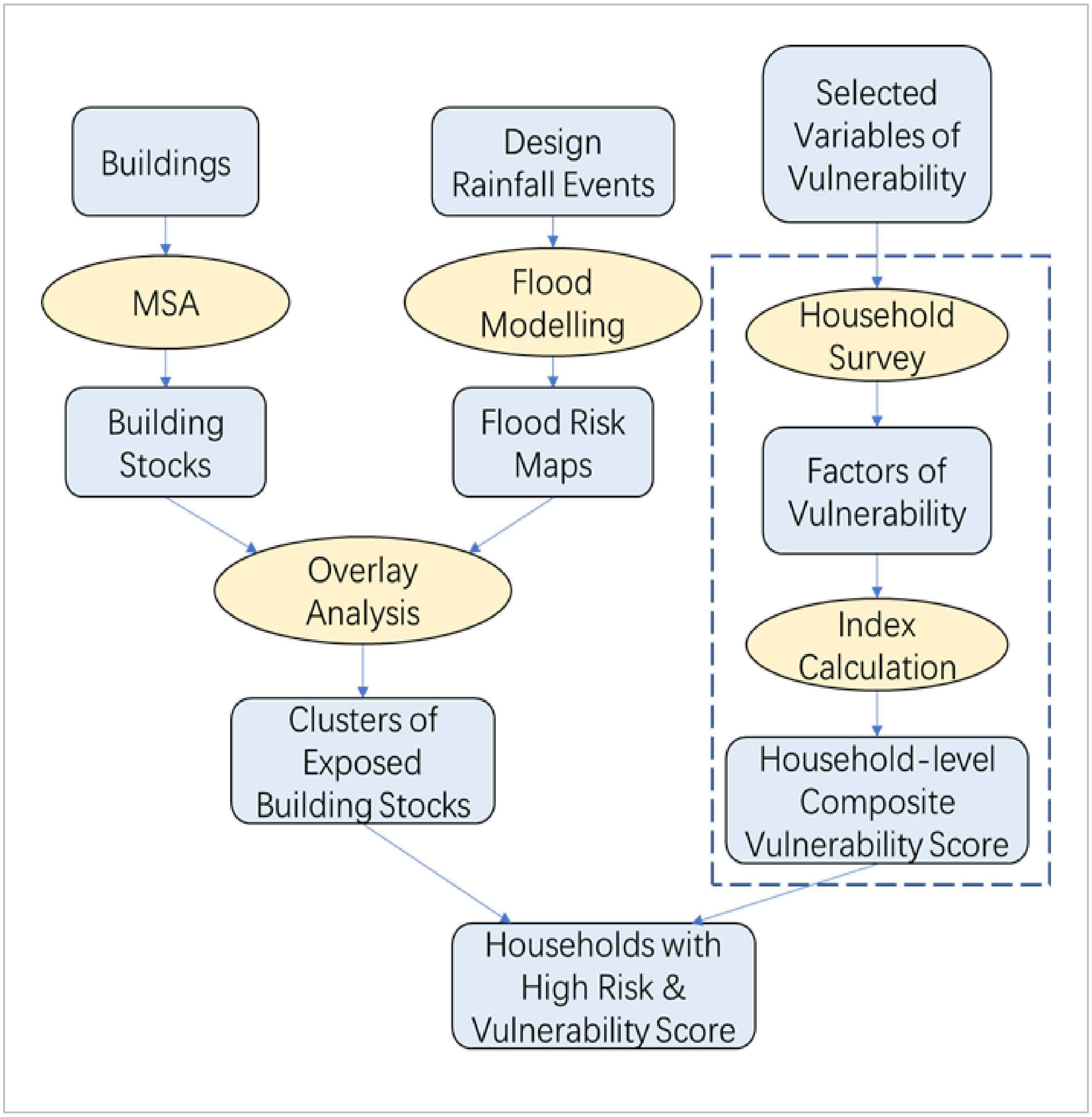

Figure 3.1: *The methodological framework for integrating the results of MSA, flood risk assessment, and vulnerability factors to identify households that are exposed and susceptive.*

3.2 Methodology for Material Stock Accounting for Buildings in Dominica

This study employs a stock-driven approach (also called bottom-up or coefficient-based approach) to account for material stocks in Dominica's buildings. In a stock-driven approach, the quantity of a type of material is derived from the product of the total inventory of items and the corresponding material intensity coefficients (Tanikawa et al., 2015). Since material stocks are directly derived from stock inventory rather than material flows, such approach enables the investigation of the spatial characteristics of the results in a defined area (Lanau et al., 2019). Although bottom-up approach can also be made dynamic by compiling a series of material stock accounts (Tanikawa et al., 2015), the stock-driven approach used in this study was static because only one "snapshot" of building stocks was taken for 2020, when the building footprints on the whole island (including informal settlements located far away from urban areas or towns) were acquired from Open Street Map (OSM).

The workflow for MSA in Dominica was adopted from Symmes et al. (2020) and includes three major steps. First, buildings are divided into different occupancy classes so that the same set of material intensity coefficients can be applied for all buildings of the same occupancy class. Following building classification, building height is derived and used to calculate gross floor area (GFA) as the approximation of the physical sizes of the buildings. The last step is based on the outputs of the first two steps, in which material stocks in buildings are estimated by applying material intensity coefficients on corresponding occupancy classes. The following subsections describe the methodology for material stock accounting in more detail.

3.2.1 Data Sources

The data sources of the geodatabase compiled for the MSA in Dominica are summarized in Table 3.1. The key data sources are: Open Street Map (OSM), which provides footprints of all the buildings on the island in 2020, Google Maps, which contains a considerable amount of building use-type information that helps building classification, as well as AERIAL DOMINICA, an unofficial organization that posts aerial videos online for public use. These aerial videos taken from drones were available in major towns and communities, so they were used to derive building heights. The aerial videos were taken within five years before 2020 and showed a good match to satellite imageries in Google Earth Pro, so this data source is considered relatively accurate. However, the building footprints from OSM had to be manually corrected for three times with reference to satellite imageries, and the building use types from Google Maps may not be up to date. Nevertheless, these data sources are capable of generating reasonable material stock analysis results, as this research intends to acquire a relatively rough estimate of building stock at the national level.

Table 3.1: *Summary of data sources of the MSA in Buildings in Dominica.*

Source	Topic
Caribbean Handbook on Risk Information Management (CHARIM)	Administrative, risk information, land-use, river channel
DomiNode	Ecology, topography, transportation, hydrology
Open Street Map	Building footprints, building use-type
Google Earth	Building use-type
AERIAL DOMINICA	Building height (number of storeys)

3.2.2 Building Classification

In stock-driven approaches, the initial step is to divide the inventory of items into groups that share the same material intensity. In the case of building stock accounting, buildings are first grouped into different occupancy classes with similar building compositions so that the same set of material intensity coefficients can be applied. In this study for Dominica, the building classification framework by Symmes et al. (2020) was adopted to assign an occupancy class code for each building. The adopted classification framework was originally developed for Grenada (a small island state near Dominica with similar cultural and environmental background) but was tailored to match the situations in Dominica by referencing the information in the aerial videos. The classification framework is based on visual interpretation of satellite imageries, field observations, and expert consultation, as discussed in detail in Symmes et al. (2020). With reference to satellite imageries and existing building use-type information in OSM, Google Map, and photos posted by users of Google Earth, each building was first assigned a first- or second-level occupancy code (e.g., 100 for institutional buildings, 110 for church and 120 for school). Next, buildings were further differentiated to a third level occupancy (e.g., 111 for Cathedral, 112 for regular community church, 121 for educational campus building and 122 for standalone elementary/secondary school building) by applying a series of decision trees which involves criteria like footprint area, spatial pattern with nearby buildings, and its spatial relationship with land use.

Listed with their codes in Table 3.2 are the 22 third-level building occupancy classes identified in Dominica. The first digit stands for the first-level use types: 100 for institutional, 200 for commercial/industrial, 300 for residential, 400 for tourism, 500 for cultural, and 600 for transport. The second and third digits present second-level use types (e.g., 110 for religious and

120 for educational) and final occupancy classes (e.g., 111 for cathedral and 112 for church). There are over 30,000 buildings on the whole island, so the strategy for building classification was to start by identifying large buildings, which could potentially be industrial buildings, supermarkets, hotels, or office buildings (Alam, 2015). The visual interpretation process also referenced the key image interpretation elements like footprint shape, pattern, size, and association with surrounding buildings (e.g., unique irregular shapes that distinguish churches from their surrounding buildings, illustrated in Figure 8 in Bradshaw, 2020). For the rest of the buildings, the assumption is that they fall into the first-level use type of residential. Based on the first-level use-types, the final building occupancy classes are derived by applying a decision tree developed by Symmes et al. (2020) for each first-level use-type, with some minor adjustments to the thresholds on footprint size that separates major hospital from minor health centre, cathedral from community church. For each building occupancy class, an example is included in Appendix A.1, showing the footprint, satellite image, and a screenshot from the aerial video.

Table 3.2: *Domain codes for each building occupancy class in Dominica.*

Code	Building Occupancy Class		
111	Cathedral	321	High-density apartment building
112	Church	322	Low-density apartment building
121	Educational campus building	330	Rural single-family dwelling
122	Standalone primary /secondary school	340	Residential single-family dwelling
131	Major hospital	411	Large multi-unit hotel building
132	Health centre	412	Small hotel/villa
140	Government office	510	Stadium
210	Commercial	520	Recreational centre
220	Urban mixed commercial	530	Historic building
230	Industrial	610	Seaport
310	Urban single-family dwelling	620	Airport

3.2.3 Building Height Estimation

After building classification, each footprint was assigned a building height in terms of its number of storeys. The workflow of building height estimation is shown in Figure 3.2. The actual building heights were acquired from visual interpretation of aerial videos. However, some buildings were not covered in any aerial video available at the time of building height estimation. For these buildings, the average height of nearby buildings of the same occupancy class with visually interpreted heights was assigned.

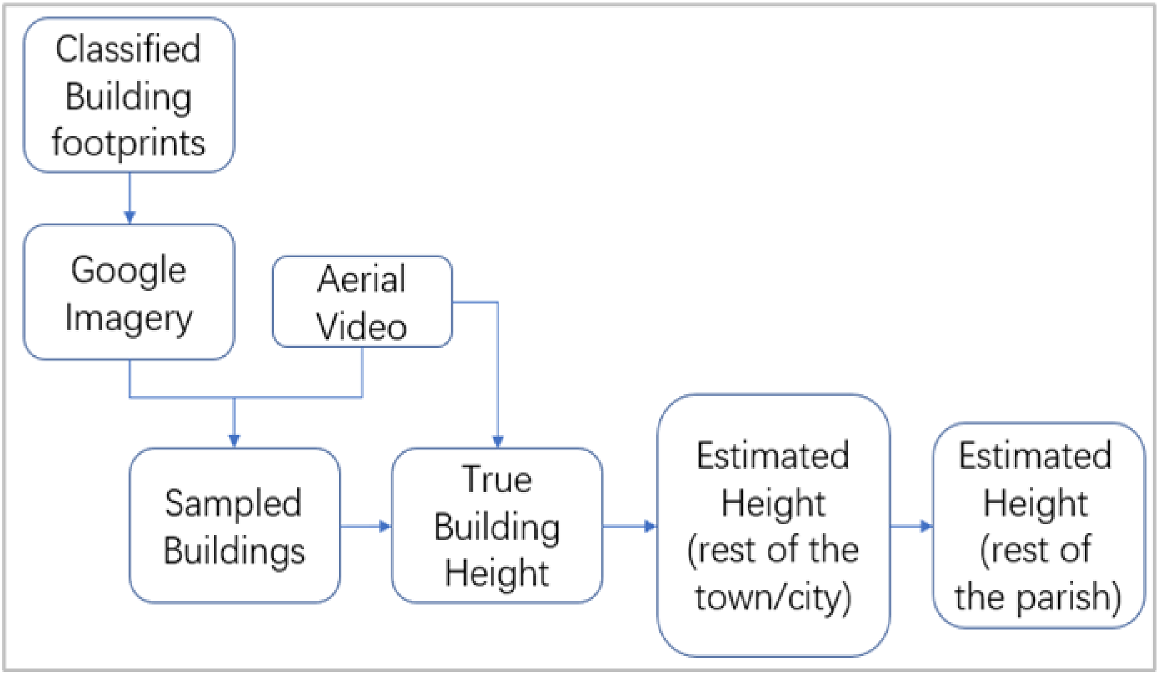

Figure 3.2: *The workflow of building height estimation using visual interpretation of aerial videos.*

Most of the towns and cities in Dominica are covered in aerial videos, and 37% of the buildings on the whole island were assigned a true building height. All the aerial videos were taken within five years before 2020 from a variety of viewing angles, making them valuable sources for the acquisition of building heights. Google Earth satellite imageries were used as base maps, on top of which the buildings in the aerial videos were linked to the building footprint vector dataset that stores building height data. In more detail, visual interpretation of building heights includes three steps: 1) overlay the classified building footprint vector dataset on top of Google Earth satellite imageries; 2) navigate to the towns or cities covered in the aerial videos and identify sampled buildings whose heights can be visually interpreted; 3) interpret the building heights of sampled buildings and store the heights in the building footprint vector dataset. The actual heights of sampled buildings were further utilized to estimate the heights of buildings far from any flight route or not covered by any viewing angle of the available aerial videos. In the same town or city, the average height of the sampled buildings of the same occupancy class was assigned to those not covered. For buildings in physically isolated towns that are not covered by any aerial video, the average height of all the other buildings of the same occupancy class, with an interpreted height, and in the same parish is assigned. The rationale is the "first law of geography" argued by Tobler (1970) that objects are more related to other objects nearby than those further away.

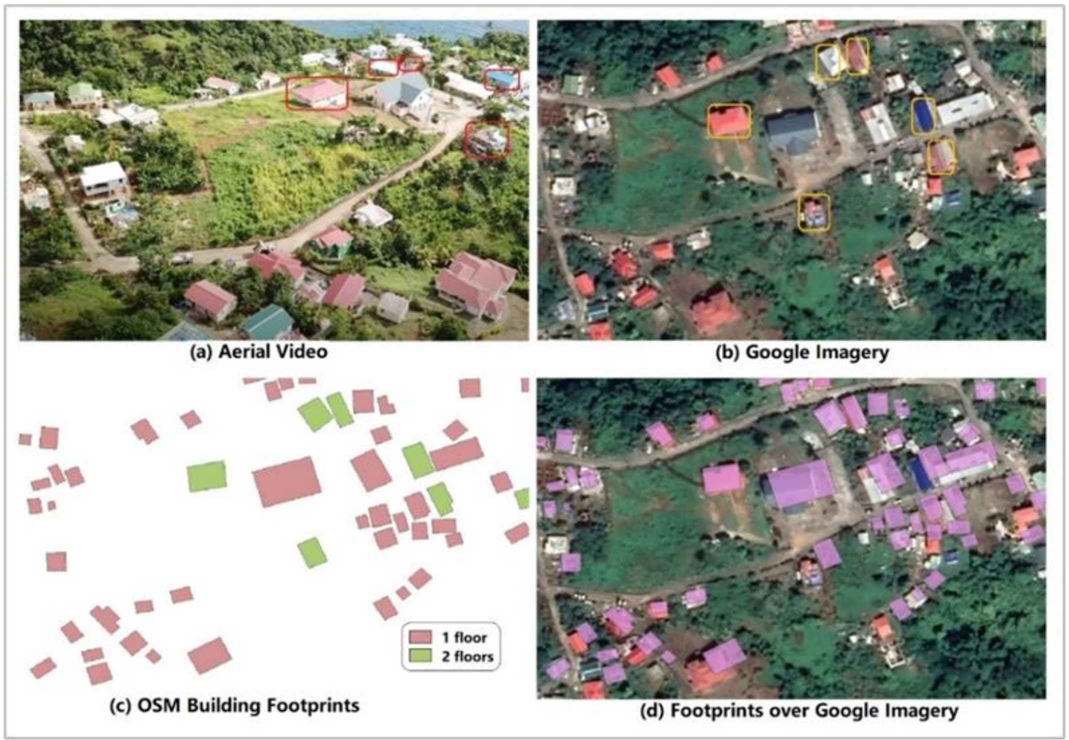

Figure 3.3: *A sample area (Vielle Case, St. Andrew Parish) for building height acquisition using aerial video.*

Figure 3.3 shows an example of a town (Vielle Case village) for building height interpretation with a combination of the aerial video, Google Earth imagery, OSM building footprint layer alone, and the footprint layer on top of Google Earth image. In this sample area, seven buildings were identified to have two floors, while the rest were confirmed as one-storey buildings. The strategy was to identify relatively tall buildings (e.g., buildings with three floors or more) for spatial orientation and link aerial videos and Google Earth satellite imageries by matching roof colours and shapes. For relatively tall buildings in the aerial videos, the shadows in Google Earth images can also provide a hint about their heights (Shao et al., 2011). Shadows can be used to derive building height by applying a trigonometric relationship involving the sun inclination angle at the time of the day and the shadow length (Irvin & McKeown, 1989). Due to the limited scope of this study and data availability, shadows are merely used as a qualitative confirmation of the visually interpreted building heights, especially for tall buildings.

3.2.4 Material Intensity

In a stock-driven material stock accounting approach, the homogeneity of the material intensity of each occupancy class is a key assumption (Augiseau & Barles, 2017), so accurate material intensity coefficients are crucial for the accuracy of the final estimated amount of MS. One reliable source for estimating material intensity is the engineering information in building construction manuals, but Dominica's data infrastructure is still under development and such information is not available. Moreover, a considerable proportion of residential buildings in Dominica were constructed under contracts with individual merchants, so they are often non-engineered even in larger cities such as Roseau and Portsmouth (Cuny, 2017). Since no in-person fieldwork observations were included in this research, the seven basic building construction styles identified in Grenada by Symmes et al. (2020) were adopted. For Dominica's building construction styles, Cuny (2017) identified the five most common housing construction types in a report of a quantitative evaluation of their performance against high winds and earthquakes. These two sets of building construction types show similarities in the general composition of primary materials (wood frame or concrete block). The comparison between the building construction styles by Symmes et al. (2020) (adopted in this study) and by Cuny (2017) is presented in Appendix A.2, with the material intensity coefficients of four types of construction materials investigated in this study: aggregate, timber, concrete, and steel.

For residential buildings only, the methodology by Symmes et al. (2020) was also adapted to derive a composite material intensity typology utilizing the shares of different construction material categories presented in the 2011 Housing and Population Census report of Dominica. Regarding material types for outer walls of residential buildings, the percentages in the 2011 census are: 27.6% for wood, 60.4% for concrete, 10.8% for wood and concrete, and 0.4% for other. Table 3.3 shows the process of allocating the composite material intensity typology. It is assumed that Concrete Structure 1 and Concrete Structure 2 (two of the building construction styles, as detailed in Appendix A.2) share the same number of buildings in the concrete construction style.

Table 3.3: *Composite material intensity typology for residential buildings in Dominica.*

Material category in the census report	**Percentage in Census 2011**	**Relevant material intensity typologies (Appendix A.2)**	**Final allocated composition in material intensity typology for residential buildings.**
Wood	27.6%	Timber Structure (100%)	Timber Structure (27.6%)
Concrete	60.4%	Concrete Structure 1 (50%) Concrete Structure 2 (50%)	Concrete Structure 1 (30.2%) Concrete Structure 2 (30.2%)
Wood and concrete	10.8%	Concrete/Timber Mix Structure (100%)	Concrete/Timber Mix Structure (10.8%)
Other	1.2%	None	0% (ignored)

3.2.5 Material Stock Accounting for Buildings

With building occupancy class, corresponding material intensity, and estimated building height, construction materials in a building can be calculated by multiplying its gross floor area (GFA) and the material intensity coefficients. At the national level, total material stock in buildings in Dominica was quantified with the equation:

$$MS_i = \sum_{OC} MI_{i,OC} \times GFA_{OC} \tag{1}$$

where

MS = total amount of material stocks in all buildings

MI = material intensity with gross floor area (GFA) as the unit for measurement (in Appendix A.2)

i = individual material class (in this research: concrete, timber, aggregate, and steel)

OC = building occupancy class (defined in Section 3.2.2)

GFA = gross floor area calculated as the production of number of floors and footprint area.

3.3 Methodology for Flash Flood Modelling in Dominica at the Island Level

Section 3.2 has focused on the methodology of material stock accounting for buildings in Dominica. However, the quantity of material stocks in buildings alone does not convey the information about the exposure to environmental hazards. From a risk management point of view, this section describes the methodology for quantifying the exposure of Dominica's MS in buildings to intense rainfall-provoked flash flooding. The magnitude of flash flooding is influenced by multiple factors, among which a high precipitation resulted from sustained high rainfall intensities is a dominating factor. In addition to heavy rainfall, the physical characteristics of the concerned catchment also affect the magnitude of flash flooding. For example, the topography, initial soil moisture and other soil physical properties, river channel dimensions, vegetation coverage, and land-use types all participate in surface flow generating processes (Doswell III et al., 1996; Marchi et al., 2010). To cope with the complex nature of flash flooding, the Open Source Limburg Soil Erosion Model (OpenLISEM, LISEM in short) was used for flood inundation modelling to integrate the multiple factors affecting the occurrence of flash flooding.

LISEM is an event-based model for simulating soil erosion and surface runoff caused by short-term rainfall (Bout et al., 2018; Starkloff et al., 2018). It was initially developed to simulate overland flow but has been extended and adapted to other applications like soil conservation (Takken et al., 1999; Hessel et al., 2003) and flood modelling (Pérez Molina, 2014; Pratomo, 2015).

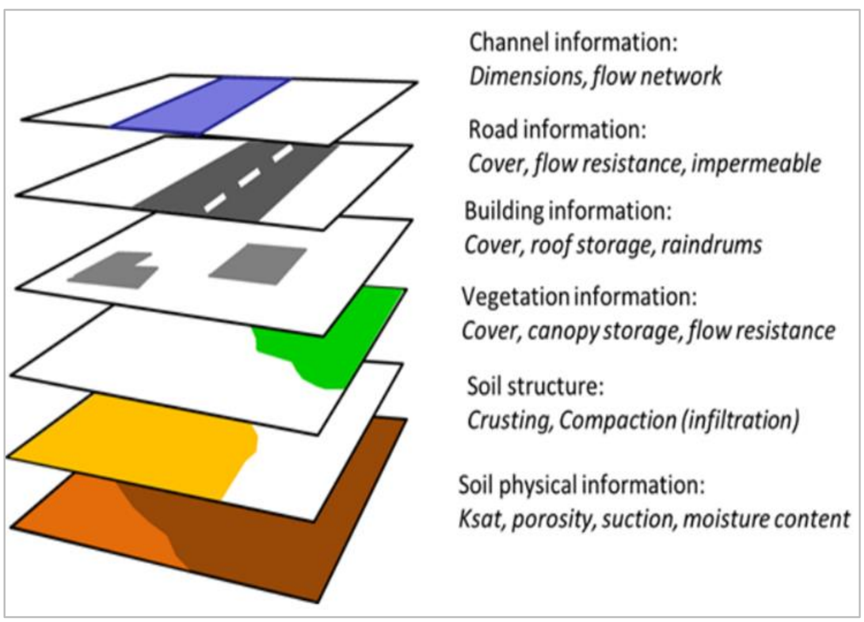

Figure 3.4: *Input data structure of the LISEM showing multiple sets of input data layers for flood modelling, adopted from Jetten (2016).*

Table 3.4: *Base input datasets and their derivatives for flood modelling using LISEM.*

Base Input Dataset	**Derived Layers**	**Processes Involved**	**Data Source**
DEM	Local drainage direction network	Surface runoff	CHARIM GeoNode (2021)
	Slope gradient	Surface runoff	
	River channel	Channel flow	
	Soil depth	Infiltration	
Soil map	Porosity	Infiltration	CHARIM GeoNode (2021)
	Saturated hydraulic conductivity	Infiltration	
	Average initial matric suction	Infiltration	
Land use map	Vegetation canopy cover	Interception	CHARIM GeoNode (2021)
	Surface roughness	Surface runoff	
	Flow resistance	Surface runoff	
Historical rainfall statistics	Design rainfall event intensity	Precipitation	Jetten (2016)
Road network	Road width	Interception, infiltration, surface runoff	CHARIM GeoNode (2021)
Building Footprints	Building size	Interception, infiltration, surface runoff	OSM (2020)

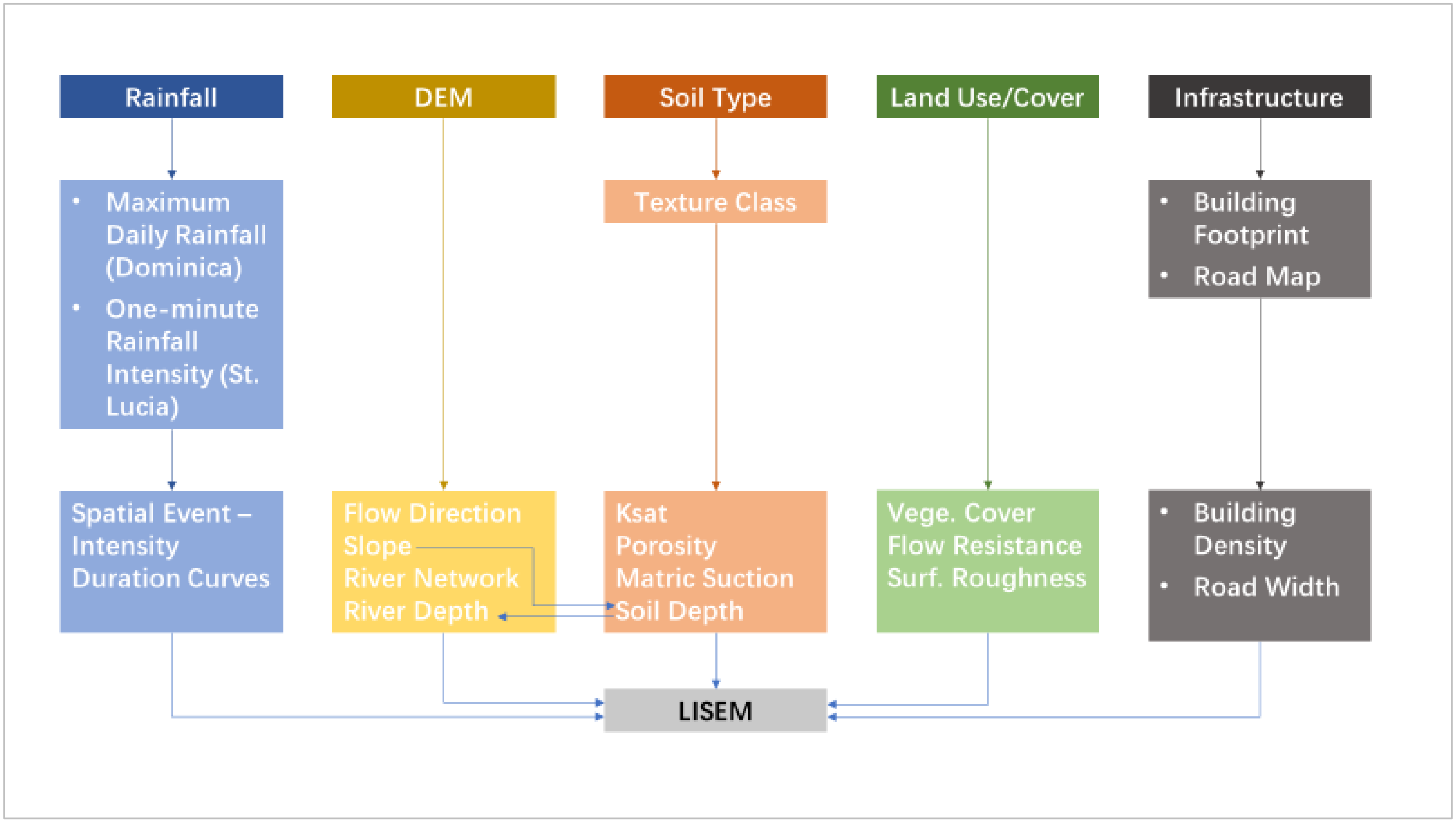

Figure 3.5: *The flow chart of deriving input data layers for LISEM from 5 basic datasets.*

Figure 3.4 presents the input data structure of LISEM. LISEM divides the concerned basin or catchment into grid cells, and for each cell aggregates surface physiography information supplied from multiple input layers. The model requires 14 input data layers in total, but most of these layers were derived from a few base maps. Figure 3.5 visualizes the derivation of the 14 input layers from five basic datasets, except for soil depth (river depth). The arrow from slope to soil depth indicates the estimation of soil depth using its relation with slope, distance to river channel, and distance to coastline (explained in Section 3.3.1.3) Table 3.4 summarizes the relevant processes of flash flooding simulation in which the input layers are involved. Details of how the input maps were derived are discussed in Section 3.3.1. To balance the precision and performance of the island-level flood model, all required input data layers were resampled to a spatial resolution of 20 m.

3.3.1 Initial Processing of Input Data Layers of Flood Modelling in LISEM

3.3.1.1 Design Rainfall Events

Rainfall is one of the fundamental input datasets for flood modelling and other hydrological simulation processes. In LISEM, rainfall data is presented as a time series of precipitation intensities describing the evolution of a rainfall event. Like other computer-based simulations, LISEM uses discrete timesteps for flood modelling. Since flash flooding has a relatively short duration, small timesteps are preferred for accurate modelling results (Bout et al., 2018). In this study, 5-min precipitation intensities were used to balance modelling quality and performance, which means rainfall intensity changed every five minutes until the simulation ended. The assumption made by Jetten (2016) that the magnitude and frequency of flood events align with the volume and frequency of the rainfall events that cause the flood events was also adopted in this study. This assumption is supported by the finding in Ogden (2016) that rainfall intensity determines peak discharges in streams in tropical forested watersheds with mountainous terrain. In this research, flood events with three different return periods were investigated: 5-year flood, 10-year flood, and 20-year flood. Return period indicates the frequency of a flood event of a given magnitude, and a flood event with a more extended return period is more extreme in terms of its magnitude and duration (Charlton, 2007). Due to the limited access to official meteorological data, the rainfall magnitude and frequency used in this research were adopted from the design storms by Jetten (2016), who applied a frequency magnitude analysis using historical maximum daily rainfall data in Dominica to generate intensity-duration-frequency curves (IDF curves) for flood events with 5 , 10 , and 20 year return periods. Also adopted was the assumption by Jetten (2016) that the whole island is subjected to spatially homogenous rainfall events due to the limited number of gauge stations in Dominica. The detailed rainfall intensity data for the three investigated rainfall events with different return periods is presented in Appendix B.1 as IDF curves.

3.3.1.2 River Channel Dimensions

As listed in Table 3.1, a river network is available on CHARIM. However, the river channels provided by CHARIM does not coincide with the valley bottoms from the DEM used in the flood model, resulting in "rivers cut across slopes, or traverse low elevated hills in the floodplain" (Jetten, 2016). Thus, a new river network was generated from the DEM. The first step of river network derivation is to create a local drainage direction network (LDD) raster map indicating the flow direction of each cell, referencing its deepest downslope neighbor. The LDD map is then used to generate a stream order map for the whole catchment referencing the stream order scheme by Strahler (1964), in which cells with no upstream cells are assigned an order of one, cells with two order one upstream neighbors are assigned order two, and so on. Finally, major river channels are derived by applying a threshold on stream order, which is an iterative process referencing satellite images to achieve the best alignment between the generated river network and the actual river network in satellite images. In this study, the highest identified stream order was eight, and five was determined to be the optimized threshold for river channel extraction, because the river network comprising cells with a stream order of five or higher showed the best match with both the total length and spatial pattern of the actual river network in the satellite images. Therefore, cells with a stream order greater than five were marked as river channel cells.

In addition to the river network, three more input maps related to river channels were produced: channel width, river depth, and flow resistance. River widths were manually acquired through visual interpretation of Google Earth satellite images. The strategy involved starting from the origin of each branch (the finest level for river width assignment in this study) before it joins another branch of higher stream order. Therefore, every location of the river of the same branch shares the same river width. The widths of most river branches were acquired from the satellite image in September 2017 (one week after Hurricane Maria) when the land surface was more exposed due to the large-scale destruction of vegetation. Figure 3.6 shows a comparison between a satellite imagery took in September 2017 and another one took in October 2018. The official dataset for river depth was not available for Dominica, so soil depth was used as an approximation to actual river depth (as described in Section 3.3.1.3). Flow resistance is a parameter related to surface roughness and is presented as Manning's *n* value in LISEM. In this study, flow resistance was set to a constant value of 0.05, based on the comparison by Jetten (2016) between field observations and typical literature values of different surface types. All the input maps related to the river channels are presented in Appendix B.2.

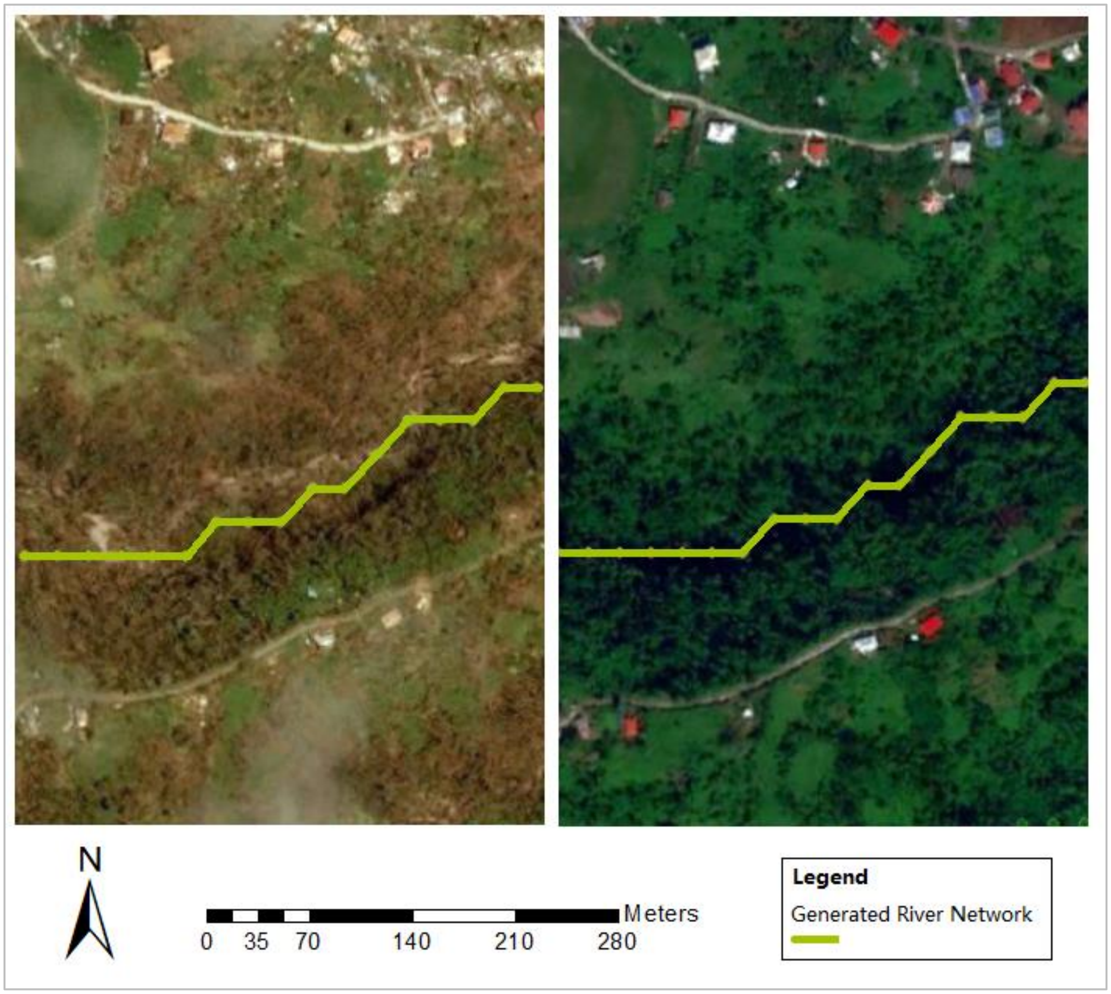

Figure 3.6: *A comparison between the satellite imagery took in September 2017 (left) and the one took in October 2018 (right).*

3.3.1.3 Soil Physical Parameters

The soil map of Dominica provided by the Soil Survey and Research Department of the University of the West Indies (Lang, 1967) was used as the base map for deriving other soil properties. In this soil map, there are 17 soil types identified in the original soil map referencing soil chemical properties such as degree of weathering and mineral composition (Lang, 1967). Due to the absence of a fieldwork to collect soil samples, the initial step was to transfer these original soil types to texture classes. The soil map follows the US convention for soil classification, so the each of the 17 soil types was translated to a soil texture class regarding the United States Department of Agriculture (USDA) texture class triangle (Jetten, 2016). With translated soil texture class, three soil physical parameters required by the LISEM are calculated by applying the pedotransfer functions on the assumed average grain size distribution of the texture class. The three soil physical parameters are: saturated hydraulic conductivity, porosity, and field capacity. The process was done using the latest version of the Soil-Plant-Air-Water (SPAW) model software package (Saxton et al., 2005), which requires the translated soil texture class as the input and automatically calculates the three soil physical parameters mentioned above. Figure 3.7 shows an example of the sandy clay soil texture class with the three concerned soil physical properties highlighted (porosity is referred to as saturation in the SPAW model software). Table 3.5 lists the three soil physical parameters of the 7 soil texture classes translated from the original 17 soil types identified in the soil map by Lang (1967).

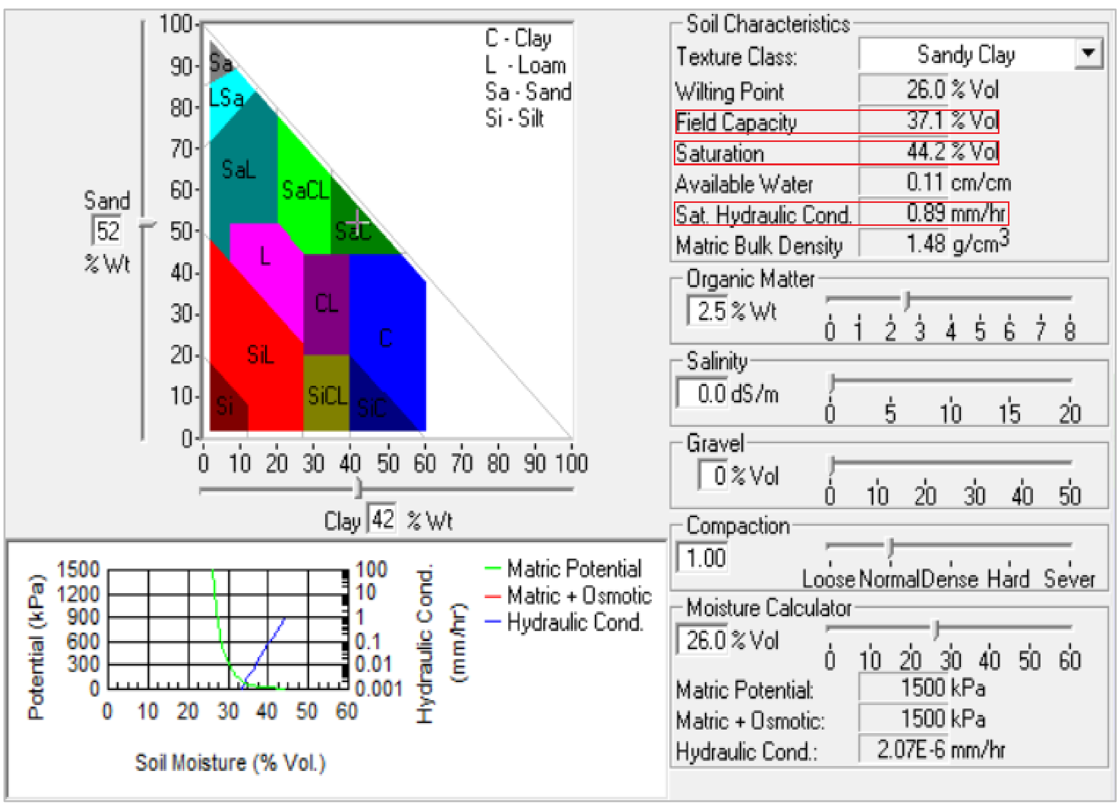

Figure 3.7: *Relevant soil physical parameters (field capacity, porosity and saturated hydraulic conductivity) of the sandy clay soil texture class automatically calculated in the SPAW model software.*

Table 3.5: *Soil texture classes and corresponding soil physical parameters.*

Soil Texture Class	Ksat (mm/h)	Porosity (% Vol)	Field Capacity (% Vol)
Clay	0.78	48.8	42.0
Clay Loam	4.56	47.2	35.0
Loamy Sand	91.26	45.7	12.1
Sand	114.05	46.3	9.4
Sandy Clay Loam	7.84	43.2	28.3
Sandy Loam	50.34	45.0	17.9
Urban	15	0.2	0.3

In addition to the three soil physical parameters determined by soil texture class, there are two other soil property maps required by the LISEM. One is a map showing wetting-front matric suction, which is a necessary parameter in the Green-Ampt (GA) infiltration model (the infiltration model used in this study). The GA infiltration model was used because soil physical parameters are assumed vertically homogeneous for the lack of detailed data in Dominica, which aligns with the assumption in the GA infiltration model that there is a clear wetting front, above which the soil is saturated (Kale & Sahoo, 2011). Wetting-front matric suction is calculated with uniform initial soil moisture at 85% of porosity, which is a typical value for the wet season when most extreme rainfall events occur in the Caribbean region. The equation adopted from Jetten (2016) for matric suction calculation is:

$$psi = a\ \theta^{-b} \qquad (2)$$

where

$b = (ln\,1500 - ln\,33)/(ln(\theta fc) - ln(\theta wp))$

$a = exp\ (ln(33) + b\ ln(\theta fc))$

1500 and 33 = matric suction for wilting point and field capacity, respectively (kPa)

The other soil property map is soil depth derived from terrain slope, relative distance to the closest river channel, and relative distance to the coastline. The equation adopted from Jetten (2016) for soil depth (in m) calculation is:

$$Soil\ depth = a((1 - S) - bD_{river} + cD_{sea}{}^{d})^{e} \qquad (3)$$

where

$S = terrain\ slope\ (bounded\ 0 - 1)$

$D_{river} = relative\ distance\ to\ the\ river\ network$

$D_{sea} = relative\ distance\ to\ the\ sea$

Scaling parameters: $a = e = 1.5, b = c = 0.5, d = 0.1$

The rationale is that soil depth tends to increase as distance to river channels increases or terrain slope and the distance to the sea decrease (Kuriakose et al., 2009). As mentioned in Section 3.3.1.2, soil depth was used as an approximation of river depth, because rivers were observed to had eroded to the rock bed (Jetten, 2016). All the input maps for soil-related properties are presented in Appendix B.3.

3.3.1.4 Buildings and Roads

In addition to the abovementioned catchment physiographic characteristics, man-made structures also affect flash flooding generation. Artificial hard surfaces can cause extra interception and obstruct infiltration and surface flow. Two input maps describing the infrastructures in Dominica were included in the flash flood modelling of this study. One is a building density map created from the building footprint layer previously used for MSA in the first part of this study. In LISEM, building density is presented as the fraction of a grid cell covered by building footprints. The other input layer is related to the road network in Dominica and was created from the road network vector dataset provided by CHARIM. The road segments in the original road network dataset are classified into three types according to road width: main highway (10 m wide), primary roads (6 m wide), and secondary roads (4 m wide). The vector dataset was converted to a raster dataset showing the width of the road segments. According to visual interpretation of the road segments against satellite images, all road segments in the dataset are paved, so they were considered impermeable in the modelling process. Thus, roads obstruct surface flow with a higher

Manning's *n* value for greater flow resistance (automatically applied in LISEM). The two infrastructure-related input maps are presented in Appendix B.4.

3.3.1.5 Hydrological Parameters Related to Land Cover

Another group of input maps is related to land cover. The original forest and land cover map provided by CHARIM was produced using Landsat and SPOT images between 1996 and 1999 (USGS, 2006). The whole island is classified into 18 land cover types, from which hydrological parameters affecting soil surface structure can be interpreted. The original 18 land cover types were reclassified into ten new land cover types to simplify the modelling process. Although some original land cover types were merged after reclassification (e.g., coastal evergreen forest and semi deciduous evergreen forest were grouped into the evergreen forest class), the reclassified land cover types are detailed enough in terms of hydrological characteristics for event-based flash flood modelling (Jetten, 2016). From the reclassified land cover map, three input maps were derived: micro surface roughness (in cm), surface flow resistance (also presented in Manning's *n*), and vegetation canopy cover. Micro surface roughness is the standard deviation of surface heights at the microscale. It is used to calculate the storage of micro ponds, whose overflow cause surface runoff at the macro scale (Jetten, 2018). Vegetation canopy cover is defined as the fraction of a cell covered by plants. It was used to calculate leaf area index (LAI) with the following equation adopted from Jetten (2018):

$$LAI = \frac{ln(1-Cover)}{-0.4} \tag{4}$$

where

$Cover = fraction\ of\ a\ grid\ cell\ cover\ by\ plants\ (in\ percentage\ area)$

LAI is a significant parameter to simulate the partition between the canopy and ground surface (Pribulick et al., 2016). In LISEM, LAI is used to calculate the maximum amount of precipitation that a plant canopy can store. All land cover-related input maps are presented in Appendix B.5.

3.3.2 Model Setup

The version of the LISEM used in this study was 6.62 beta (05.03.2021). There are few options in LISEM for surface flow simulation. This study used the option that combines 1D kinematic wave and 2D dynamic wave. Both overland flow and channel flow were simulated as 1D kinematic wave (using local drainage direction only), while the overbank flow was simulated as 2D dynamic wave (using DEM) and was calculated with the full Saint-Venant equations. This combination of 1D kinematic wave and 2D dynamic wave emphasizes flooding generated from the overflowing of rivers rather than regular surface runoff, because fluvial flooding is more common during heavy rainfall as rivers, stream and other channels tend to overflow their banks (Dominica News Online, 2022). Detailed explanations for the water balance equations for 1D kinematic wave and 2D dynamic shallow water flow simulation can be found in Jetten (2018). The extra options for simulating interception and infiltration were set as default because no relevant datasets were available to optimize these options. All LISEM run options are shown in Appendix B.6.

3.3.3 Calculating Exposed MS in Buildings in Dominica

After flood inundation areas are identified in the flood model, the next step is to quantify the amount of material stocks in buildings exposed to flash flooding. Output flood inundation areas of LISEM are stored as raster datasets. These raster datasets were converted to polygon shapefiles and imported into ArcGIS for further overlay analysis. Quantify the amount of exposed building MS and identifying buildings affected by the simulated flood events are necessary. An individual building footprint was used as the basic unit to investigate the exposure of buildings to simulated flash flooding events. As a result, this study assumed that a building was either not affected at all or affected as a whole. A building footprint is considered exposed to potential flash flooding events if it intersects any flooded areas in the polygon shapefile converted from the flood extent raster dataset from the LISEM.

3.4 Methodology for Household-level Vulnerability Assessment

In addition to hazard exposure, vulnerability is another element of hazard risk. Hazard exposure approaches the concept of hazard risk from a physical perspective and refers to the coincidence of lives or properties and the locations involved in physical hazards events (Kron, 2002), while vulnerability reflects the social part of hazard risk and is defined as the degree to which lives and properties can be impacted (Cutter et al., 2008).

The first two parts of the methodological framework presented in Figure 3.1 aim collectively to reveal clusters of exposed MS in buildings in Dominica. Following these two parts, the third part of the methodological framework aims to investigate the vulnerability aspect of hazard risk. This part of the research is mainly based on the Social Vulnerability Index (SoVI) approach initially developed for the United States by Cutter et al. (2003), except that the socioeconomic variables have to be collected at the household level as primary data, because census data is aggregated to the parish level or the nation level in Dominica to protect the household-level confidentiality (Central Statistics Office of Dominica, 2011; Flowerdew, 2011). As is shown in Figure 3.1, the vulnerability assessment part of this research has three major steps. Accordingly, the rest of this subsection will discuss the methodologies for the selection of commonly used variables for social factors of vulnerability, the design of a household survey to collect primary data, and the combination of these variables to calculate a composite vulnerability score for each household exposed to the simulated flooding events.

3.4.1 Selection of Socioeconomic Variables

3.4.1.1 Initial Selection of Socioeconomic Variables

This research adapts the SoVI methodology for the quantification of household-level vulnerability to environmental hazards. The SoVI methodology derives socioeconomic indicators from census variables, and these socioeconomic indicators are independent from each other and can be further combined into a summary score indicating general vulnerability to environmental hazards (Cutter, Boruff & Shirley, 2003). Since disaggregated and georeferenced census data of small island states in the Caribbean is usually not available to the public (Cumberbatch et al., 2020), the first step is collecting relevant variables from the literature and tailoring these variables so that they can be specifically applied at the household level in Dominica.

The SoVI research by Cutter, Boruff & Shirley (2003) served as a starting point for the selection of variables related to social factors contributing to vulnerability to environmental hazards. The original 42 census variables in the SoVI research were expanded by searching the adaptations or variants of the SoVI methodology in other contexts. Three digital databases were used for the search: University of Waterloo Library, Wilfrid Laurier University Library, University of Guelph Library and Google Scholar. The keywords for the search were: SoVI, environmental hazard, social vulnerability, Caribbean and flood. Based on the search results, six previous studies were identified, with three focusing on small island states in the Caribbean region (Boruff & Cutter, 2007; Cumberbatch et al., 2020; St. Bernard, 2007) and the other three focusing on China (Chen et al., 2013), Zimbabwe (Mavhura, Manyena & Collins, 2017) and the United States (Flanagan et al., 2011), respectively. Appendix C.1 lists the 57 variables extracted from the aforementioned studies, and these variables were grouped into 18 categories reflecting different concepts of vulnerability such as socioeconomic status, gender, occupation, and so on.

3.4.1.2 Adaptation of the Selected Variables to a New Context

Adaptation of indicators for vulnerability to environmental hazards are crucial because vulnerability heavily depends on geographical and cultural backgrounds (Brooks, Adger & Kelly, 2005). Therefore, the relevant variables collected from literature must be contextualized before they are mapped to the associated questions to be included in the survey. Following the guideline by Holand & Lujala (2013), this research adopted three types of variable accommodation: conceptual accommodation, technical accommodation, and geographic accommodation.

Conceptual accommodation responds to the question *Does the vulnerability concept captured by a variable apply for the new context?* If the answer is negative, modifications are necessary to correct the disparities in vulnerability concepts between the original and the new setting (Holand & Lujala, 2013). As a result, some variables identified in literature were omitted from the final collection because they are not typical in the new context. For example, mobile homes are relatively common in North America, but in Dominica there is a lack of records of this type of residence. For the variables whose associated vulnerability concepts are valid in the new context, minor revisions regarding the counterparts in the new context were still required. One example is the variables for the percentages of non-white and non-Anglo population, which reflect the race and ethnicity aspect of vulnerability in the original SoVI research as ethnic minorities are likely to encounter cultural and language barriers that hinder their access to post-hazard funding (Cutter, Boruff & Shirley, 2003). In this research, these variables were adapted by switching to the existence of Amerindian, White, East Indian, Chinese, Syrians and Lebanese population, because 84.8% of Dominica’s total population are Afro-Caribbean descent (Central Statistics Office of Dominica, 2011).

Technical accommodation and geographical accommodation are respectively the second and the third step for variables adaptation if the vulnerability concepts reflected by the variables do apply for the new setting. Technical accommodation examines data availability and responds to the question *Is census data that is required to construct relevant variables collected or available to the public?* Geographic accommodation builds on the previous two questions and responds to the question *If the vulnerability concepts apply for the new context and data is available to the public*, *is the data shared at the appropriate scale?* Viewing these two questions collectively, the answer is simply negative in the context of this research, because census data is aggregated to the parish level before dissemination in Dominica to maintain confidentiality (Central Statistics Office of Dominica, 2011; Flowerdew, 2011). However, since this research attempted to design a household-level survey instrument to collect primary data, both technical accommodation and geographical accommodation are an inherent part of the methodology workflow. Variables adapted to the context of Dominica through the aforementioned three types of accommodations are listed in Table 3.6, along with the rationale behind these variables and whether a variable increases or decrease household-level vulnerability to environmental hazards. How these adapted variables were mapped to associated questions in the designed household survey will be described in Section 3.4.2.

Table 3.6: *Variables of household-level vulnerability adapted to the context of Dominica.*

Concept of Vulnerability	**Variable Name**	**Rationale**	**+/-**[1]
Age	*Percentage of family members aged below five*	Both sides of the age spectrum result in limited mobility for evacuation (Cutter et al., 2000), and burden of care in hazard aftermath (Morrow, 1999).	+
	Percentage of family members aged above 65		+
Education	*Percentage of family members 18 years or older with a high school diploma*	A higher level of education results in a better understanding of hazard warning and recovery information (Center & John, 2000; Tierney, 2006), and a better chance to survive hazard events (Frankenberg et al., 2013). Access to hazard information may also be facilitated by a higher computer literacy rate (St. Bernard, 2007).	-
	Percentage of family members 18 years or older with exposure to tertiary level education		-
	Percentage of family members 15 years or		-

	older with computer literacy		
Socioeconomic Status	*Per capita income*	Income level is usually the best indicator for the ability to absorb losses due to hazard events through insurance and other means (Chen et al., 2013; Cutter et al., 2000).	-
	Percentage of unemployed family members		+
Residential Property	*Monetary value of owner-occupied housing*	The value of housing affects potential losses and houses that are more expensive are usually more costly to repair (Center & John, 2000; Cutter et al., 2000).	+
	Number of vehicles per family member	Transportation out of evacuation zones is problematic for household without a vehicle (Flanagan et al, 2011; Morrow, 1999).	-
Renters	*Monetary value of renter-occupied housing*	Renters often lack financial resources to own a house, and sometimes have limited shelter options if temporary lodging is too expensive (Morrow, 1999).	+
Gender	*Percentage of female family members 18 years or older*	Women is recognized as a social group with higher levels of vulnerability due to family care responsibilities, traditional gender roles and gender discrimination (Forhergill, 1996).	+
Family Structure	*Total number of family members (sleeping at least four days per week)*	Households with more family members are overcrowded, thus encounter difficulties during evacuation (Tierney, 2006). Single-parent families are usually dependent on social resources and have more stress taking care of the dependents (Cutter et al., 2003).	+
	Ratio of parents to children (under 18 years old)		-

	Ratio of family members to the number of bedrooms		+
Special Needs	*Percentage of family members with a disability*	People with disabilities are disproportionately affected and more likely to require transportation, medical care or assistance with their daily activities during and after hazard events (Cutter et al., 2003; Flanagan et al, 2011; Morrow, 1999)	+
Isolated Household	*Percentage of family members who are not ethnic majorities*	Ethnic minorities are more likely to encounter language and cultural barriers that makes them unfamiliar to the region and makes it difficult for them to assess post-disaster funding (Chen et al., 2013; Cutter et al., 2014; Morrow, 1999).	+
	Percentage of family members five years or older and whose first language is not English		+

[1]Positive (+) means increased vulnerability; negative (-) means decreased vulnerability.

3.4.2 Design and Implementation of a Resident Survey Instrument to Assess Household-level Vulnerability

Questionnaire surveys are commonly used tools in human geography when primary data about people, their attitudes and behavior is required. Based on the 17 variables (listed in Table 3.6) adapted for Dominica, a resident survey was developed to collect the information about household-level vulnerability to environmental hazards. Appendix C.2 shows the resident survey consisting of 16 questions developed with reference to the general guidelines for quantitative survey design (Bryman & Bell, 2019; Flowerdew & Martin, 2005).

3.4.2.1 The Development of Survey Questions

The 17 variables listed in Table 3.6 are the experimental or independent variables which are possibly the predictors of vulnerability to environmental hazards (Flowerdew & Martin, 2005).

In addition, all the 17 variables are used to measure the characteristics of the households themselves (e.g., per capita income and number of vehicles), rather than people's behaviour and attitudes, which are more difficult to elicit due to their complexities and susceptibility to the quality the survey design (Rattray & Jones, 2007). Moreover, all the properties measured by the 17 variables are interval or ratio in nature, which makes them more appropriate to be elicit from closed questions (Bird, 2009). Closed questions are presented with a set of fixed alternatives, and with the extra clarification provided by the available answers, respondents can understand a question better, which promotes standardization in both how the questions are asked and how the answers are recorded (Bryman & Bell, 2019).

Most questions in the resident survey are presented in an explicit manner asking the exact numerical values required to populate the adapted variables. However, to maintain a decent level of confidentiality for two variables reflecting sensitive information, namely *Per capita income* and *Monetary value of owner-occupied housing*, multiple mutually-exclusive categories were created and listed with letter labels (e.g., A. EC$0 to EC$1000, B. EC$1001 to EC$2000). Although categorical values are not as precise as interval values, this type of question is still preferable to the lack of response if participants directly refuse to answer the question (Flowerdew & Martin, 2005).

3.4.2.2 Sampling and Piloting of the Resident Survey

To maintain statistical reliability of the results collected from the resident survey, usually at least thirty respondents are required by most statistical tests (Bryman & Bell, 2019), while there is always a trade-off between decreasing sample size to save time or costs and increasing sampling bias (Flowerdew & Martin, 2005). As is shown in Figure 3.1, a sampling procedure is inherent in the methodological framework, in which high concentrations of exposed MS to the simulated flooding events are potential samples for vulnerability. The rational is that small island states with limited natural and economical resources need to pinpoint the households with both high exposure and vulnerability to lower the overall loss due to potential hazard events in a more cost-effective manner. In this research, it was decided that recruitment would be focused on the town of Portsmouth as it was a cluster of exposed MS in buildings identified via flood modelling (shown in Figure 4.10). A total number of 346 residential buildings exposed to the 20-year flood scenario were selected as a sample.

With the identified sample, the resident survey would be conducted on a door-to-door base via physical copies of the questionnaire during fieldwork. The author (also the interviewer) would distribute the printed questionnaires, explain its purpose, and inform the potential participants of a draw in appreciation of the time given for a higher response rate. The questionnaire is self-explanatory and can be completed without the assistance of the interviewer, so the finished questionnaires would be collected three days after the distribution by revisiting the households.

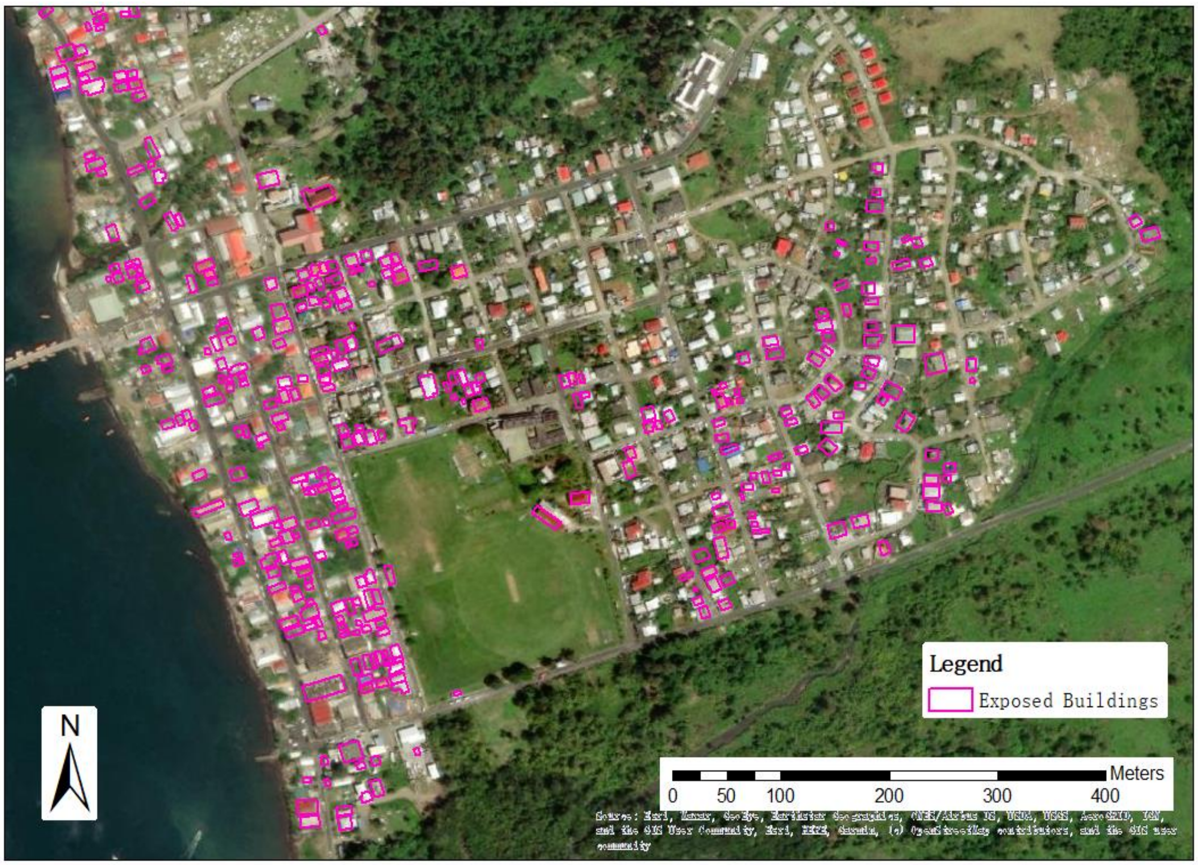

Figure 3.8: *Exposed buildings in the city of Portsmouth as a sample for the resident survey.*

3.4.2.3 Data Analysis for Information Collected from the Resident Survey

Data analysis methods should be carefully considered during the aftermath of a fieldwork, as they are critical for the elicitation of new insight and information (Flowerdew & Martin, 2005). Following the methodology adapted from the original SoVI research by Cutter, Boruff & Shirley (2003), this research would apply a principal components analysis (PCA) to derive a composite vulnerability score for each household participating the resident survey. PCA is a multivariate statistical method for data reduction by combining variables into mutually-exclusive dimensions, or principal components, which account for a sufficient amount of the variance in the original input variables (Chu, Tan & Mortsch, 2021; Cutter, Boruff & Shirley, 2003). In this research, the aim of applying a PCA is to identify a few uncorrelated indicators that can explain the majority of be variance among all surveyed households and can be further combined into a summary vulnerability score.

Data normalization is a necessary step before performing a PCA to ensure all input features are in the same scale, because in a PCA higher numerical values are considered to be of higher significance, which would result in biased outputs (Dutt, 2021). In this research, most variables are fundamentally percentages which range from 0 to 1, but for interval variables, the following equation can be used to standardize the values:

$$z_i = \frac{x_i - \min(x)}{\max(x) - \min(x)} \tag{5}$$

With the inputs of all the 17 variables, a PCA generates 17 principal components (PCs) via linear commination of the original variable, and each new variable is assigned an eigenvalue representing the proportion of variance it can capture (Oulahen et al., 2015). This research follows the methodology by Cutter, Boruff & Shirley (2003) and select PCs with an eigenvalue greater than 1.0 as the vulnerability factors, which can be further combined into a composite vulnerability score for each household using the following equation:

$$SoVI\ Adapted = \pm F1 \pm F2 \pm \cdots \pm Fn \tag{6}$$

where *Fi* represents the PCs and the sign before each PC is determined by its composition of the original 17 variables and whether they are negatively (decreases) or positively (increases) household vulnerability, as indicated in Table 3.6. For example, if the majority of the original variables consisted in a PC increases household vulnerability to environmental hazards, the sign of that PC would be adjusted to positive and vice versa (Chu, Tan & Mortsch, 2021; Cutter, Boruff & Shirley, 2003). Based on the methodology described above, the resulting adapted SoVI values indicates household-level vulnerability and a larger value means more susceptible to the impacts of environmental hazards.

4 Results

4.1 Results of Material Stock Accounting for Dominica's Buildings

This subsection presents the results of material stock accounting for buildings in Dominica using the methodology described in Section 3.2. First, the basic statistics of the building heights derived from aerial videos are examined. Following the determination of building heights, the calculated material stocks in buildings in 2020 are presented by material category and building use-type. Finally, the spatial distribution of estimated material stocks in buildings is examined to identify clusters of material stocks in buildings in Dominica.

4.1.1 Estimation of Building Heights in Dominica by Building Use-type

This subsection presents the results of the building height acquisition methodology described in Section 3.2.3. The total number of buildings in Dominica covered by the aerial videos available online is 12,430 (about 37% of the total number of buildings on the whole island). In this research, the height a building is presented in the term of the number of floor levels it has. The average height of these 12,430 buildings is 1.18 floor levels. The heights of all the buildings captured by the aerial videos range from 1 floor level to 6 floor levels (e.g., the financial centre of the government).

To further examine the building heights collected from the aerial videos, Table 4.1 shows the basic statistics of these building heights by building use-type. Some building heights are fractions, and a building with 1.5 or 2.5 floor levels is built with a partial top floor to accommodate for more space (an example is shown in Figure A.2). All building use-types share the same minimum floor level of one, but the maximum floor level varies across different building use-types. The highest value of maximum floor level is identified in the institution use-type at six, and the lowest value is observed in the transportation use-type at 1.5. The mean floor level for all building use-types are below two storeys, and the mean building height also varies cross different building use-types. Commercial/industrial buildings have the largest average building height at 1.6 floor levels, followed by cultural buildings (1.5 floor levels), institutional and tourism buildings (1.4 floor levels), residential buildings (1.2 floor levels), and transportation buildings (1.1 floor levels). These values also demonstrate that no significant positive correlation is found between the maximum building height and the mean building height. For example, the commercial/industrial building use-type has the largest mean building height at 1.6 floor levels, while its maximum building height is smaller than that of the residential building use-type with a lower mean building height at 1.2 floor levels.

For the amount of variation of building heights collected from the aerial videos of each building use-type, the lowest standard deviation is identified in the transportational use-type, which could be due to the limited number of samples as there are only 24 buildings of the transportational use-type. The same explanation can be applied to the cultural use type with the highest standard deviation but also a limited number of samples (28 buildings). The residential use-type has the second-lowest standard deviation, with the largest number of samples (11,512 buildings). This reflects the finding during the process of visual interpretation from the aerial videos that most residential buildings in Dominica are single-storey dwellings.

Table 4.1: *Basic statistics of sampled buildings with an actual number of floors.*

Building Use-type	Number of Buildings	Minimum Floor Level	Mean Floor Level	Maximum Floor Level	Standard Deviation
Institutional	181	1	1.4	6	0.656
Commercial/Industrial	422	1	1.6	4	0.600
Residential	11,512	1	1.2	5	0.392
Tourism	263	1	1.4	5	0.707
Cultural	28	1	1.5	3	0.780
Transportational	24	1	1.1	1.5	0.165

The pie charts in Figure 4.1 show the overall shares of building samples with different floor levels compared to those in Grenada collected from a fieldwork by De Kroon (2020). The pie charts indicate a higher percentage of one-storey buildings in Dominica (83.35%) than that in Grenada (50%). As a result, the total shares of two- and three-storey buildings in Dominica is relatively small at 15% and 0.88%, respectively. Given the two island states' similar historical and cultural backgrounds, there is a potential overestimation of the number of one-storey buildings in Dominica, though in De Kroon (2020) only 703 buildings were sampled in six communities across Grenada, while 12,430 buildings were sampled across the whole island of Dominica in this research.

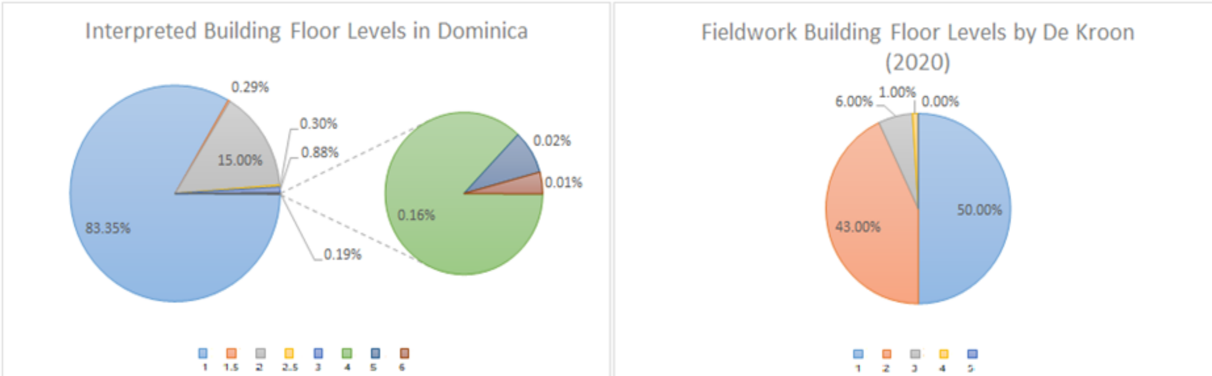

Figure 4.1: *Pie charts of buildings floor levels in Dominica compared to building floor levels in Grenada collected from fieldwork by De Kroon (2020).*

4.1.2 Material Stocks in Buildings by Material Category

Total material stocks in buildings of Dominica in 2020 was estimated at 6,574 kt. Given Dominica's population in 2020, the per capita material stocks in buildings was 91 t/cap. Figure 4.2 shows the percentage shares of the four material categories investigated in this study. Concrete accounts for the largest share of total MS in buildings at 85.66%, followed by aggregate (7.62%), timber (3.74%), and steel (2.97%). This reveals the dominance of buildings with a concrete structure in Dominica.

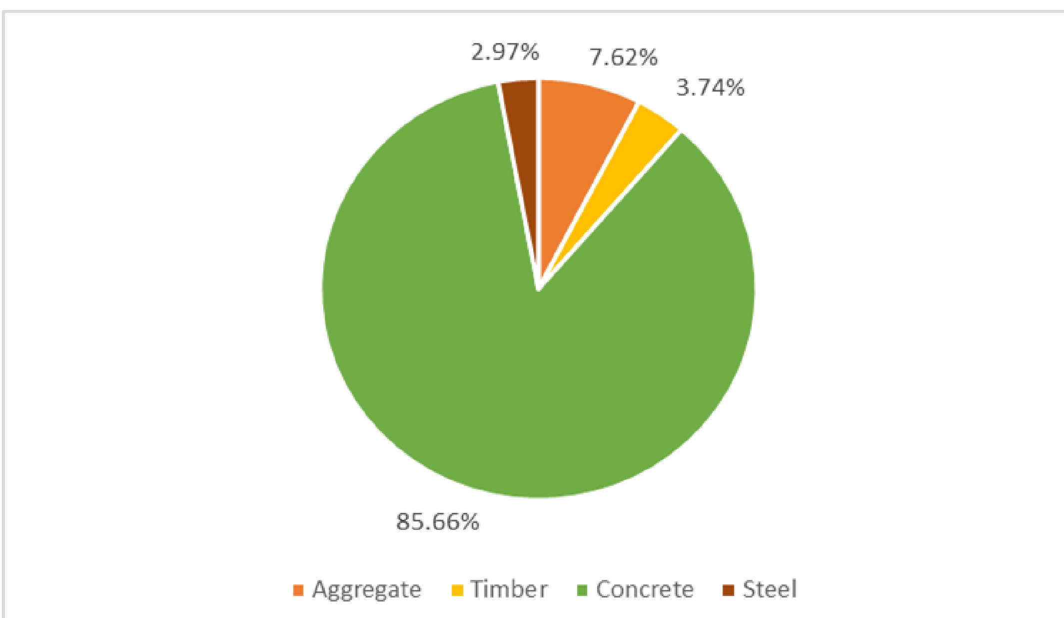

Figure 4.2: *Total share (in %) of material stocks in buildings of Dominica by material category.*

4.1.3 Material Stocks in Buildings by Building Use-type

Figure 4.3 shows the distribution of material stocks by different building use types. The X-axis presents the percentage share of each building use type to the total number of buildings in Dominica following the building use type names. The blue columns present the percentage shares of the building MS contained in different building use-types. The orange line shows the ratio of the proportion of MS contributed by each building use-type to its share of the total number of buildings in Dominica, reflecting the overall material intensity of each building use type. In 2020, MS in buildings of Dominica was dominated by the residential building use-type at 75.93%, followed by industrial/commercial buildings at 11.1%, institutional buildings at 7.23%, tourism buildings at 4.79%, and cultural and transportation buildings contributing to less than 1%. Moreover, no apparent positive correlation is identified between the number of buildings of each use type and its overall material intensity. On the contrary, building use-types with more footprints tend to have lower overall material intensity. For example, residential buildings have the lowest MS-to-footprint number ratio, while they occupy the largest share of total MS.

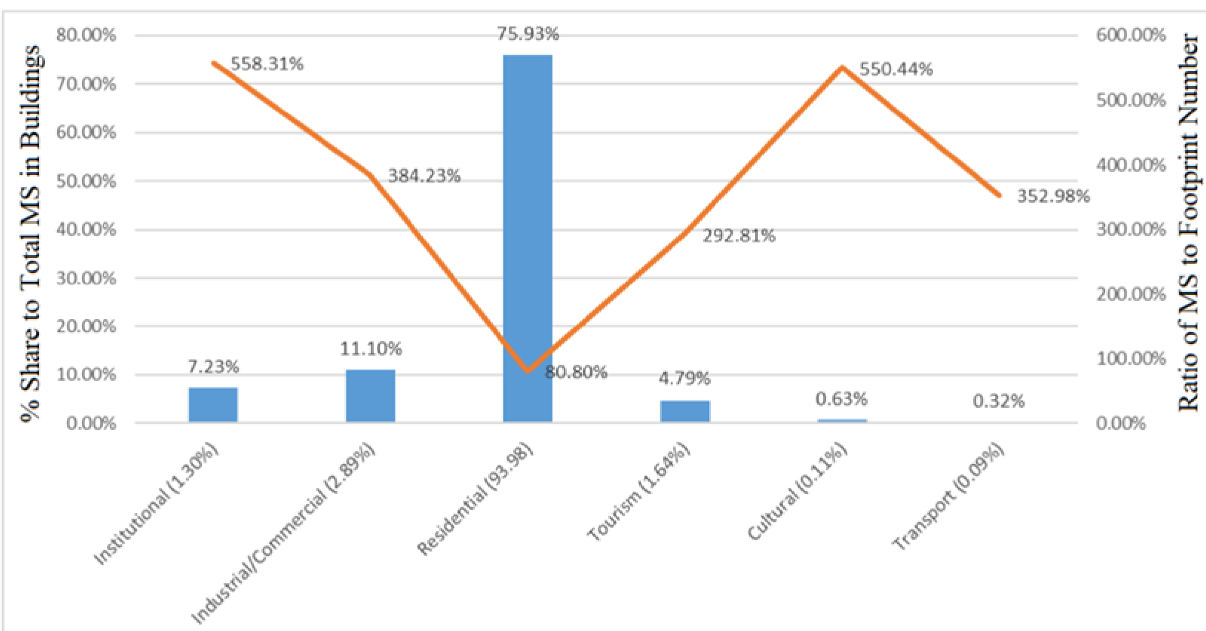

Figure 4.3: *Material stocks in buildings by building use-type with overall material intensity.*

The absolute values of MS in different building use-types by material category are presented in Table 4.2 regarding per capita values. It can be found that for all the four material categories, the residential building use-type is the largest sink. In Figure 4.4, MS in buildings are broken down by material category for each building use type. For all building use-types, concrete has the largest share (above 80%), reflecting the dominance of concrete structure buildings in Dominica. Moreover, for all building use-types, aggregate accounts for the second-largest percentage share of MS in buildings at around 10%. The largest share of timber is observed in the residential use-type at 4.38%. For steel, the cultural building use-type is identified as the most steel-intensive building use-type. Not much difference is observed in the composition of material category among building use-types since concrete dominates the percentage share of total MS in buildings. The percentage shares of the four material categories in all building use-types are similar to the aggregated results shown in Figure 4.2, which means construction types are equally shared across different building use-types in Dominica. Except for the residential use-type, the percentage share of steel is higher than that of timber, reflecting a steel-intensive for all non-domestic building use-types. However, the opposite is true for the residential use type. Since the residential use-type accounts for 94% of all buildings in Dominica, the percentage share of steel is actually lower than that of timber in the aggregated results shown in Figure 4.2.

Table 4.2: *Per capita material stocks by material category and building use-type.*

Building Use-Type	**Aggregate (t/cap)**	**Timber (t/cap)**	**Concrete (t/cap)**	**Steel (t/cap)**	**Total (t/cap)**
Institutional	0.61	0.15	5.68	0.21	6.66
Commercial/Industrial	0.90	0.22	9.27	0.27	10.65
Residential	5.26	3.24	62.99	1.68	73.17
Tourism	0.36	0.05	3.17	0.22	3.80
Cultural	0.06	0.00	0.42	0.05	0.54
Transportation	0.03	0.00	0.26	0.02	0.31

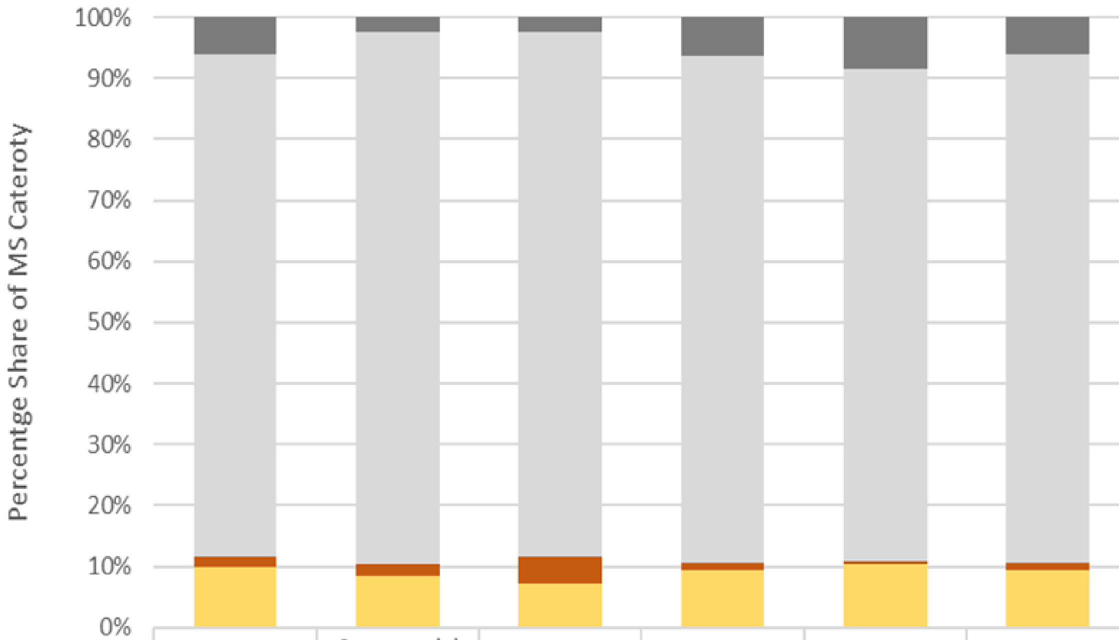

	Institutional	Commercial /Industrial	Residential	Tourism	Cultural	Transport
Steel	6.15%	2.35%	2.49%	6.31%	8.51%	6.13%
Concrete	82.34%	87.17%	85.98%	82.98%	80.56%	83.17%
Timber	1.66%	2.06%	4.38%	1.23%	0.54%	1.26%
Aggregate	9.85%	8.43%	7.14%	9.48%	10.40%	9.43%

Figure 4.4: *Material Stocks broken down by material category (in %) in Dominica for 2020.*

4.1.4 The Spatial Distribution of Material Stocks in Buildings

The spatial distribution of MS in buildings in Dominica is only investigated at the national scale. The methodology described in Section 3.2.4 for material stock accounting assumes that buildings of the same occupancy class share the same material intensity typology, so the individual-building resolution cannot be achieved. Breaking the island into 10,000 m^2 cells, Figure 4.5 shows the distribution of accumulated MS in buildings in Dominica in 2020. The cell size of 100 m corresponds to the average distance between blocks in dense urban areas like the capital city Roseau. Clusters of high MS accumulation are represented by dark yellow and red, while low accumulation is represented by the green colours (colours are classified by the Natural Breaks-Jenks methodology for better variances between classes). The largest cluster of material stocks in buildings is identified in the parish of St. George along the southwestern coast of the island, where the capital city Roseau is located. The second-largest cluster can be seen in the parish of St. John along the northwestern coast, where Portsmouth is located.

Figure 4.6 shows the distribution of building MS at the district level. The district boundaries do not coincide with the parish boundaries, and the relationship between district and parish is unknown. However, district is the smallest geographic unit because the spatial data for census enumeration district is not available. The district-level map confirms that building MS tends to accumulate near the coast rather than in the mountainous interior areas where two protected areas (national parks) are located. The map also conveys that the island's western coast is more material intensive than the eastern coast, showing a radial pattern emerging from the capital city Roseau but blocked by the two protected areas.

The distribution of building MS by building use type is also examined at the district level, as presented in Figure 4.7. Institutional, commercial/industrial, cultural, and residential MS is mainly concentrated near the capital city in St. George at 65.4%, 50.1%, 72.2%, and 34.6%, respectively. A high accumulation of tourism MS (46.3%) is identified along the island's northwestern coast, where Portsmouth, the second-largest city in Dominica, is located. A high concentration of MS in the transportation use type is observed in the northern district where the two airports (Roseau-Canefield Airport and Douglas-Charles Airport) are located.

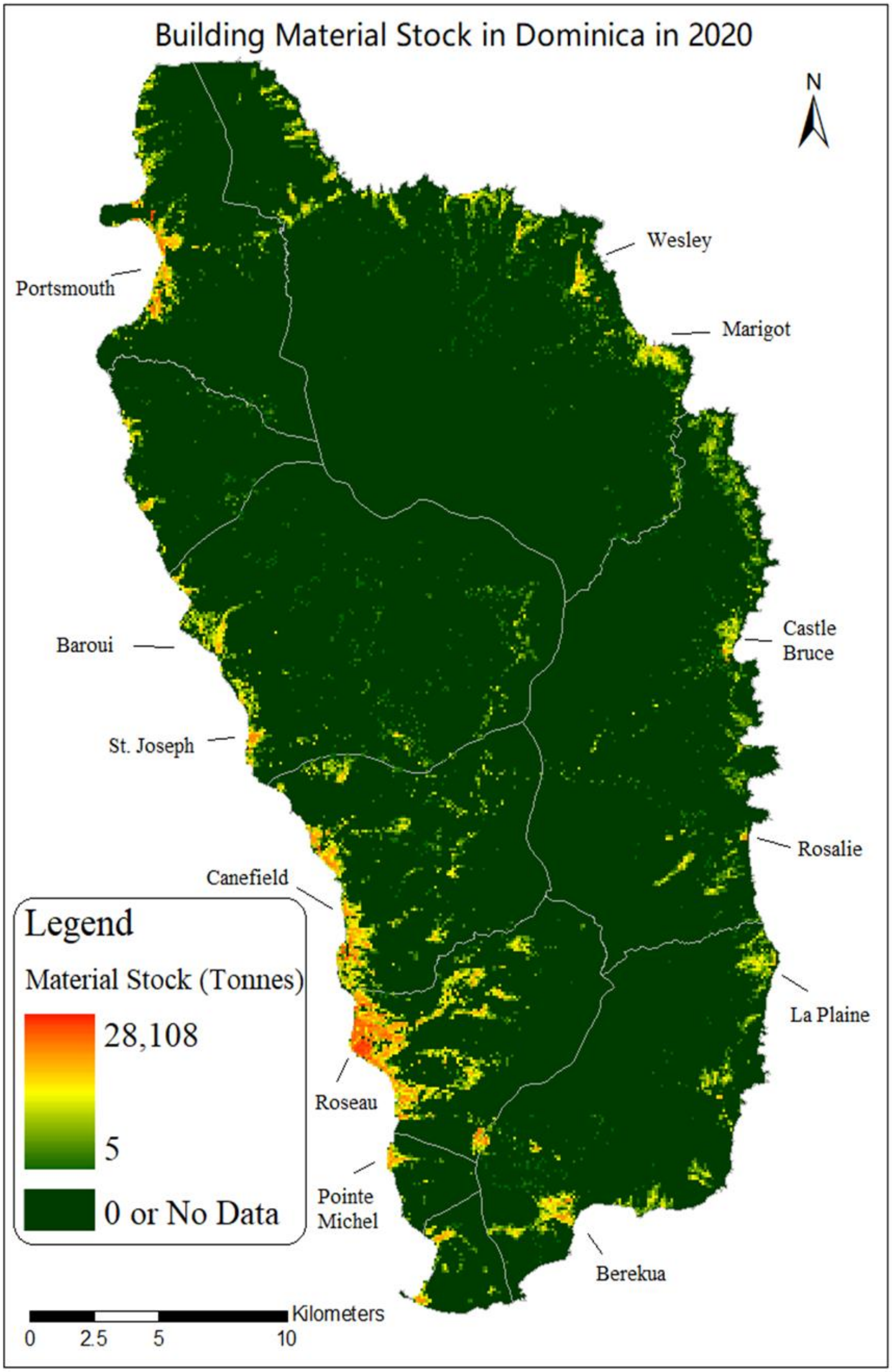

Figure 4.5: *Accumulation of MS in Dominica's buildings in 2020, shown with 10,000 m² cell resolution.*

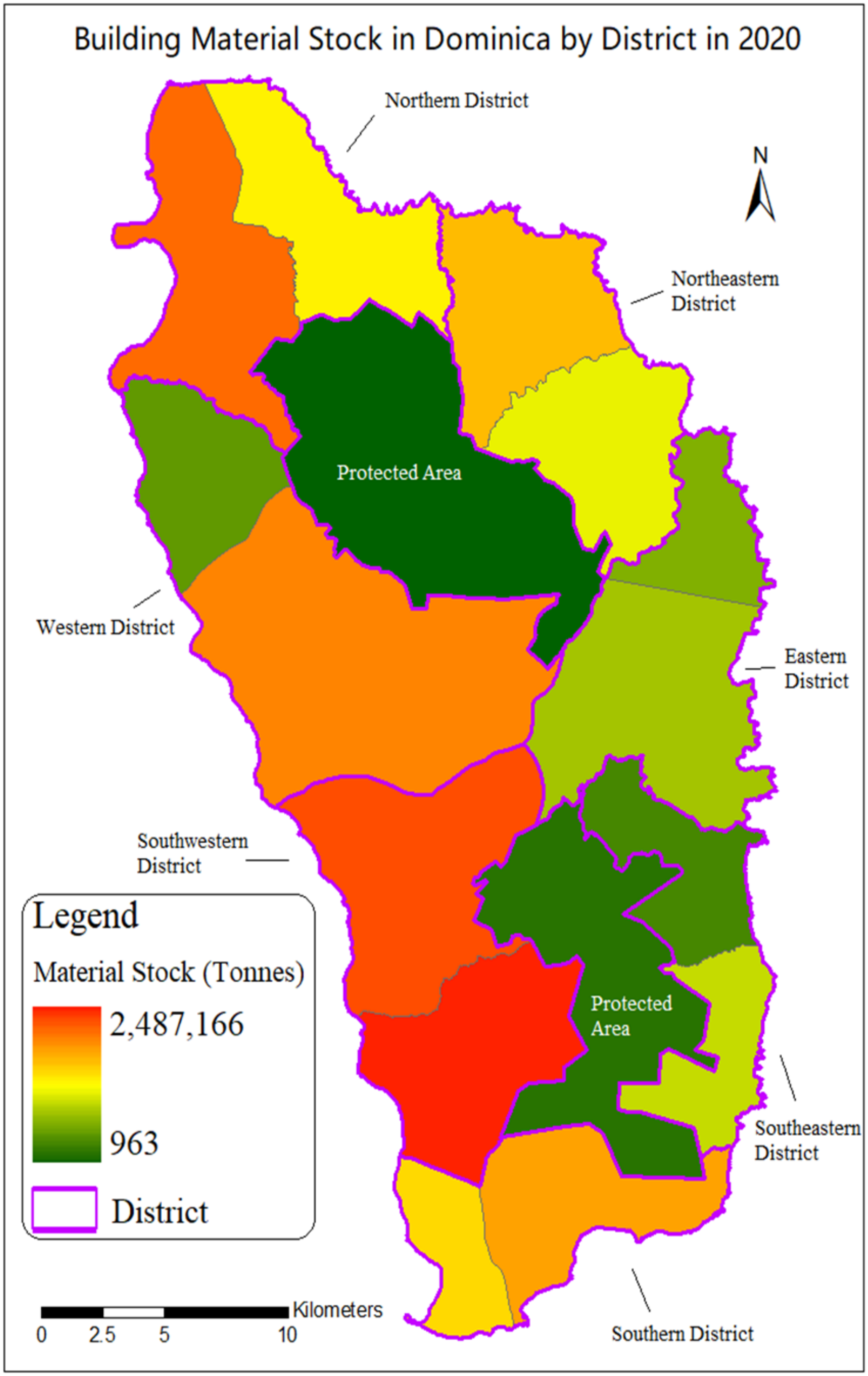

Figure 4.6: *Material Stocks in Dominica's buildings in 2020, by district.*

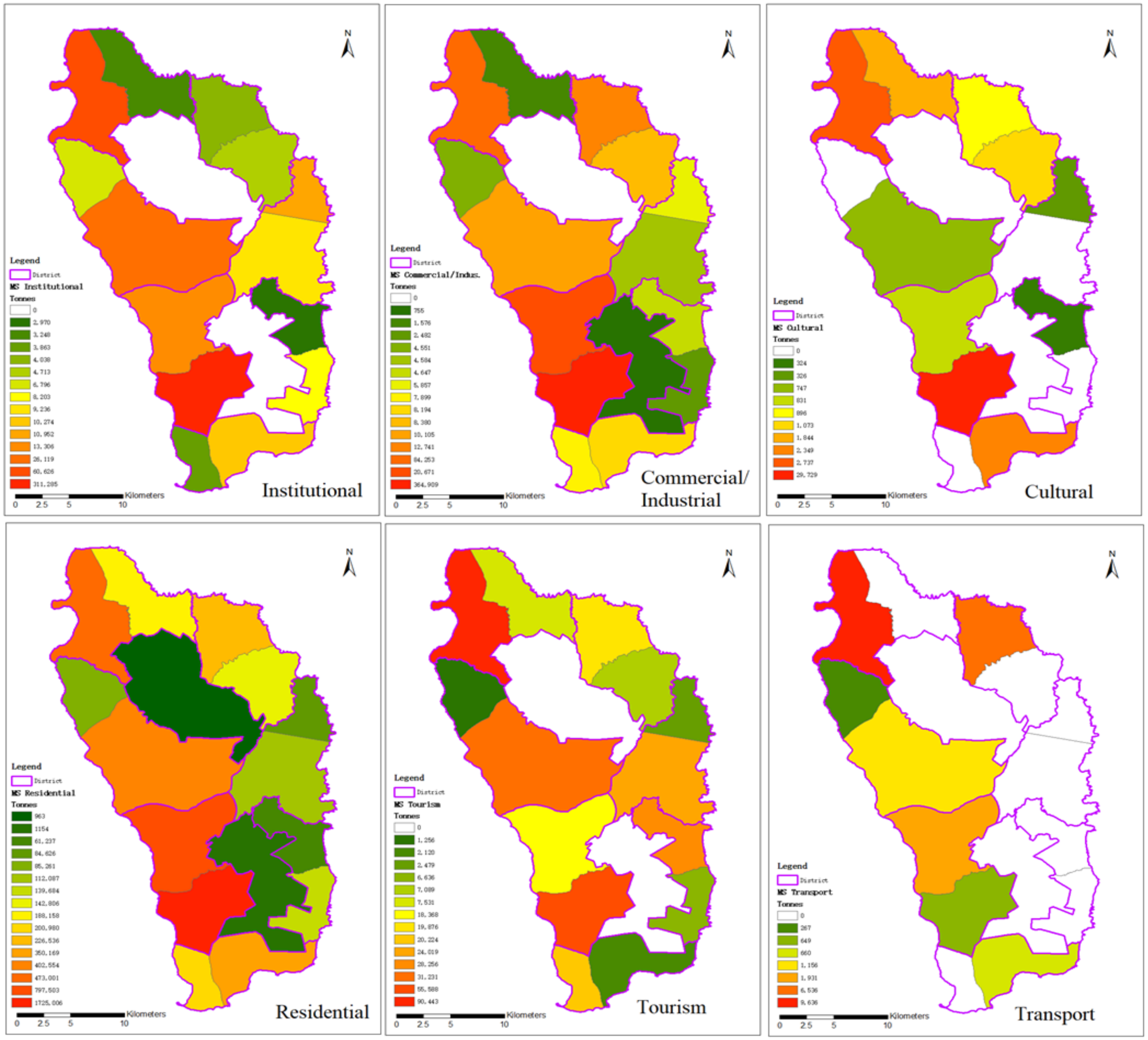

Figure 4.7: *Distribution of material stocks in Dominica's buildings in 2020 by building use-type at the district level.*

4.2 Results of Flood Modelling and Exposure of MS in Dominica's Buildings

The following subsections present the results of flash flood modelling described in Section 3.3. Flood extent is summarized for flash flood hazard events with return periods of 5 years, 10 years, and 20 years. The impact of the simulated flood events on MS in buildings in Dominica is also described, with the quantity and spatial distribution of MS at risk examined at the island scale.

4.2.1 Flood Modelling Results

Significant outputs of flood inundation modelling are flood extent, flood start time, maximum flood height, and flood volume. In this study, only flood extent was used to investigate the exposure of building MS to flash flooding in Dominica. Flood height and flood start time are not accurate enough for flood modelling at the island scale due to relatively low spatial resolution (Jetten, 2016). Flood volume is essential for calibrating a flood model by referencing on-site river discharge records of selected catchment, but it is not discussed in this research for the lack of relevant hydrological data in Dominica.

In this research, flood extent (flooded area) consists of cells with a maximum flood height of over 0.05 m. Flood depth under 0.05 m is considered harmless, according to a discussion with stakeholders in a previous CHARIM project (Jetten, 2016).

Basic statistics of the flood extents of the three designed flash flood events are listed in Table 4.3. The total flooded area for the 5-year, 10-year, and 20-year events are 4.1 km^2, 5 km^2, and 5.7 km^2, respectively. Thus, there is a positive relationship between flood extent and flood magnitude. However, the difference in flood extent is relatively small, as there is only an increase of 20% in flood extent from the 5-year flood event to the 10-years flood event, and a rise of 17% from the 10-year flood event to the 20-year flood event.

Table 4.3: *Flooded area of the flood hazard for three return periods.*

Return Period	Rainfall Depth (mm)	Rainfall Duration (min)	Flood Extent (km^2)
5 years	217	195	4.1
10 years	267	265	5.0
20 years	315	330	5.7

Figure 4.8 shows the spatial distributions of flooded areas (flooded cells are buffered by 20 m for better recognition at the island scale). For all three flood magnitudes, flooded cells

concentrate along the west coast of the island. It is found that the increase in flood extent from flood events of small magnitude to that of larger magnitude is mainly caused by the occurrences of entirely new flooded areas. For example, the 10-year flood extent includes few obvious clusters of flooded cells along the southeastern coast of the island, which are not observed in the 5-year flood extent map. Similar new clusters are identified along the northeastern and eastern coast in the 20-year flood extent map.

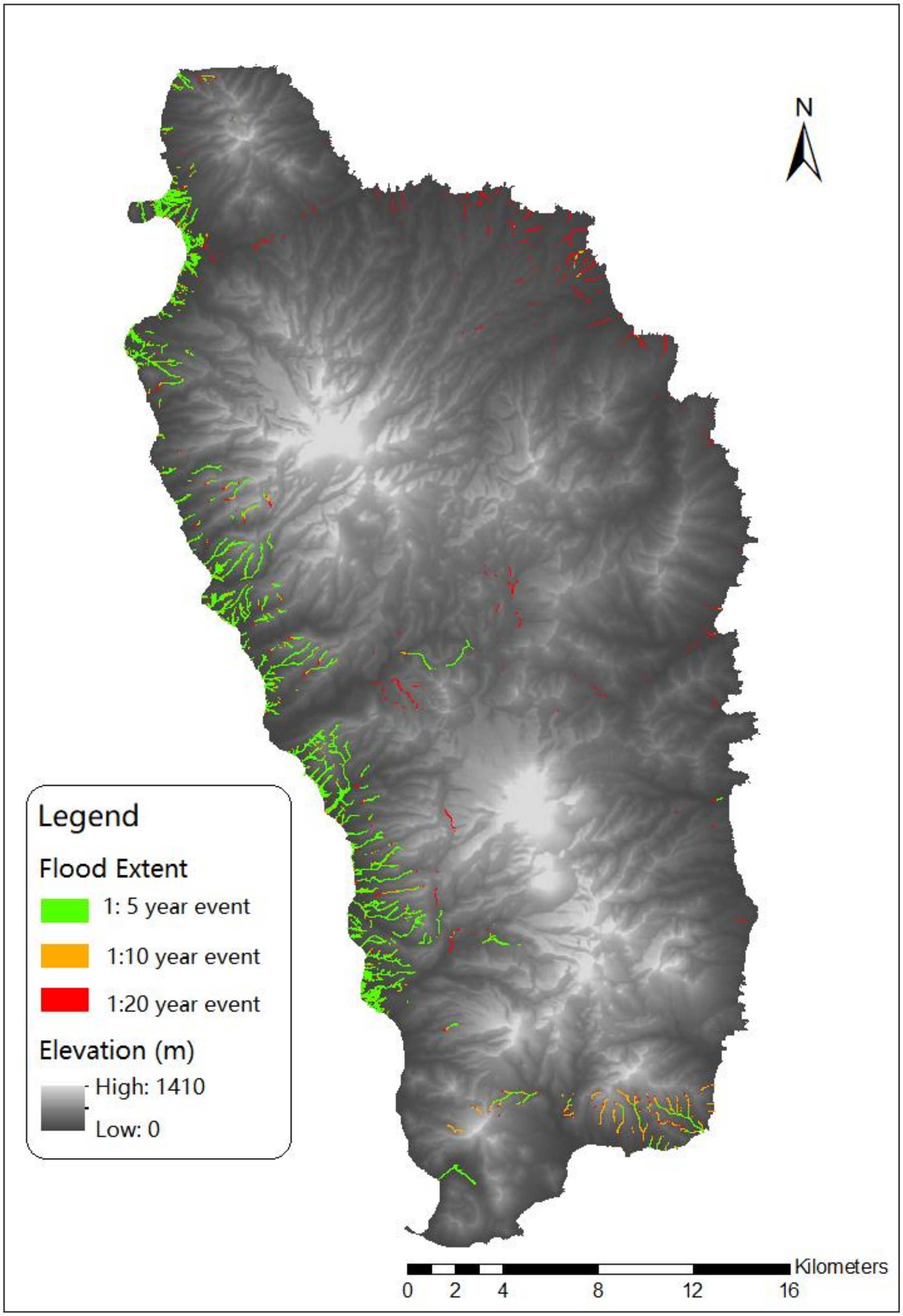

Figure 4.8: *Maps of flood extent for the flood hazard event for three return periods.*

4.2.2 Impact of Flash Flooding on Material Stocks in Dominica Buildings

Previous sections have shown the results of material stock accounting and flash flood modelling separately. Linking the results of material stock accounting, the following subsections describe the impact of the simulated flash flood hazard events on MS in buildings in Dominica. The number of exposed buildings and the quantity of contained MS are shown by considering flood magnitude, building use type, and material category.

4.2.2.1 Total Affected Material Stocks in Buildings in Dominica

Total MS in buildings affected by the design flash flood events with different return periods are shown in Table 4.4. In terms of affected buildings on the island, the 5-year flood event accounts for the least number of exposed building footprints at 2,781, followed by the 10-year flood event and 20-year flood event at 3,030 and 3,274, respectively. When exposed MS is considered, flood events of greater magnitude also result in more exposed MS. However, the differences in exposed MS between the three simulated flood events are small, as there is only an increase of 1% from less extreme events to more extreme events.

Table 4.4: *Summary of total affected buildings by the flash flood hazard event for three return periods.*

Return Period	Number of Buildings Affected	MS Exposed (kt)	% of MS Exposed
5 years	2,781	1,162	17%
10 years	3,030	1,232	18%
20 years	3,274	1,302	19%

The spatial distributions of exposed buildings in the three investigated flood events are presented in Figure 4.9. The spatial pattern of exposed buildings corresponds to the spatial pattern of flooded areas, demonstrating that the most affected buildings are located along the west coast of the island, with some entirely new clusters of affected buildings by 10-year and 20-year flash flood events along the southeastern and southwestern coast. When presented in 10,000 m^2 cells, the affected MS in buildings by the three simulated flood events did not show much difference, so only the map of the 20-year flood event is included (Figure 4.10). Comparing the spatial distribution of exposed buildings and that of contained MS, it is found that there is an overlap between high concentrations of building MS at risk and clusters of buildings exposed to flash flooding.

Following the national-scale distributions of exposed buildings and MS, Figure 4.11 focuses on the local-scale distribution of exposed buildings in the capital city of Roseau to the three flash flooding scenarios, with the flood extent maps overlaid on a satellite imagery. Due to the low-quality DEM used in this research, there is a misalignment between the artificially generated river network and the river network in the satellite imagery. Therefore, the exposure of buildings located on the southern coast of the Roseau River could be overestimated, and vice versa for buildings on the northern part of the city. However, even with this data precision issue, it is found that riverbank overflows are not the major reason for flash flooding in urban areas such as Roseau. Apart from inundated cells along the river network, other flooded areas exist across high-density build-up zones. Possible reasons for this distribution pattern are obstructed infiltration and surface flow by a high density of man-made structures.

Also focusing on the capital city of Roseau, Figure 4.12 breakdowns the amount of exposed MS in individual buildings by material category. The distributions of exposed aggregate, concrete, and steel are similar with some of the institutional buildings (e.g., the government headquarter and the financial centre), educational buildings (e.g., Convent high school), health buildings (e.g., Princess Margaret Hospital), and recreational buildings (e.g., Windsor Park Stadium) being the biggest sink. These non-domestic buildings tend to have a larger footprint area and multiple floors, resulting in relatively large gross floor areas. Compared with the aforementioned three material categories, exposed timber does not concentrate in the health buildings and recreational buildings in Roseau. This is because these two types of buildings are in a reinforced concrete structure with no timber involved in their constructions.

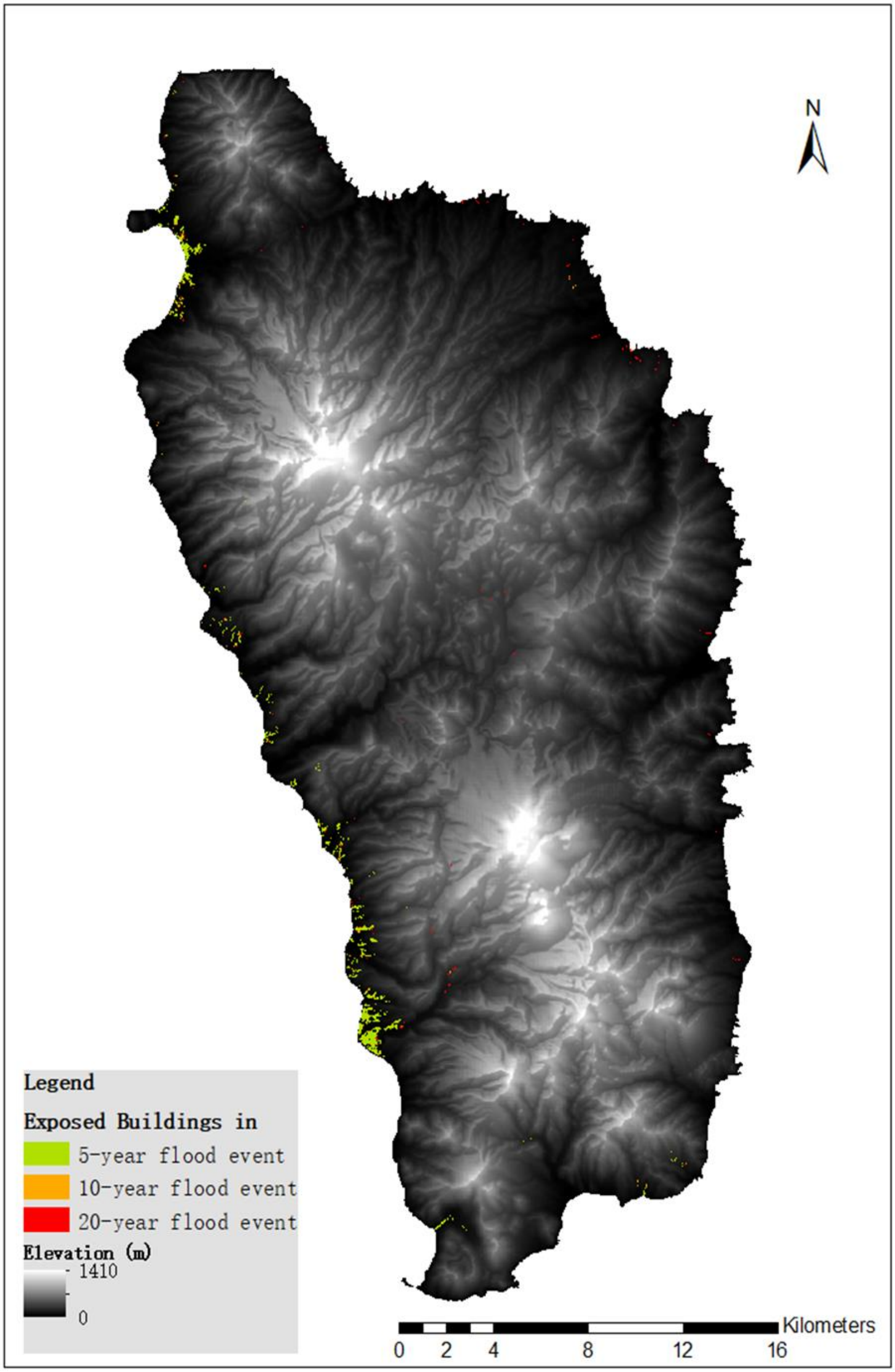

Figure 4.9: *Maps of exposed buildings to the flood hazard event for three return periods.*

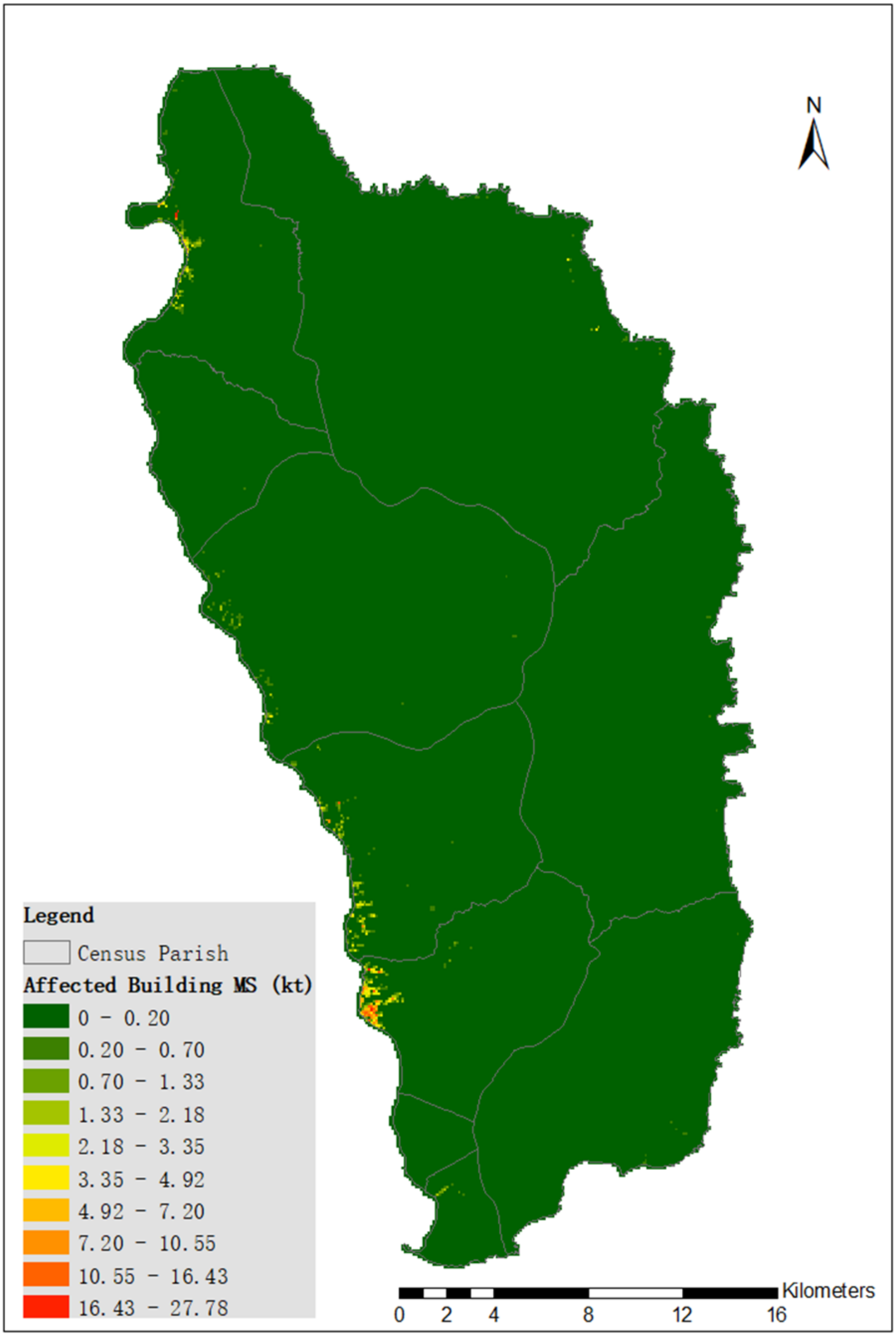

Figure 4.10: *Maps of exposed material stocks in buildings to the flood hazard event for three return periods.*

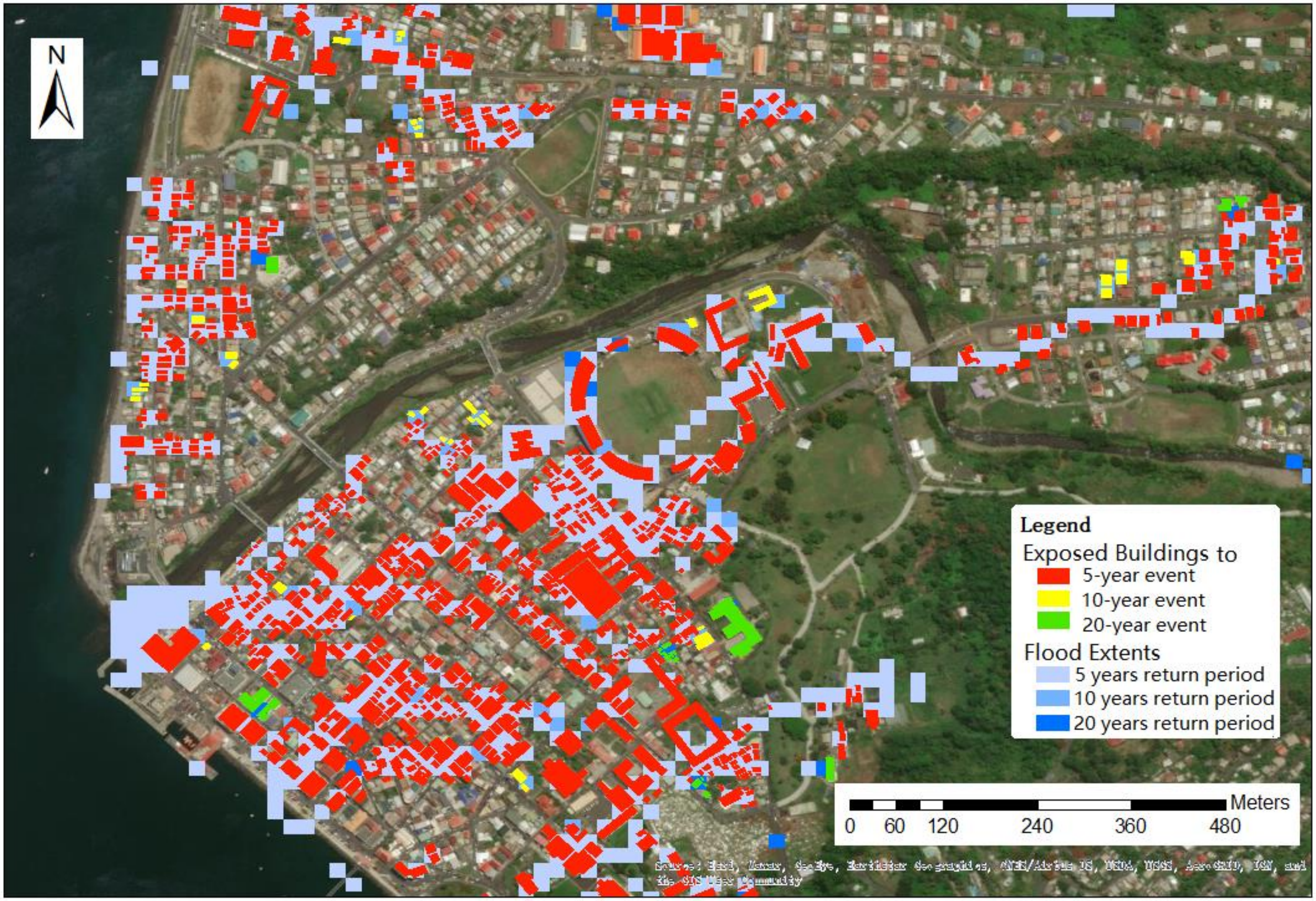

Figure 4.11: *A local-scale map of exposed buildings in the capital city of Roseau and the flood extents over satellite imagery.*

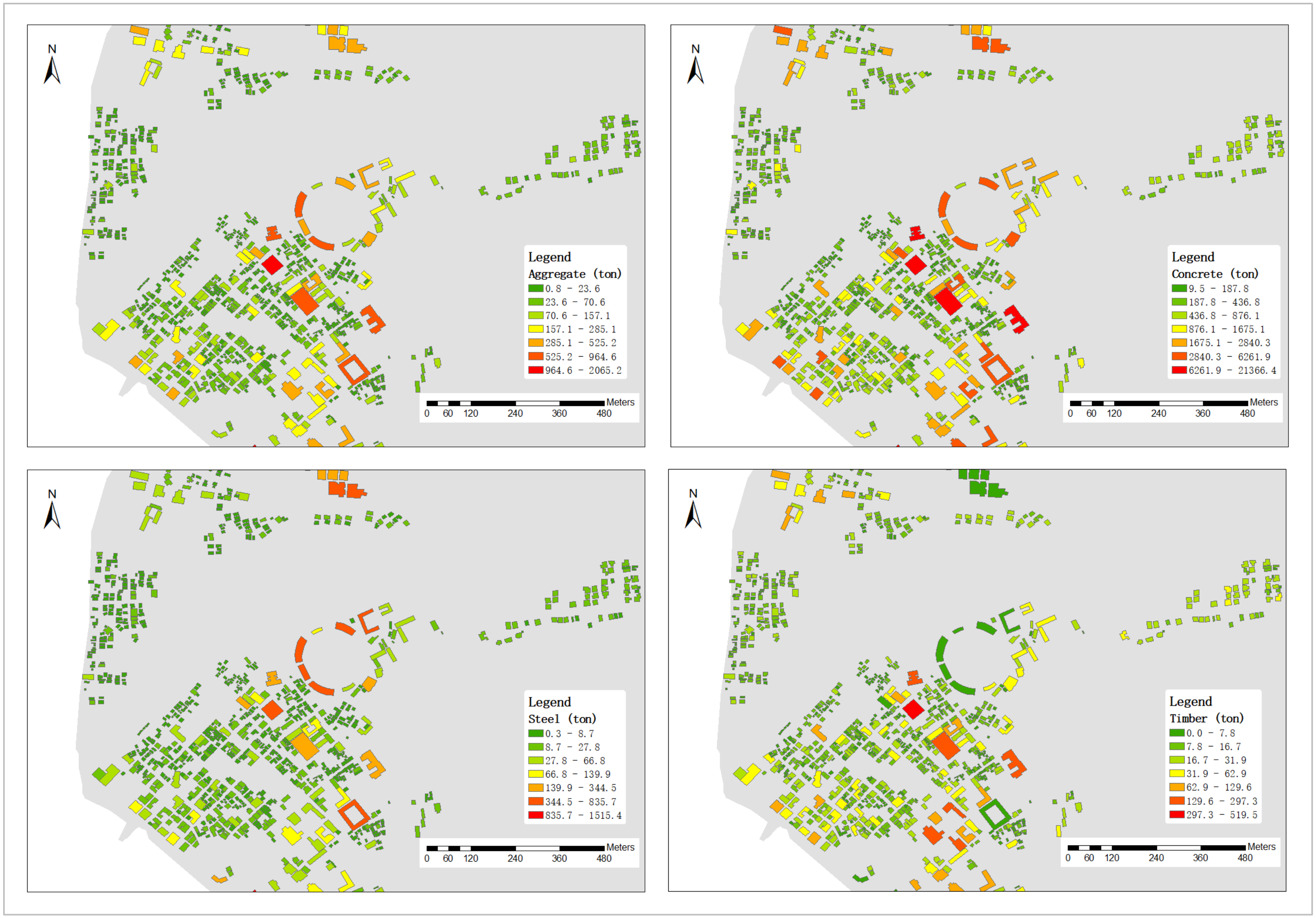

Figure 4.12: *The local-scale distribution of MS of each category in buildings in the city of Roseau. Top left: aggregate; Top right: Concrete; Bottom left: steel; Bottom right: timber.*

4.2.2.2 Affected Material Stocks in Buildings by Material Category

In terms of types of materials affected (Figure 4.11), hardly any difference was observed between the share of each material category among the three simulated flash flood events. This is because the increase in the quantity of total impacted MS from small magnitude events to large magnitude events is relatively small (about 1%, as discussed in the previous subsection). The distribution of affected stocks by material category is similar to the distribution of total MS in Buildings without considering flood impacts (Figure 4.2), demonstrating that construction types are similarly shared in affected buildings. Concrete accounts for the highest share of affected MS in buildings at about 85.9%. Aggregate is the second-largest material category accounting for 8.2% of total affected materials, followed by timber at about 3% and steel at about 2.9%.

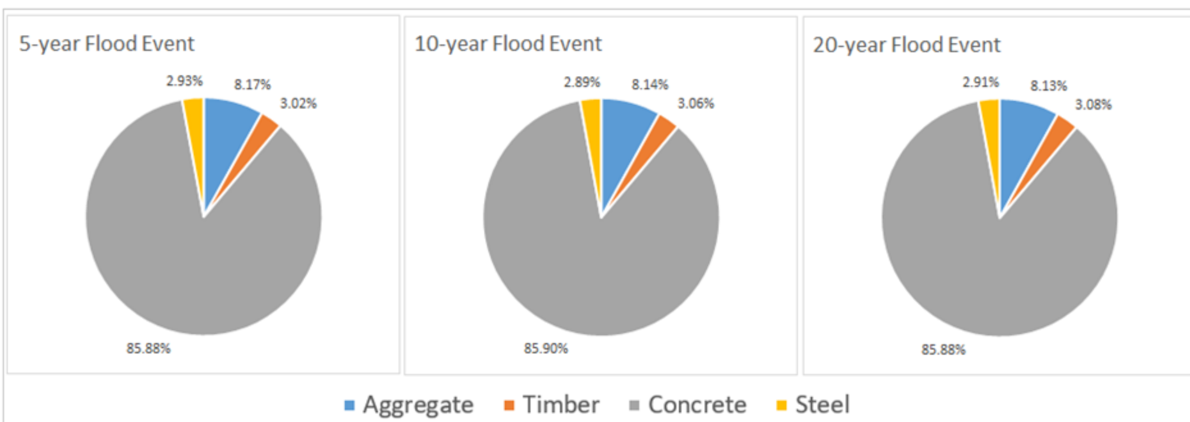

Figure 4.13: *Total share (in %) of exposed material stocks in buildings of Dominica to flood hazard event for the three return periods by material category.*

4.2.2.3 Affected Material Stocks in Buildings by Building Use-type

The results of affected MS in buildings of different use types are summarized in Table 4.5. In terms of absolute value, the residential sector is most affected by all three simulated flood events, with 554 kt, 609 kt, and 652 kt of MS exposed respectively to the 5-year, 10-year, and 20-year flash flooding scenarios. In terms of percentage of total MS of the use type, cultural buildings are most exposed to the simulated flood events, with 64.9% of total materials exposed in all the three simulated flash flood events due to their proximity with the coast. Institutional and commercial/industrial buildings are moderately affected with 41.6-45.7% and 41.9-43.5% of total materials exposed, respectively, though the quantity of exposed MS in institutional buildings is lower in terms of absolute value. It was also found that transportation buildings show the largest increase in exposed materials across different flood magnitudes, with 7.1% and 27.2% more at-risk materials from the 5-year event to the 10-year event, and from the 10-year event to the 20-year event, respectively.

Table 4.5: *Summary of affected buildings by building use-type for the three simulated flood events. Units: kt.*

Return Period:	5-year Flood Event		10-year Flood Event		20-year Flood Event	
Building Use-type	**Exposed MS**	**% of Use-type MS**	**Exposed MS**	**% of Use-type MS**	**Exposed MS**	**% of Use-type MS**
Institutional	200	41.6%	208	43.3%	219	45.7%
Commercial/ Industrial	322	41.9%	326	42.4%	333	43.5%
Residential	554	10.5%	609	11.6%	652	12.4%
Tourism	57	20.9%	59	21.6%	61	22.2%
Cultural	25	64.9%	25	64.9%	25	64.9%
Transportation	5	20.4%	6	27.5%	12	54.7%

The spatial distribution of affected MS by building use type at the district level is shown in Figure 4.12 and Figure 4.13. For institutional, commercial/industrial, residential, and cultural buildings, the highest concentration of affected material stocks is in the southwestern district, where the capital city is located. For tourism and transportation buildings, most at-risk material stocks are found in the northern district where the town of Portsmouth is located. When the results of the three simulated flood events for all building use types are compared, it is found that flood magnitude did not significantly affect the distribution of impacted MS in buildings at the district level, because the orders of different districts regarding affected MS within them did not change with flood magnitude. However, the 10-year and 20-year flood events did result in more exposed MS in the eastern districts. One exception is the cultural use type, which shows no distinction of affected material stocks across flood events of different return periods.

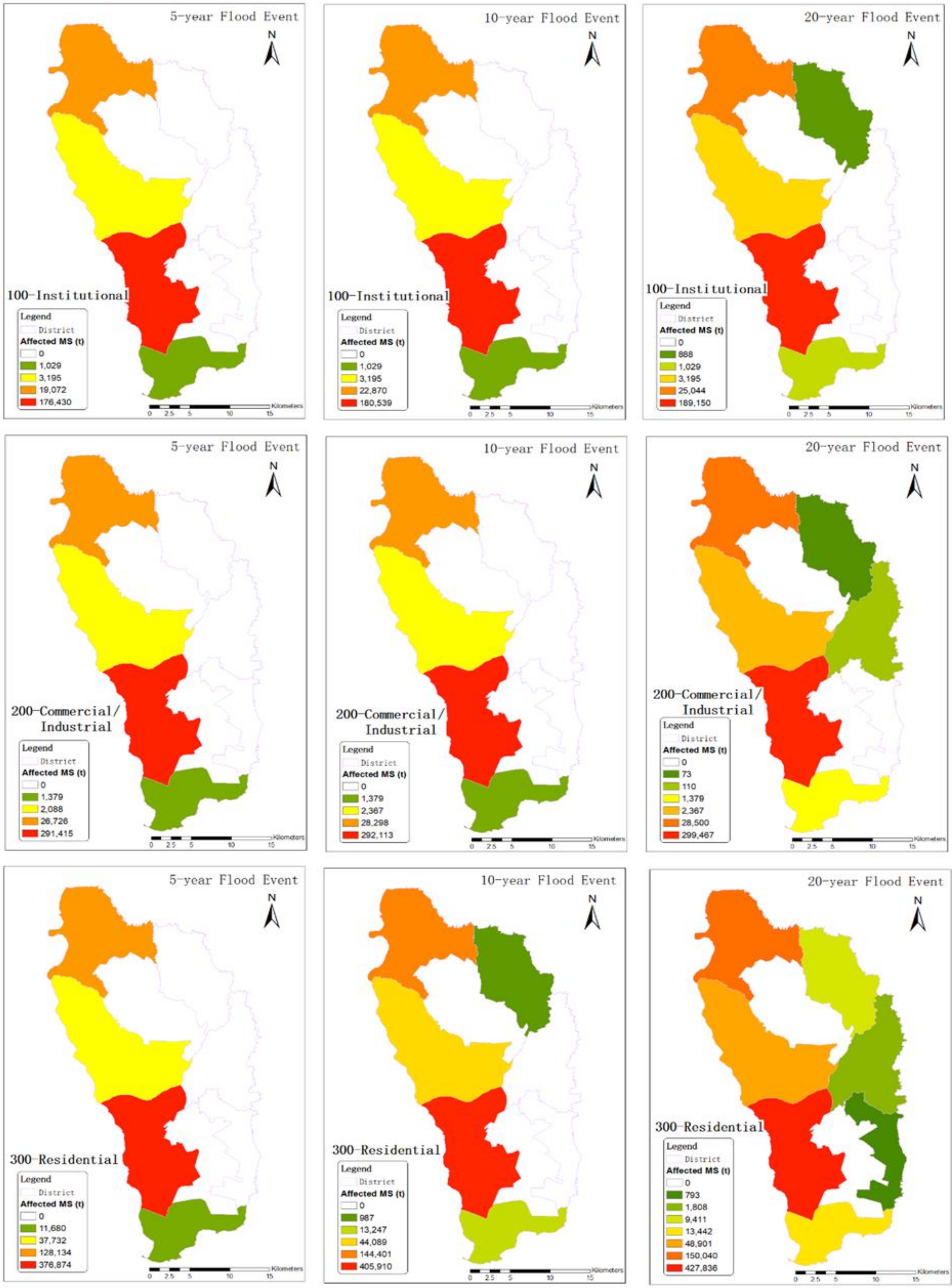

Figure 4.14: *Affected MS by building use type (institutional, commercial/industrial, and residential) in 5-year, 10-year, and 20-year flood events, presented at the district level.*

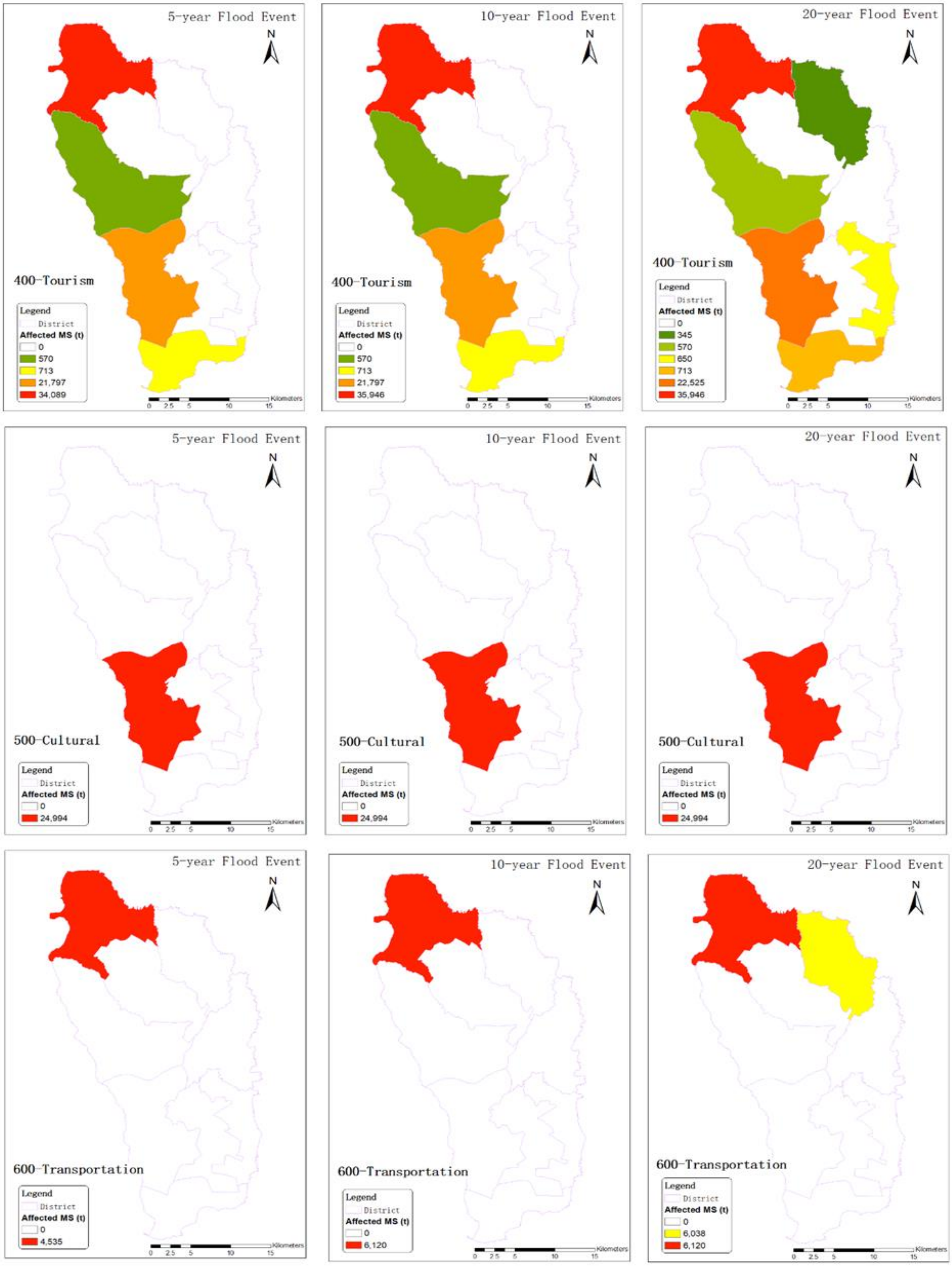

Figure 4.15: *Affected MS by building use type (tourism, cultural, and transportation) in 5-year, 10-year, and 20-year flood events, presented at the district level.*

5 Discussion & Conclusion

This section concludes the thesis by discussing the key findings from both the material stock accounting and the flash flood modelling, as well as how the research questions are addressed by the results. Also considered are directions for future work about material stocks and environmental hazards, followed by a brief summary of the entire research project.

5.1 Material Stocks in Buildings in Dominica and Spatial Distribution

The first research question of this study is about the quantity and spatial distribution of MS in buildings in Dominica. To answer this question, a material stock accounting analysis was conducted to capture a “screenshot” of 2020, when the building footprints were acquired from Open Street Map (OSM).

5.1.1 Material Stocks in Buildings in Dominica

The quantity of Dominica’s in-use material stocks in buildings in 2020 is estimated at 6,574 kt, equivalent to 91 t/capita, given Dominica’s population of the year. Table 5.1 lists the results from similar MS studies conducted in both developed and developing societies also at the national scale. When these results are compared, it is found that per capita values of MS in buildings in developed countries are not necessarily larger than the per capita values in small island states. For example, among the three small island states in Table 5.1, only Antigua & Barbuda (A&B) has a lower per capita value than Japan and Germany. When material density is considered, the same conclusion can be reached for per area values.

Previous studies also indicate that a high per capita value of MS in buildings does not always accompany a high per area value (at least to the same extent). Regarding A&B as a benchmark, the per capita value of Germany is 315% larger than that in A&B, while the difference between corresponding per area values is only 176%. Another example is the comparison between Dominica and Japan: the per capita MS in buildings of Japan is lower than that of Dominica, while the per area value of Japan is almost twice as large as that of Dominica. Although the abovementioned disagreement between per capita and per area values of Japan and Dominica is mainly caused by different population densities, the extent of this disagreement can reveal some information about the proportions of different housing styles. For example, Japan has a relatively high per area MS in buildings due to its high population density, but this may be offset by more single-family dwellings, which have a greater impact on per area value than per capita value.

Considering the three small island states in the Caribbean region in Table 5.1, their per capita MS in buildings show some disparities, with Dominica's per capita value in the middle range, but its per area value being amongst the lowest. Again, this misalignment between per capita and area values is mainly due to population density, with Grenada having the largest population density at 311 people per km^2, followed by A&B at 223 people per km^2 and Dominica at 96 people per km^2. In summary, based on the results from this research a limited number of material stock accounting studies conducted at the national scale, MS in buildings are proven to be site-specific, necessitating the adaptation of the methodology framework of this thesis for other study areas.

Table 5.1: *Per capita and per area MS in buildings of this research and previous studies.*

Country	**Year**	**MS in Buildings (t/cap)**	**MS in Buildings (t/km^2)**	**Source**
Japan	2010	60 (193%)	20,107 (188%)	Tanikawa et al., 2015
Germany	2010	128.6 (415%)	29,427 (276%)	Ortlepp et al., 2016; Ortlepp et al., 2018
Grenada	2014	125 (403%)	40,207 (377%)	De Kroon, 2020
Antigua & Barbuda	2004	31 (100%)	10,677 (100%)	Bradshaw, 2019
Dominica	2020	91 (294%)	8,754 (82%)	Current Study

5.1.2 Spatial Distribution of Material Stocks in Buildings in Dominica

From a building use type point of view, it is found that except for tourism and transport buildings, MS in all building use types are clustered near the capital city Roseau in St. George parish. This spatial pattern reflects the population and building distributions mentioned in Section 1.5 that 30% of Dominica's population live in St. George, and 25% of buildings are located in the capital city Roseau, which can also explain the high concentration of MS in buildings in the corresponding district in Figure 4.6. Being Dominica's economic and political center, Roseau is where many institutional buildings are clustered. Some examples are government offices like the Dominica Government Headquarters and the country's financial center, educational campus buildings of Dominica State College, as well as major buildings of Princess Margaret Hospital.

Buildings of the institutional use type are assigned relatively intense material intensity typology (e.g., Concrete Structure 2 or Reinforced Concrete Structure) and often appear as a cluster (e.g., buildings of the Princess Margaret Hospital). For MS in commercial/industrial buildings, tourist agencies, vehicle rentals, insurance companies, and banks are common in Roseau because the Roseau Ferry Terminal accounts for over 50% of annual visitors arriving by sea (Central Statistics Office of Dominica, 2010). For MS in cultural buildings, Roseau also has the Windsor Park Stadium, the country's only stadium. In addition, since non-domestic buildings tend to be higher than domestic buildings in general, the larger proportion of non-residential buildings in St. George makes its average building floor level (1.64 storeys) larger than the national average value of 1.26 floors. All the factors mentioned above contribute to the high concentration of total MS in buildings in St. George and around the capital city Roseau.

MS in tourism buildings are distributed differently from that of the aforementioned building use types, with the highest concentration identified in the parish of St. John along the northwestern coast of Dominica. Although tourism buildings are spread throughout the island, about 24% of total tourism buildings are located near Portsmouth, the second-largest city in Dominica. Like the capital city Roseau, Portsmouth also has a seaport, but it only accounts for 5% of annual visitors arriving by sea (Central Statistics Office of Dominica, 2010). Thus, this high concentration of MS in tourism buildings might be resulting from the clustering of tourist attractions. For instance, a few public beaches (e.g., Coconut Beach and Ripaton Beach) can be found along the coast near Portsmouth. In addition, not far from Portsmouth is the Cabrits National Park, where Fort Shirley is located. The construction of Fort Shirley traces back to the 1700s, and it is one of the limited cultural sites for visitors interested in the history of Dominica (UNESCO, 2021). Thus, new resorts tend to be built in St. John. For example, the recently-built 5-star hotel, Cabrits Kempinski Resort, is located near Portsmouth, which also helps to explain the high concentration of MS observed in tourism buildings, since this multi-unit large hotel accounts for nearly 7% of total MS in tourism buildings in Dominica.

5.2 Dominica’s Material Stocks in Buildings Affected by Flash Flooding

The second research question of this study is about the quantity and spatial distribution of MS in buildings exposed to flash flooding in Dominica. To answer this question, flash flood modelling was conducted to derive the extent of flash flood events with different return periods. The following sections summarize the results and explain why these results occur.

5.2.1 Flooded Area in Dominica

The total flooded area in Dominica is 4.1 km^2, 4.9 km^2, and 5.7 km^2 for 5-year, 10-year, and 20-year flash flood events, respectively. Given Dominica's landmass of 750km^2, only a small proportion (less than 1%) of the island is impacted by the simulated flash flood events. In terms of total rainfall depth, the 5-year, 10-year, and 20-year flood events are triggered by precipitation of 220.3 mm, 270 mm, and 317.6 mm, respectively. The increase in total rainfall depth is nearly 50% from the 5-year rainfall event to the 20-year rainfall event, while the increase in corresponding flood extent was not proportional at about 39%. This illustrates that total rainfall depth is not the only factor affecting flood extent in Dominica when a flash flood hazard is investigated at the national level. From a flood generation mechanism perspective, rainfall amount, intensity, duration, and spatial distribution all influence flood extent (Bracken et al., 2008). Therefore, although this was not the case in Dominica, it is possible that flood events with larger return periods and rainfall depths do not necessarily result in a larger flood extent.

The locations of flooded areas provide essential information of where flood-related risks can be expected. When the spatial distribution of flooded areas is examined, it is evident that most of the inundated areas are located along the west coast of the island. This spatial pattern could be caused by lower infiltration rates along the west coast. The infiltration maps of the three simulated flash flood events are presented in Appendix B.7, showing an overlap between flooded areas and areas with low infiltration values. The soil texture of these areas is clay, whose saturated hydraulic conductivity is relatively low. Therefore, when the soil is saturated after a certain point from the start of the rainfall event, its infiltration capacity cannot manage further intense precipitation, leading to high overland flow as flooding. Knowledge of the influence of soil property on flood modelling results uncovers the need for more detailed soil maps or fieldwork observations to acquire more accurate soil properties, including porosity, initial soil moisture, and saturated hydraulic conductivity.

Also discovered are entirely new flooded areas on the southwestern coast in the 10-year flood event, and on the northeastern coast and in more inland mountainous zones in the 20-year flood event. Two previous projects assessing flash flood susceptibility in Dominica exist (CIPA, 2006; Jetten, 2016), which also produced qualitative flash flood maps as primary results (Figure

5.1). According to the flood extent map by CIPA (2006), most of the flooded areas are located near the west coast of the island, which is similar to the pattern of flooded areas identified in this research. However, a major difference is that the flooded areas in the CIPA project are more extensive, especially along the west coast. Compared with the result of the CHARIM project, less flash flood risk is identified along the east coast in this study, with a smaller number of flooded areas distributed on the east side. Although both the CHARIM project and this study employed the same model for flood simulation, flood areas in the CHARIM project show a more extensive and continuous pattern along major rivers, while flooded areas in this study are more dispersed and distributed along drainage lines. This is important because an over estimate of flood extents could put extra burden on government finance in small island states with limited budgets. In addition, the spatial pattern of flooded areas in this research would suggest Dominica putting more emphasis on developing better drainage systems, especially in urban areas, as a complement to regular flood risk reduction approaches like floodwalls and levees.

One contribution of this research to the original flood modelling in the CHARIM project is the derivation of a more accurate river width input map, as the original river width map was derived by extrapolating river width data from another basin, so it was not site-specific. Artificial river networks were used in both the CHARIM project and this study, but this research was able to identify a smaller number of river channels, where the locations and widths match the actual rivers identified in satellite imagery. Another contribution of this study is a more accurate building density map derived from manually corrected building footprints with reference to satellite imagery (Section 3.2.2). In the CHARIM project, the footprint area for buildings outside Roseau was assumed to be 70 m^2, which is smaller than the average size of 103 m^2 of all the building footprints in Dominica (manually corrected). Therefore, the dispersed pattern of flooded areas along drainage lines identified in this research is probably resulting from fewer river channels gathering overland flow to main river branches, as well as higher building density leading to surface flow obstruction. Despite the two improved input maps mentioned above, it is uncertain whether they are the only factors for the different patterns of the flooded areas observed in this study. Except for the two improved input maps, the rest of the input maps used in the CHARIM project were unavailable, making it difficult to replicate the entire modelling process.

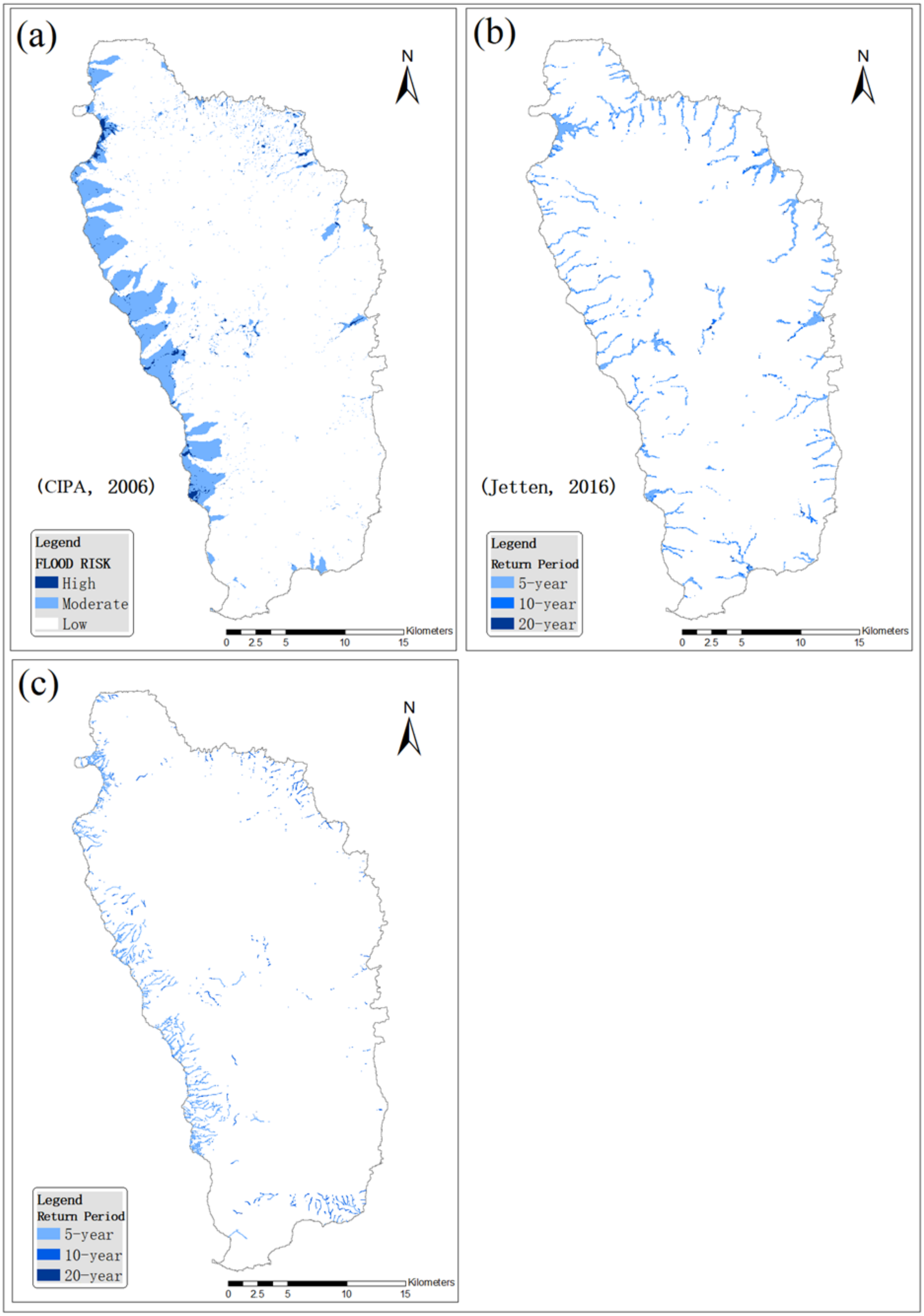

***Figure 5.1**: Flash flooding extent generated in (a) the US-AID funded multi-hazard assessment project by CIPA (2006); (b) the CHARIM project by Jetten (2016); and (c) current study.*

5.2.2 Affected Buildings and Contained Material Stocks

The numbers of buildings affected by flash flooding were 2,781, 3,030, and 3,274, respectively, in the 5-year, 10-year, and 20-year events. Table 5.2 is used to comparatively summarise the affected buildings and the contained material stocks in Dominica regarding a multi-hazard assessment project (CIPA, 2006), the CHARIM project (Jetten, 2016), and this research. For the multi-hazard assessment project, only the high hazard class resulting from a 2-year rainfall event is included, because the low hazard class covering the whole island is considered as non-flooded area, and the medium hazard class can be interpreted as runoff area contributing to actual flooding near river channels (Jetten, 2016). When exposed buildings are investigated together with flood extent, it is observed that there is a positive relationship between the number of affected buildings and flooded area for all three flood modelling projects. This positive relationship suggests that most buildings in Dominica were located without considering flood risk. This finding agrees with the statement by Barclay et al. (2019) that much of Dominica's population is concentrated in areas with high disaster risk due to historical illegal settlements in unoccupied lands.

When the results of the CHARIM project and current study are compared, it is found that the increase in the number of affected buildings does not bring an increase of the same scale in exposed material stocks in Dominica. For example, for all three flood scenarios, the number of affected buildings in the CHARIM project is about twice the number of affected buildings in this research. However, the difference in corresponding exposed MS is relatively small at 1-4%. This unmatched increase pattern can be explained by the location of these extra exposed buildings in the CHARIM project. As discussed in the previous subsection, there are more affected buildings identified along the east coast of Dominica in the CHARIM project. The mean gross floor area (GFA) of buildings on the eastern side of Dominica is 88 m^2, which is smaller than the average GFA of all the buildings on the island at 145 m^2. Therefore, since all building occupancy classes are similar in total material intensity, smaller GFA is the main cause of the unmatched increase patterns of exposed buildings and MS.

Table 5.2: *Quantitative summary of affected buildings and contained material stocks by flood extent in different flood risk assessment projects.*

Source	**Return Period**	**Number of Buildings Affected**	**% of Buildings Affected**	**MS Exposed (kt)**	**% of MS Exposed (kt)**
Multi-hazard Assessment Project (CIPA, 2006)	2 years	2,605	7.8%	959	14%
CHARIM Project (Jetten, 2016)	5 years	4,862	14.5%	1,213	18%
	10 years	6,101	18.3%	1,509	22%
	20 years	6,122	18.3%	1,513	22%
Current Study	5 years	2,781	8.3%	1,162	17%
	10 years	3,030	9.1%	1,232	18%
	20 years	3,274	10.0%	1,032	19%

5.3 Incorporating Vulnerability Factors

Once the results of material stock accounting and flash flood modelling reveal the quantity and spatial distribution of flash flood-prone MS in buildings in Dominica, the third research question is about the effect of social characteristics on household level-vulnerability to flash flooding. To answer this research question, 17 variables for social factors of vulnerability to environmental hazards were collected from the literature and adapted to the context of Dominica. Based on these 17 adapted variables, a resident survey instrument was designed to collect primary data following general guidelines for quantitative survey design (Bryman & Bell, 2019; Flowerdew & Martin, 2005). This survey was not conducted in the field for this research due to the COVID-19 pandemic, which resulted in travel restrictions that prevented surveys to be conducted on-site and in-person in Dominica. If these variables can be collected through the implementation of the designed resident survey, they can be used to calculate a composite vulnerability score following the methodology described in Section 3.4.2.3 for each household that participates in the survey. This quantitative information can help local government to evaluate hazard risk from a vulnerability perspective by cal. Relevant future work and possible deliverables are discussed in Section 5.4.3.

5.4 Limitations & Future Work

Small island states are generally limited in terms of spatial data availability, and all the assumptions in the methodology are related to this issue. This section begins with the limitations of the material stock accounting process, followed by what can be improved in the flash flood modelling process. Finally, this section also discusses probable future work related to material stocks and environmental hazards to extend the scope of current research.

5.4.1 Material Stock Accounting in Dominica

Building classification is a fundamental step in bottom-up MSA approaches. The goal of building classification is to group buildings into the least possible number of occupancy classes, while material intensity homogeneity within every single occupancy class can still be achieved. The existing footprints dataset for buildings in Dominica only covers buildings in the capital city of Roseau. The rest of the buildings on the island are stored as points without essential properties like footprint area for material stock accounting. Therefore, OSM building footprints were used instead for all buildings in Dominica to ensure that footprints inside and outside Roseau were collected from a consistent source.

This study adopts the building classification framework and the material intensity coefficients developed by Symmes et al. (2020) for Grenada, another Caribbean island nation. Although the two island nations are similar in geographical background, material intensity coefficients are unique to individual buildings for gradient slope and soil type, among other physical attributes of the lands they are built on, as well as societal and economic factors like time of construction, technologies available, and owner's budgets (Sprecher et al., 2021). Data sources for building classification in Dominica were limited to Google Maps, OSM, aerial videos and Google Earth images. Considering the site-specific nature of building use-type and material intensity, one of the most significant improvements of the material stock accounting in Dominica can come from future field work to conduct on-site validations of the building use types and calibration of relevant material intensity coefficients through interviews on local construction experts.

The strategy of identifying remarkable non-residential buildings and assuming the rest to be residential buildings could result in an overestimation of the number of residential buildings. According to Dominica's census report, there were 25,133 residential buildings in 2011 (Central Statistics Office of Dominica, 2011), while there were 31,403 buildings in Dominica classified as residential buildings in this research. Again, a fieldwork to conduct on-site validations of the building occupancy classes is essential for the calibration of this offset in the proportion of residential buildings. Another point to investigate during future fieldworks is whether some residential buildings are used as villas during the tourist season in Dominica. According to Central Statistics Office of Dominica (2010), 45% of visitors from outside the Caribbean region in 2010 stayed in private homes rather than hotels. This phenomenon could cause bias in the relationship between MS in buildings and associated services because a considerable amount of MS should be regarded as providers for both residential and tourism services.

Building height is another reason the methodology used in this research cannot achieve an individual building-resolution MS accounting. Except for the footprint area, the OSM building footprint dataset does not include many attributes of the buildings in Dominica, so building heights were derived from visual interpretation of aerial videos, which improves to some extent the accuracy of MS accounting compared with simply assuming the same height for buildings within the same occupancy class. With 37% of the buildings in Dominica covered by the aerial videos, the heights of the rest of the buildings were derived from buildings with an actual height of the same occupancy class and in the same parish. However, the number of buildings with an interpreted height cannot be controlled within occupancy classes or parishes. This would lead to biased results if there is a limited number of buildings with an interpreted height within a specific occupancy class or parish. In addition, this method of acquiring building heights may not be applicable in other areas because aerial videos are not commonly available.

A more accurate way to obtain buildings heights for material stock accounting would be using remote sensing data like high-resolution DSM (Digital Surface Model) generated from a LiDAR (Light Imaging Detection and Ranging) survey. In 2018, a LiDAR topography survey was conducted in Dominica under the Disaster Vulnerability Reduction Project. Despite the careful manual correction of the OSM footprint dataset, there could be a few artificial errors that remain in this data layer (e.g., the misalignment between footprints and actual buildings in the images or multiple footprints overlapping each other). Thus, in addition to building heights, the LiDAR dataset is also helpful for the development of an entirely new building footprint dataset that is more accurate than the OSM dataset used in current research. Since LiDAR datasets are usually difficult to access and time-consuming if processed at the island scale, it is recommended that the first step for future work is to focus on a smaller area (e.g., one catchment in hydrology) and compare the new results with those in current research.

5.4.2 Flash Flood Modelling in Dominica

As discussed in the methodology section, it is assumed that the whole island is subjected to spatially homogenous rainfall events in the flood modelling process implemented in this study. The design rainfall events adopted from Jetten (2016) were derived from records of only two rain gauge stations located separately at the two airports in Dominica. However, the spatially homogenous rainfall distribution pattern is not realistic when applied to the entire island state. It is found that annual total precipitation is actually higher in central areas in Dominica due to the orographic effect that produces extremely concentrated precipitation when a tropical cyclone passes over high mountains (Houze, 2012). If the rain gauge station network in Dominica is improved, the lack of detailed rainfall data could be solved by using rainfall interpolation methods. For example, Mair & Fares (2011) conducted a comparative study evaluating the performances of traditional and geostatistical rainfall interpolation methods in mountainous tropical island settings. While low errors still exist in interpolated rainfall, geostatistical interpolation methods (e.g., ordinary kriging) that incorporate the pattern of spatial dependence would improve the accuracy of flash flood modelling by adding some spatial variability to the rainfall input map (Goovaerts, 2000; Mair & Fares, 2011).

The river network was artificially generated from the DEM. The river channels were derived by applying a threshold on stream order, and river width was manually interpreted from satellite imagery. Therefore, the river network and relevant river parameters cannot perfectly reflect the actual river system in Dominica. There is a consensus that flood models are sensitive to the quality of DEM (Yu & Lane, 2006), but it is uncertain how sensitive is the flood model in this research to river parameters. Thus, it is recommended that future research conducts a sensitivity analysis of river dimensions. It is also recommended to calibrate the flood model by referencing images or videos of potential flood events in the future.

Since flood risk was examined at the national level in Dominica, only flood extent is considered to be accurate among other flood properties. Thus, the sole criterion for identifying MS exposed to potential flash flooding risk is whether the building footprint intersects any flooded area. Although clusters of flooded buildings and contained MS can be located at the national level using the current methodology, exposure cannot be quantified for individual buildings because based on the simplified methodology buildings are either affected as a whole or not affected at all. This does not reflect reality because even if the simulated flood extent fully covers a building, it may withstand the impact of flooding for its good inherent structural resistance (Prieto et al., 2018). One solution is to investigate flash flood risk at the local level (e.g., in a catchment with a high concentration of affected MS identified in the national-scale simulations) so that more flood characteristics can be applied. For example, Kreibich et al. (2009) argue that flow velocity and water depth can be combined to indicate total flow energy, which is proven to be a significant physics-based parameter influencing the structural damage of domestic buildings in the context of flash flooding in Germany. With these extra flood properties, it is possible to calculate the degree of damage caused by the simulated flood event for an individual building, which can be further used to quantify the actual amount of lost MS within that building. While the highest concentration of buildings MS is identified in the capital city of Roseau, local-scale flood simulations in urban areas are sensitive to the resolution of the DEM used, because significant topographic features such as man-made structure greatly affect flow dynamics (Haile & Rientjes, 2005). This issue can also be solved by incorporating a more detailed DEM generated from LiDAR data to better representing the model domain (Haile & Rientjes, 2005). Given the multiple potential applications of LiDAR data in both MSA and flash flood modelling, as well as the high computing requirements for LiDAR data processing, it is recommended that the local government share the existing LiDAR datasets to facilitate preparedness for hazard response and recovery. It should also be noted that sediment transportation was not involved in the simulations, despite the fact that the extra forces caused by high sediment loads cannot be ignored (Marvi, 2020). Therefore, even with accurate flood properties derived from local-level simulations, the exposed MS could be underestimated in the current study because the effect of sediment transportation was not included.

5.4.3 Directions for Future Work

As discussed in Section 2.3.1, the risk of an environmental hazard encompasses three components: 1) hazard characteristics including intensity, extent, and duration; 2) exposure of lands or population; 3) vulnerability defined as the susceptibility of the exposed lands or people due to social factors (UNISDR, 2015). Using Dominica as a case study, this research has focused on the first two components by modelling the impact of flash flooding events of different magnitudes on the accounted material stocks in buildings. However, vulnerability as the third component of hazard risk is equally important because the same hazard event can cause different degrees of damage to different households for their various levels of susceptibility. For example, Dominica's low-income families tend to live in houses of low resilience against environmental hazards and reside in informal settlements in low-lying areas far away from urban areas or towns, where high flood risk can be expected (Barclay et al., 2019). This suggests that the impact of environmental hazards is a function of both physical exposure and social factors contributing to vulnerability.

Different methodologies can be used to incorporate vulnerability in the framework of the current study (mentioned in Section 2.4), but primary data collection is necessary to bridge the data gap between hazard exposure and vulnerability. A draft household survey (in Appendix C.2) was designed to collect primary date about household vulnerability to environmental hazards. It is recommended that future studies utilize this resident survey instrument to investigate household-level social factors of vulnerability to environmental hazards. If information of household vulnerability can be collected using the household survey, the flood risk can be quantified from both social (socioeconomic factors contributing to vulnerability) and physical (hazard exposure) perspectives. Together with the flash flood exposure investigated in this study, social vulnerability as a multidimensional concept can help the government identify the households that have difficulty responding to and recovering from potential flooding events (Cutter et al., 2003).

In addition to buildings, roads are also a significant sink of construction materials. Different from buildings and other discrete structures with clear footprints, roads are comprised of a network of continuous structures and can contain construction materials that are comparable to or more than building material stocks (Tanikawa et al., 2015). Considering MS in seven end-use types in Japan in 2010, 43% of the materials were in buildings, and 26 % were in roads (Tanikawa et al., 2015). For developing countries, it is also found that approximately 40% of the construction materials were used to expand and maintain the road network in Vietnam from 2003 to 2013 (Nguyen et al, 2019). For small island states in the Caribbean region, the amount of building material stock was 14,012 kt in 2014 in Grenada, and the amount of road material stock was estimated at 4,375 kt (De Kroon, 2020; Ye, 2022). Therefore, road material stock should not be neglected in material stock accounting for a more complete investigation of the entire built environment in Dominica. From an environmental hazard perspective, roads in addition to buildings are also severely affected. More specifically in flash flooding events, the degree of structural damage of inundated roads sections are significantly affected by flow velocity, and due to the paved structure of roads, both road surface and road foundation are equally crucial in MS exposure analysis (Kreibich et al., 2009; Tanikawa et al., 2014). In Dominica, informal settlements where low-income families live are usually linked by coastal roads, so if these roads are damaged, those families are easily isolated, which prevents efficient aid to be transferred from other parts of the island (Barclay et al., 2019). Thus, it is necessary to pay more attention to roads in both material stock accounting and hazard exposure analysis.

5.5 Recommendations

The following section outlines some generalized recommendations for decision-makers and practitioners on how this research can be used in the context of hazard risk reduction to achieve certain Sustainable Development Goals (SDGs; UN, 2023) not limited in Dominica, but in other small island states as well.

Small island states heavily rely on imports of construction materials due to the scarcity of natural and human resources and a limited scope of economic diversification. Utilizing in-use material stock account at the building level, urban planning specialist will be able to identify clusters of construction materials, which could be potential maintenance hotspots (Pauliuk et al., 2014). Since building stock is linked to the services, decision makers will also be informed about the distribution of essential services across the island, and accordingly adjust development plans to achieve a more coordinated development (Kunz et al., 2013). However, data infrastructure in small island states is often underdeveloped, posing challenges for both stock-driven and flow-driven material stock analysis. Nevertheless, it is recommended that small island states adapt the material stock analysis approach in this research to first acquire a rough material stock account at the island scale. This island-level material stock account could serve as a base point for further material flow analysis, which would support the efficient use of natural resources and help reduce waste generation, as stated in SDG 12.2 and 12.5. Decision makers could operationalize material flow analysis by promoting the application of Building Information Model (BIM) in the construction of institutional buildings and even in residential buildings under contracts with individual merchants to track the amount of material used for construction and maintenance throughout the whole lifecycle (Smith, 2014).

An environmental hazard event is a common incident in which MS is converted to waste, even long before the ends of expected lifespans (Tabata et al., 2018). In small island states with limited natural resources, disaster waste is a part that cannot be neglected in ordinary construction and demolition (C&D) waste estimation and management. The material stock analysis part of this research paves the way for estimating the quantity and distribution of material stocks and associated services exposed to potential hazard events. It is recommended that stakeholders in small island states combine the results of material stock analysis and hazard risk mapping to pinpoint clusters of exposed material stocks, which could help local governments prioritize funding for local scale hazard risk assessment. This would promote SDG 11.b, which encourages the implementation of local disaster risk reduction strategies.

After revealing the exposure of material stocks to environmental hazards, the resident survey instrument developed in this research could be used by small island states as a template to involve the vulnerability aspect of hazard risk. The survey instrument could be improved by incorporating more physical factors contributing to vulnerability, such as presence of basement, height of lowest opening, building age, and wall material (masonry or non-masonry) (Granger et al., 1999; Menoni et al., 2006; Kappes, Papathoma-Köhle & Keiler, 2012). In the reality of limited budgets, it is recommended that governments of small island states pilot the survey in previously identified clusters of exposed material stocks. This would help small island states initiate proactive emergency preparedness plans before a hazard event or optimize priority settings in evacuation actions during a hazard event for a better emergency response, which aligns with sustainable development goal 11.5 (protecting people in vulnerable situations).

5.6 Conclusion

Dominica and other small island states are on the frontlines of climate crisis and are disproportionately affected by climate-related hazards, as small island states contribute to less than 1% of global greenhouse gas emission but are more vulnerable to extreme events and sea-level rise due to their unique social, physical, institutional, and environmental characteristics (UNDP, 2017). Using a bottom-up approach, this study is the first attempt of material stock accounting in Dominica. Both the quantity and spatial distribution of material stocks in buildings were examined, providing a knowledge base that can help policymakers understand the spatial patterns of different material categories in different building occupancy classes across the island. The results of the material stock analysis created a 'snapshot' of MS in buildings for 2020, showing that MS in buildings concentrate in major towns along the coastline. With the help of annual inflow and outflow data, this 'snapshot' can be used as a base point for material flow analysis, providing a flow-based perspective from which predictions of the future amounts of material stocks can be made. However, a few assumptions exist in the material stock accounting methodology, as the building classification framework and the material intensity coefficients were adopted from another research conducted another Caribbean small island state. This research also linked the results of material stock analysis to the impacts of environmental hazards in the context of small island states. Focusing specifically on flash flooding, this research found that about 17%, 18% and 19% of MS in buildings in Dominica were exposed to 5-year, 10-year and 20-year flash flood events, respectively. In terms of the spatial distribution of these exposed MS in buildings, it was also found that high concentrations of exposed MS were located along the western coast of the island, mainly in the capital city of Roseau and other towns. In terms of methodological contribution, this study developed a methodological framework for small island states to estimate hazard risk as a function of hazard exposure and vulnerability of impacted people and properties. The vulnerability assessment part of the methodological framework was not tested in current research due to the travel restrictions on the in-person survey implementation, so it is recommended that future studies conduct a fieldwork for both the validation of the assumptions in the material stock analysis and implementing the resident survey instrument to test the reliability of the entire methodological framework.

Several previous projects have focused on flash flooding risk assessment using flood inundation modelling in Dominica, but this is a novel study investigating the impacts of such type of environmental hazard on the building sector. Most of the input datasets for flood modelling are adopted from the previous CHARIM project, but this study improves the quality of the river width dataset using visual interpretation based on satellite images. The accuracy of the building density input dataset was also enhanced by using a more complete building footprint dataset manually corrected by referencing satellite images. Based on the improved flood modelling, this research found that flood extent might be overestimated in the CHARIM project, probably due to the denser river network used in the CHARIM project that channel more water to the outlets. Future improvements regarding more accurate exposure of material stocks in buildings could include not only more-accurate input datasets, but also incorporate building performance against flooding and hazard intensity variables. Combining the results of material stock accounting and flood inundation modelling will allow policy makers to understand the quantity and spatial pattern of material stocks in buildings exposed to flash flooding in Dominica.

References

Adger, W. N. (2006). Vulnerability. *Global environmental change, 16*(3), 268-281.

Alam, M. (2015). *Application of national census data for vulnerability assessment and spatial planning in Grenada* (Master's thesis, University of Twente).

Anju, B., Drissia, T. K., & Nowshaja, P. T. (2021, March). One dimensional hydrodynamic modelling of pamba river for identifying the flood vulnerability. In *IOP Conference Series: Materials Science and Engineering* (Vol. 1114, No. 1, p. 012023). IOP Publishing.

Arora, M., Raspall, F., Cheah, L., & Silva, A. (2019). Residential building material stocks and component-level circularity: The case of Singapore. *Journal of Cleaner Production*, *216*, 239-248.

Augiseau, V., & Barles, S. (2017). Studying construction materials flows and stock: A review. *Resources, Conservation and Recycling*, *123*, 153-164.

Babinard, J., Bennett, C. R., Hatziolos, M. E., Faiz, A., & Somani, A. (2014, February). Sustainably managing natural resources and the need for construction materials in Pacific island countries: The example of South Tarawa, Kiribati. In *Natural resources forum* (Vol. 38, No. 1, pp. 58-66).

Barclay, J., Wilkinson, E., White, C. S., Shelton, C., Forster, J., Few, R., ... & Honychurch, L. (2019). Historical trajectories of disaster risk in Dominica. *International Journal of Disaster Risk Science*, *10*(2), 149-165.

Becken, S., Mahon, R., Rennie, H. G., & Shakeela, A. (2014). The tourism disaster vulnerability framework: An application to tourism in small island destinations. *Natural Hazards*, *71*(1), 955-972.

Bird, D. K. (2009). The use of questionnaires for acquiring information on public perception of natural hazards and risk mitigation–a review of current knowledge and practice. *Natural hazards and earth system sciences*, *9*(4), 1307-1325.

Borga, M., Stoffel, M., Marchi, L., Marra, F., & Jakob, M. (2014). Hydrogeomorphic response to extreme rainfall in headwater systems: flash floods and debris flows. *Journal of Hydrology*, *518*, 194-205.

Boruff, B. J., & Cutter, S. L. (2007). The environmental vulnerability of Caribbean island nations. *Geographical Review*, *97*(1), 24-45.

Bout, B., Jetten, V., De Roo, A., Wesseling, C., & Ritsema, C. (2018). OpenLISEM-Multi-Hazard Land Surface Process Model. *Enschede, Netherlands: University of Twente-Faculty of Geo-Information and Earth Observation (ITC)*.

Bracken, L. J., Cox, N. J., & Shannon, J. (2008). The relationship between rainfall inputs and flood generation in south–east Spain. *Hydrological Processes: An International Journal*, *22*(5), 683-696.

Bradshaw, J., Jit Singh, S., Tan, S. Y., Fishman, T., & Pott, K. (2020). GIS-based material stock analysis (MSA) of climate vulnerabilities to the tourism industry in Antigua and Barbuda. *Sustainability*, *12*(19), 8090.

Bryman, A. (2016). *Social research methods: Fifth Canadian Edition*. Oxford university press.

Canevari-Luzardo, L., Bastide, J., Choutet, I., & Liverman, D. (2017). Using partial participatory GIS in vulnerability and disaster risk reduction in Grenada. *Climate and Development*, *9*(2), 95-109.

Casulli, V., & Stelling, G. S. (1998). Numerical simulation of 3D quasi-hydrostatic, free-surface flows. *Journal of Hydraulic Engineering*, *124*(7), 678-686.

Center, E. H. J. H. I., & John, H. H. (2000). *The hidden costs of coastal hazards: Implications for risk assessment and mitigation*. Island Press.

Central Statistics Office of Dominica. (2010). Travel Report 2010. Available at https://stats.gov.dm/wp-content/uploads/2019/06/Annual_Travel_Report_-2010.pdf

Central Statistics Office of Dominica. (2011). Population and Housing Statistics 2011. Available at https://stats.gov.dm/wp-content/uploads/2020/04/2011-Population-and-Housing-Census.pdf

Charlton, R. (2007). *Fundamentals of fluvial geomorphology*. Routledge.

Chen, W., Cutter, S. L., Emrich, C. T., & Shi, P. (2013). Measuring social vulnerability to natural hazards in the Yangtze River Delta region, China. *International Journal of Disaster Risk Science*, *4*(4), 169-181.

CIPA. (2006). Development of a landslide hazard map and multihazard assessment of Dominica, West Indies. *US-AID/COTS programme*. Available at http://doccentre.dlis.gov.dm/cgi-bin/koha/opac-detail.pl?biblionumber=43307/

Condeixa, K., Haddad, A., & Boer, D. (2017). Material flow analysis of the residential building stock at the city of Rio de Janeiro. *Journal of Cleaner Production*, *149*, 1249-1267.

Cuny, F. C. (2017). *Vulnerability Analysis of Traditional Housing in Dominica*. INTERTECT.

Cumberbatch, J., Drakes, C., Mackey, T., Nagdee, M., Wood, J., Degia, A. K., & Hinds, C. (2020). Social Vulnerability Index: Barbados–A Case Study. *Coastal Management*, *48*(5), 505-526.

Cutter, S. L., Ash, K. D., & Emrich, C. T. (2014). The geographies of community disaster resilience. *Global environmental change*, *29*, 65-77.

Cutter, S. L., Barnes, L., Berry, M., Burton, C., Evans, E., Tate, E., & Webb, J. (2008). A place-based model for understanding community resilience to natural disasters. *Global environmental change*, *18*(4), 598-606.

Cutter, S. L., Boruff, B. J., & Shirley, W. L. (2003). Social vulnerability to environmental hazards. *Social science quarterly*, *84*(2), 242-261.

Cutter, S. L., Emrich, C. T., Morath, D. P., & Dunning, C. M. (2013). Integrating social vulnerability into federal flood risk management planning. *Journal of Flood Risk Management*, *6*(4), 332-344.

Cutter, S. L., Mitchell, J. T., & Scott, M. S. (2000). Revealing the vulnerability of people and places: A case study of Georgetown County, South Carolina. *Annals of the association of American Geographers*, *90*(4), 713-737.

Daigo, I., Iwata, K., Oguchi, M., & Goto, Y. (2017). Lifetime distribution of buildings decided by economic situation at demolition: D-based lifetime distribution. *Procedia CIRP*, *61*, 146-151.

Dalrymple, T. (1960). *Flood-frequency analyses, manual of hydrology: Part 3* (No. 1543-A). USGPO.

Deetman, S., Marinova, S., van der Voet, E., van Vuuren, D. P., Edelenbosch, O., & Heijungs, R. (2020). Modelling global material stocks and flows for residential and service sector buildings towards 2050. *Journal of Cleaner Production*, *245*, 118658.

De Kroon, K. (2020). *Linking Services to Material Stocks: A GIS-based material stock-service analysis from island and city perspectives* (Master's thesis, University of Waterloo).

Doswell III, C. A., Brooks, H. E., & Maddox, R. A. (1996). Flash flood forecasting: An ingredients-based methodology. *Weather and Forecasting*, *11*(4), 560-581.

Eastern Caribbean Central Bank. (2021). THE COMMONWEALTH OF DOMINICA: Contribution of Gross Domestic Product by Economic Activity in Constant Prices in

Percentage (%). Available at <https://www.eccb-centralbank.org/statistics/gdp-datas/country-report/6> [Accessed 28 August 2021].

EM-DAT. (2022). The International Disaster Database. Available at: <https://www.emdat.be/> [Accessed 27 March]

European Commission. (2016). EU Overview of Methodologies Used in Preparation of Flood Hazard and Flood Risk Maps [online], Publications Office of the European Union, Luxembourg, 2016. ISBN 978-92-79-54718-8. Available at: <https://bit. ly/38Qb79K> [Accessed 6 September 2020].

Fischer-Kowalski, M., Swilling, M., Von Weizsacker, E. U., Ren, Y., Moriguchi, Y., Crane, W., ... & Sewerin, S. (2011). Decoupling*: natural resource use and environmental impacts from economic growth*. United Nations Environment Programme.

Fishman, T., Schandl, H., Tanikawa, H., Walker, P., & Krausmann, F. (2014). Accounting for the material stock of nations. *Journal of Industrial Ecology*, *18*(3), 407-420.

Flanagan, B. E., Gregory, E. W., Hallisey, E. J., Heitgerd, J. L., & Lewis, B. (2011). A social vulnerability index for disaster management. *Journal of homeland security and emergency management*, *8*(1).

Flowerdew, R., & Martin, D. (Eds.). (2005). *Methods in human geography: a guide for students doing a research project*. Pearson Education.

Fothergill, A. (1996). Gender, risk, and disaster. *International journal of mass emergencies and disasters*, *14*(1), 33-56.

Frankenberg, E., Sikoki, B., Sumantri, C., Suriastini, W., & Thomas, D. (2013). Education, vulnerability, and resilience after a natural disaster. *Ecology and society: a journal of integrative science for resilience and sustainability*, *18*(2), 16.

Fu, C., Zhang, Y., Deng, T., & Daigo, I. (2021). The evolution of material stock research: From exploring to rising to hot studies. *Journal of Industrial Ecology*.

Fuchs, S. (2009). Susceptibility versus resilience to mountain hazards in Austria-paradigms of vulnerability revisited. *Natural Hazards and Earth System Sciences, 9*(2), 337-352.

Galasso, C., Pregnolato, M., & Parisi, F. (2021). A model taxonomy for flood fragility and vulnerability assessment of buildings. *International Journal of Disaster Risk Reduction*, *53*, 101985.

Galasso, C., & Senarath, S. U. (2014). A Statistical Model for Flood Depth Estimation in

Southeast Europe. In *Vulnerability, Uncertainty, and Risk: Quantification, Mitigation, and Management* (pp. 1415-1424).

Gassner, A., Lederer, J., Kovacic, G., Mollay, U., Schremmer, C., & Fellner, J. (2021). Projection of material flows and stocks in the urban transport sector until 2050–A scenario-based analysis for the city of Vienna. *Journal of Cleaner Production*, 127591.

Goovaerts, P. (2000). Geostatistical approaches for incorporating elevation into the spatial interpolation of rainfall. *Journal of hydrology*, *228*(1-2), 113-129.

Government of the Commonwealth of Dominica. (2017). Post-disaster needs assessment: Hurricane Maria, September 18, 2017. Available at: <https://www.gfdrr.org/sites/default/files/publication/Dominica_mp_012418_web.pdf> [Accessed 18 October 2021].

Granger, K., Jones, T. G., Leiba, M., & Scott, G. (1999). Community risk in Cairns: a multi-hazard risk assessment. *Australian Journal of Emergency Management, The*, *14*(2), 25-26.

Haile, A. T., & Rientjes, T. H. M. (2005). Effects of LiDAR DEM resolution in flood modelling: a model sensitivity study for the city of Tegucigalpa, Honduras. *Isprs wg iii/3, iii/4*, *3*, 12-14.

Holand, I. S., & Lujala, P. (2013). Replicating and adapting an index of social vulnerability to a new context: a comparison study for Norway. *The Professional Geographer*, *65*(2), 312-328.

Holding, S., Allen, D. M., Foster, S., Hsieh, A., Larocque, I., Klassen, J., & Van Pelt, S. C. (2016). Groundwater vulnerability on small islands. *Nature Climate Change*, *6*(12), 1100-1103.

Houze Jr, R. A. (2012). Orographic effects on precipitating clouds. *Reviews of Geophysics*, *50*(1).

Huntington, T. G. (2006). Evidence for intensification of the global water cycle: Review and synthesis. *Journal of Hydrology*, *319*(1-4), 83-95.

IPCC. (2019). The Ocean and Cryosphere in a Changing Climate. Available at: <https://www.ipcc.ch/srocc/> [Accessed 18 October 2021].

Irvin, R. B., & McKeown, D. M. (1989). Methods for exploiting the relationship between buildings and their shadows in aerial imagery. *IEEE Transactions on Systems, Man, and Cybernetics*, *19*(6), 1564-1575.

Jetten, V. (2016). CHARIM project Dominica national flood hazard map methodology and validation report. Available at: <https://www.cdema.org/virtuallibrary/images/DOMFloodReport.pdf> [Accessed 6 October, 2021].

Jetten, V. (2018). OpenLISEM–Multi-Hazard Land Surface Process Model–Documentation & User Manual.

Jia, D. D., Zhou, J. Y., Shao, X. J., & Zhang, X. B. (2014). Three-dimensional flow structures and suspended-sediment transport in the dam area of large reservoir. In *Applied Mechanics and Materials* (Vol. 501, pp. 1981-1985). Trans Tech Publications Ltd.

Kale, R. V., & Sahoo, B. (2011). Green-Ampt infiltration models for varied field conditions: A revisit. *Water resources management*, *25*(14), 3505-3536.

Kalt, G., Thunshirn, P., Wiedenhofer, D., Krausmann, F., Haas, W., & Haberl, H. (2021). Material stocks in global electricity infrastructures–An empirical analysis of the power sector's stock-flow-service nexus. *Resources, Conservation and Recycling*, *173*, 105723.

Kappes, M. S., Papathoma-Koehle, M., & Keiler, M. (2012). Assessing physical vulnerability for multi-hazards using an indicator-based methodology. *Applied Geography*, *32*(2), 577-590.

Kastridis, A., Kirkenidis, C., & Sapountzis, M. (2020). An integrated approach of flash flood analysis in ungauged Mediterranean watersheds using post-flood surveys and unmanned aerial vehicles. *Hydrological Processes*, *34*(25), 4920-4939.

Kelfoun, K., Druitt, T., de Vries, B. V. W., & Guilbaud, M. N. (2008). Topographic reflection of the Socompa debris avalanche, Chile. *Bulletin of Volcanology*, *70*(10), 1169-1187.

Krausmann, F., Richter, R., & Eisenmenger, N. (2014). Resource use in small island states: Material flows in Iceland and Trinidad and Tobago, 1961–2008. *Journal of industrial ecology*, *18*(2), 294-305.

Krausmann, F., Wiedenhofer, D., Lauk, C., Haas, W., Tanikawa, H., Fishman, T., ... & Haberl, H. (2017). Global socioeconomic material stocks rise 23-fold over the 20th century and require half of annual resource use. *Proceedings of the National Academy of Sciences*, *114*(8), 1880-1885.

Kreibich, H., Piroth, K., Seifert, I., Maiwald, H., Kunert, U., Schwarz, J., ... & Thieken, A. H. (2009). Is flow velocity a significant parameter in flood damage modelling?. *Natural Hazards and Earth System Sciences*, *9*(5), 1679-1692.

Kron, W. (2002). Keynote lecture: Flood risk= hazard× exposure× vulnerability. *Flood defence*, 82-97.

Kunz, N. C., Moran, C. J., & Kastelle, T. (2013). Conceptualising "coupling" for sustainability implementation in the industrial sector: a review of the field and projection of future research opportunities. *Journal of cleaner production, 53,* 69-80.

Kuriakose, S. L., Devkota, S., Rossiter, D. G., & Jetten, V. G. (2009). Prediction of soil depth using environmental variables in an anthropogenic landscape, a case study in the Western Ghats of Kerala, India. *Catena*, *79*(1), 27-38.

Lanau, M., Liu, G., Kral, U., Wiedenhofer, D., Keijzer, E., Yu, C., & Ehlert, C. (2019). Taking stock of built environment stock studies: Progress and prospects. *Environmental science & technology*, *53*(15), 8499-8515.

Liang, H., Dong, L., Tanikawa, H., Zhang, N., Gao, Z., & Luo, X. (2017). Feasibility of a new-generation nighttime light data for estimating in-use steel stock of buildings and civil engineering infrastructures. *Resources, Conservation and Recycling*, *123*, 11-23.

Lichtensteiger, T., & Baccini, P. (2008). Exploration of urban stocks. *detail*, *5*(6), 16.

Mazzorana, B., Simoni, S., Scherer, C., Gems, B., Fuchs, S., & Keiler, M. (2014). A physical approach on flood risk vulnerability of buildings. *Hydrology and Earth System Sciences, 18*(9), 3817-3836.

Marchi, L., Borga, M., Preciso, E., Sangati, M., Gaume, E., Bain, V., ... & Pogačnik, N. (2009). Comprehensive post-event survey of a flash flood in Western Slovenia: observation strategy and lessons learned. *Hydrological Processes: An International Journal*, *23*(26), 3761-3770.

Marchi, L., Borga, M., Preciso, E., & Gaume, E. (2010). Characterization of selected extreme flash floods in Europe and implications for flood risk management. *Journal of Hydrology*, *394*(1-2), 118-133.

Marvi, M. T. (2020). A review of flood damage analysis for a building structure and contents. *Natural Hazards*, *102*(3), 967-995.

Mair, A., & Fares, A. (2011). Comparison of rainfall interpolation methods in a mountainous region of a tropical island. *Journal of hydrologic engineering*, *16*(4), 371-383.

Mathew, A. E., Kumar, S. S., Vivek, G., Iyyappan, M., Karthikaa, R., Kumar, P. D., ... & Usha, T. (2021). Flood impact assessment using field investigations and post-flood survey. *Journal of Earth System Science*, *130*(3), 1-10.

Matthews, E., Amann, C., Bringezu, S., Fischer-Kowalski, M., Hüttler, W., Kleijn, R., ... &

Weisz, H. (2000). The weight of nations. *Material outflows from industrial economies World Resources Institute, Washington*.

Mavhura, E., Manyena, B., & Collins, A. E. (2017). An approach for measuring social vulnerability in context: The case of flood hazards in Muzarabani district, Zimbabwe. *Geoforum*, *86*, 103-117.

McCarthy, J. J., Canziani, O. F., Leary, N. A., Dokken, D. J., & White, K. S. (Eds.). (2001). *Climate change 2001: impacts, adaptation, and vulnerability: contribution of Working Group II to the third assessment report of the Intergovernmental Panel on Climate Change* (Vol. 2). Cambridge University Press.

Menoni, S., Galderisi, A., Ceudech, A., Federico, N., Delmonaco, G., & Margottini, C. (2006). Harmonised hazard, vulnerability and risk assessment methods informing mitigation strategies addressing land-use planning and management. *ARMONIA PROJECT, Deliverable*, *5*.

Müller, D. B. (2006). Stock dynamics for forecasting material flows—Case study for housing in The Netherlands. *Ecological economics*, *59*(1), 142-156.

Nguyen, T. C., Fishman, T., Miatto, A., & Tanikawa, H. (2019). Estimating the material stock of roads: the vietnamese case study. *Journal of Industrial Ecology*, *23*(3), 663-673.

Nugent, A. D., & Rios-Berrios, R. (2018). Factors leading to extreme precipitation on Dominica from Tropical Storm Erika (2015). *Monthly Weather Review*, *146*(2), 525-541.

Nunez, C. (2023) Hurricanes, Cyclones, and Typhoons Explained. Available at https://education.nationalgeographic.org/resource/hurricanes-cyclones-and-typhoons-explained/

Obernosterer, R., Brunner, P. H., Daxbeck, H., Gagan, T., Glenck, E., Hendriks, C., ... & Reiner, I. (1998). Urban metabolism the city of Vienna. *Materials accounting as a tool for decision-making in environmental policy. 4th European Commission Programme for Environment and Climate. Institute of Water Quality and Waste management. Vienna University of Technology, Vienna*.

Ogden, F. L. (2016). Evidence of equilibrium peak runoff rates in steep tropical terrain on the island of Dominica during Tropical Storm Erika, August 27, 2015. *Journal of Hydrology*, *542*, 35-46.

Ortlepp, R., Gruhler, K., & Schiller, G. (2016). Material stocks in Germany's non-domestic buildings: a new quantification method. *Building Research & Information*, *44*(8), 840-862.

Ortlepp, R., Gruhler, K., & Schiller, G. (2018). Materials in Germany's domestic building stock: calculation model and uncertainties. *Building Research & Information*, *46*(2), 164-178.

Oulahen, G., Mortsch, L., Tang, K., & Harford, D. (2015). Unequal vulnerability to flood hazards:"ground truthing" a social vulnerability index of five municipalities in Metro Vancouver, Canada. *Annals of the Association of American Geographers*, *105*(3), 473-495.

O'Connor, J. E., & Costa, J. E. (2004). *The world's largest floods, past and present: their causes and magnitudes* (Vol. 1254). Geological Survey (USGS).

O'Dell, A. (1988). An evaluation of the house condition measurements in the context of the English house condition survey. In *CIB Conference, Tällberg*.

Papathoma-Köhle, M., Schlögl, M., & Fuchs, S. (2019). Vulnerability indicators for natural hazards: An innovative selection and weighting approach. *Scientific Reports*, *9*(1), 15026.

Pauliuk, S., Fishman, T., Heeren, N., Berrill, P., Tu, Q., Wolfram, P., & Hertwich, E. G. (2021). Linking service provision to material cycles: A new framework for studying the resource efficiency–climate change (RECC) nexus. *Journal of Industrial Ecology*, *25*(2), 260-273.

Pauliuk, S., Venkatesh, G., Brattebø, H., & Müller, D. B. (2014). Exploring urban mines: Pipe length and material stocks in urban water and wastewater networks. *Urban Water Journal*, *11*(4), 274-283.

Peled, Y., & Fishman, T. (2021). Estimation and mapping of the material stocks of buildings of Europe: a novel nighttime lights-based approach. *Resources, Conservation and Recycling*, *169*, 105509.

Petzold, J., & Magnan, A. K. (2019). Climate change: thinking small islands beyond Small Island Developing States (SIDS). *Climatic change*, *152*(1), 145-165.

Prakash, M., Rothauge, K., & Cleary, P. W. (2014). Modelling the impact of dam failure scenarios on flood inundation using SPH. *Applied Mathematical Modelling*, *38*(23), 5515-5534.

Pratomo, R. A. (2015). *Flash Flood Behaviour on a Small Caribbean Island: A Comparison of Two Watersheds in Grenada*. University of Twente Faculty of Geo-Information and Earth Observation (ITC).

Pribulick, C. E., Foster, L. M., Bearup, L. A., Navarre-Sitchler, A. K., Williams, K. H., Carroll, R. W., & Maxwell, R. M. (2016). Contrasting the hydrologic response due to land cover and climate change in a mountain headwaters system. *Ecohydrology*, *9*(8), 1431-1438.

Prieto, J. A., Journeay, M., Acevedo, A. B., Arbelaez, J. D., & Ulmi, M. (2018). Development of structural debris flow fragility curves (debris flow buildings resistance) using momentum flux rate as a hazard parameter. *Engineering Geology*, *239*, 144-157.

Pérez Molina, E. (2014). *Modelling urban growth and flooding interactions with cellular automata in Kampala, Uganda* (Master's thesis, University of Twente).

Rattray, J., & Jones, M. C. (2007). Essential elements of questionnaire design and development. *Journal of clinical nursing*, *16*(2), 234-243.

Saxton, K. E., & Willey, P. H. (2006). The SPAW model for agricultural field and pond hydrologic simulation. *Watershed models. CRC Press, Boca Raton, Fl*, 401-435.

Shao, Y., Taff, G. N., & Walsh, S. J. (2011). Shadow detection and building-height estimation using IKONOS data. *International journal of remote sensing*, *32*(22), 6929-6944.

Singh, S. J., Fischer-Kowalski, M., & Haas, W. (2018). The sustainability of humanitarian aid: The Nicobar islands as a case of 'complex disaster'. In *The Asian Tsunami and Post-Disaster Aid* (pp. 143-165). Springer, Singapore.

Singh, S. J., Fischer-Kowalski, M., & Chertow, M. (2020). Introduction: The metabolism of islands. *Sustainability*, *12*(22), 9516.

Smith, P. (2014). BIM implementation–global strategies. *Procedia engineering*, *85*, 482-492.

Smith, R. B., Schafer, P., Kirshbaum, D. J., & Regina, E. (2009). Orographic precipitation in the tropics: Experiments in Dominica. *Journal of Atmospheric Sciences*, *66*(6), 1698-1716.

Spielman, S. E., Tuccillo, J., Folch, D. C., Schweikert, A., Davies, R., Wood, N., & Tate, E. (2020). Evaluating social vulnerability indicators: criteria and their application to the Social Vulnerability Index. *Natural hazards*, *100*, 417-436.

Sprecher, B., Verhagen, T. J., Sauer, M. L., Baars, M., Heintz, J., & Fishman, T. (2021). Material intensity database for the Dutch building stock: Towards Big Data in material stock analysis. *Journal of Industrial Ecology*.

Starkloff, T., Stolte, J., Hessel, R., Ritsema, C., & Jetten, V. (2018). Integrated, spatial distributed modelling of surface runoff and soil erosion during winter and spring. *Catena*, *166*, 147-157.

Strahler, A. N. (1964). Part II. Quantitative geomorphology of drainage basins and channel networks. *Handbook of Applied Hydrology: McGraw-Hill, New York*, 4-39.

St Bernard, G. (2007). Measuring social vulnerability in Caribbean States. University of the West Indies (UWI).

Symmes, R., Fishman, T., Telesford, J. N., Singh, S. J., Tan, S. Y., & De Kroon, K. (2020). The weight of islands: Leveraging Grenada's material stocks to adapt to climate change. *Journal of Industrial Ecology*, *24*(2), 369-382.

Tabata, T., Zhang, O., Yamanaka, Y., & Tsai, P. (2016). Estimating potential disaster waste generation for pre-disaster waste management. *Clean Technologies and Environmental Policy*, *18*(6), 1735-1744.

Tanikawa, H., Fishman, T., Hashimoto, S., Daigo, I., Oguchi, M., Miatto, A., ... & Schandl, H. (2021). A framework of indicators for associating material stocks and flows to service provisioning: Application for Japan 1990–2015. *Journal of Cleaner Production*, *285*, 125450.

Tanikawa, H., Fishman, T., Okuoka, K., & Sugimoto, K. (2015). The weight of society over time and space: A comprehensive account of the construction material stock of Japan, 1945–2010. *Journal of Industrial Ecology*, *19*(5), 778-791.

Tanikawa, H., Managi, S., & Lwin, C. M. (2014). Estimates of lost material stock of buildings and roads due to the Great East Japan Earthquake and tsunami. *Journal of Industrial Ecology*, *18*(3), 421-431.

Takken, I., Beuselinck, L., Nachtergaele, J., Govers, G., Poesen, J., & Degraer, G. (1999). Spatial evaluation of a physically-based distributed erosion model (LISEM). *Catena*, *37*(3-4), 431-447.

Tayefi, V., Lane, S. N., Hardy, R. J., & Yu, D. (2007). A comparison of one-and two-dimensional approaches to modelling flood inundation over complex upland floodplains. *Hydrological Processes: An International Journal*, *21*(23), 3190-3202.

Teng, J., Jakeman, A. J., Vaze, J., Croke, B. F., Dutta, D., & Kim, S. (2017). Flood inundation modelling: A review of methods, recent advances and uncertainty analysis. *Environmental modelling & software*, *90*, 201-216.

Tierney, K. (2006). Social inequality, hazards, and disasters. *On risk and disaster: Lessons from Hurricane Katrina*, 109-128.

Tobler, W. R. (1970). A computer movie simulating urban growth in the Detroit region. *Economic geography*, *46*(sup1), 234-240.

UNDP. (2017, September). *Small Island Nations at the frontline of climate action*. Retrieved from United Nations Development Programme:
https://www.undp.org/content/undp/en/home/presscenter/pressreleases/2017/09/18/smallisland-nations-at-the-frontline-of-climate-action-.html

UN (United Nation). (2023). THE 17 GOALS. Retrieved from: https://sdgs.un.org/goals

UNESCO (United Nations Educational, Scientific and Cultural Organization). (2021). Fort Shirley. Available at: < https://whc.unesco.org/en/tentativelists/6020> [Accessed 6 October, 2021].

UNDRR (United Nations Office for Disaster Reduction). (2015). Sendai Framework for Disaster Risk Reduction 2015 – 2030. Sendai: UN Publications. [online] Available at: <https://www.preventionweb.net/files/43291_sendaiframeworkfordrren.pdf> [Accessed 6 September 2020].

U.S. Environmental Protection Agency (2015) Climate change in the United States—benefits of global action. Benefits of Global Action. *Environmental Protection Agency, Office of Atmospheric Programs*. EPA 430-R-15-001, p 94

Venkatesh, G., Hammervold, J., & Brattebø, H. (2009). Combined MFA-LCA for analysis of wastewater pipeline networks: Case study of Oslo, Norway. *Journal of Industrial Ecology*, *13*(4), 532-550.

Wang, T., Zhou, J., Yue, Y., Yang, J., & Hashimoto, S. (2016). Weight under Steel Wheels: Material Stock and Flow Analysis of High-Speed Rail in China. *Journal of Industrial Ecology*, *20*(6), 1349-1359.

Wiedenhofer, D., Steinberger, J. K., Eisenmenger, N., & Haas, W. (2015). Maintenance and expansion: modelling material stocks and flows for residential buildings and transportation networks in the EU25. *Journal of Industrial Ecology*, *19*(4), 538-551.

Wilhelmsen, A. M. (1982). Methods for surveying and describing the building stock. In *Proceeding of the CIB W* (Vol. 70, p. 1981).

World Meteorological Organization. (2022). Storm Surge. Available at: https://public.wmo.int/en/our-mandate/focus-areas/natural-hazards-and-disaster-risk-reduction/storm-surge

Yan, K., Di Baldassarre, G., Solomatine, D. P., & Schumann, G. J. P. (2015). A review of low-cost space-borne data for flood modelling: topography, flood extent and water level. *Hydrological processes*, *29*(15), 3368-3387.

Yu, D., & Lane, S. N. (2006). Urban fluvial flood modelling using a two-dimensional diffusion-wave treatment, part 1: mesh resolution effects. *Hydrological Processes: An International Journal*, *20*(7), 1541-1565.

Zhang, B., Wu, B., Ren, S., Zhang, R., Zhang, W., Ren, J., & Chen, Y. (2021). Large-scale 3D numerical modelling of flood propagation and sediment transport and operational strategy in the Three Gorges Reservoir, China. *Journal of Hydro-environment Research*, *36*, 33-49.

Appendix A. Supplementary Information for MS Accounting in Dominica

A.1 Occupancy Class Examples

Each building occupancy class is given an example in this appendix. The building footprint (with a colored background showing land use), the Google Imagery, and the screenshot of the aerial video (or Google Photo) are presented together.

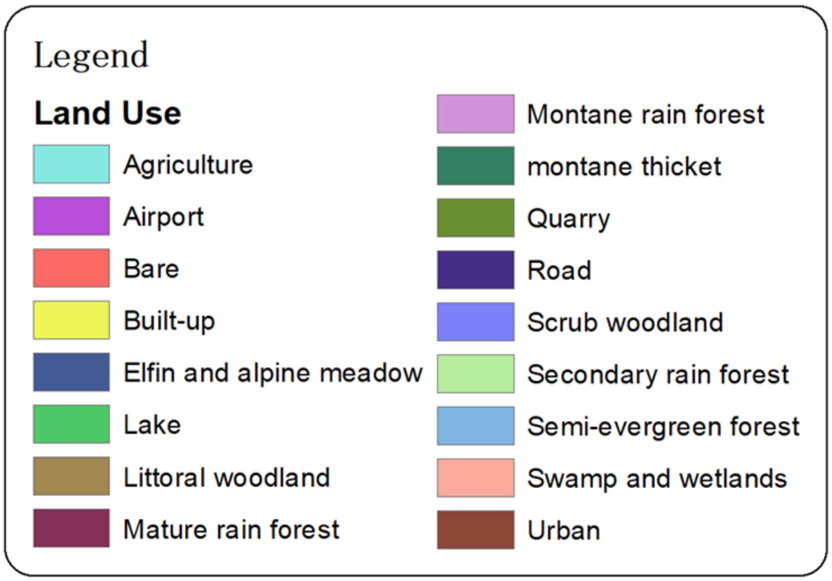

Figure A.1: *Background colors used to distinguish land use as one of the criteria of building classification.*

A.1.1 Institutional Buildings - 100

A.1.1.1 Cathedral - 111

Gospel Mission Church (Brick Historical Structure)

(Aerial video screenshot) (Google Imagery, 2018) (OSM building footprint)

Figure A.2: *An example of the cathedral building occupancy class (code 111) in Brick Historical Structure.*

A.1.1.2 Church - 112

Marigot Methodist Church (Concrete Structure 2)

(Aerial video screenshot) (Google Imagery, 2018) (OSM building footprint)

Figure A.3: *An example of the church building occupancy class (code 112) in Concrete Structure 2.*

A.1.1.3 Educational Campus Building - 121

Dominica State College (Concrete Structure 2)

(Aerial video screenshot) (Google Imagery, 2021) (OSM building footprint)

Figure A.4: *An example of the educational campus building occupancy class (code 121) in Concrete Structure 2.*

A.1.1.4 Standalone School - 122

Colihaut Primary School (Concrete Structure 2)

(Aerial video screenshot) (Google Imagery, 2018) (OSM building footprint)

Figure A.5: *An example of the standalone school building occupancy class (code 122) in Concrete Structure 2.*

A.1.1.5 Major Hospital - 131
Portsmouth Hospital (Reinforced Concrete Structure)

(Aerial video screenshot) (Google Imagery, 2021) (OSM building footprint)

Figure A.6: *An example of the major hospital building occupancy class (code 131) in Reinforced Concrete Structure.*

A.1.1.3 Health Center - 132
New Castle Bruce Health Center (Concrete Structure 2)

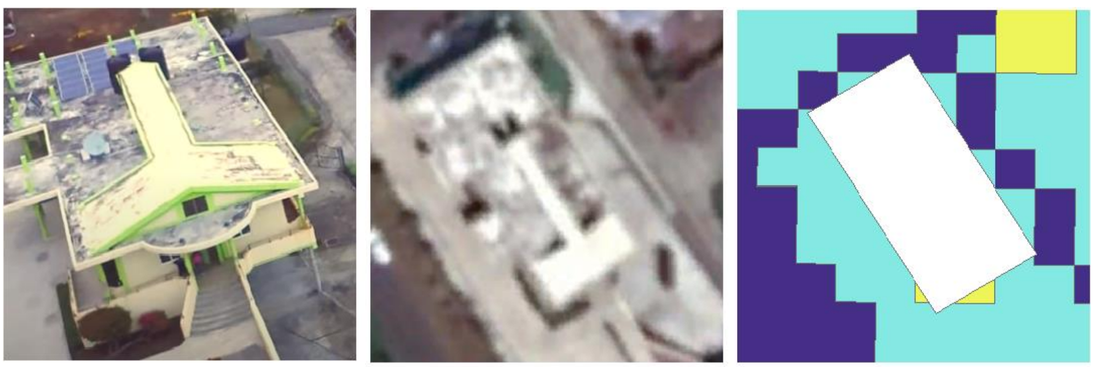

(Aerial video screenshot) (Google Imagery, 2018) (OSM building footprint)

Figure A.7: *An example of the health centre building occupancy class (code 132) in Reinforced Concrete Structure.*

A.1.1.4 Government Office - 140
Dominica Government Headquarters (Reinforced Concrete Structure)

(Aerial video screenshot) (Google Imagery, 2021) (OSM building footprint)

Figure A.8: *An example of the government office building occupancy class (code 140) in Reinforced Concrete Structure.*

A.1.2 Industrial/Commercial - 200

A.1.2.1 Commercial - 210

Calibishie Tourist Center (Concrete Structure 2)

(Aerial video screenshot) (Google Imagery, 2021) (OSM building footprint)

Figure A.9: *An example of the commercial building occupancy class (code 210) in Concrete Structure 2.*

A.1.2.2 Urban Mixed Commercial - 220

Courts (Concrete Structure 2)

(Aerial video screenshot) (Google Imagery, 2021) (OSM building footprint)

Figure A.10: *An example of the urban mixed commercial building occupancy class (code 220) in Concrete Structure 2.*

A.1.2.3 Industrial - 230

Dominica Brewery & Beverages (Composite Industrial Structure)

(Aerial video screenshot) (Google Imagery, 2020) (OSM building footprint)

Figure A.11: *An example of the industrial building occupancy class (code 230) in Composite Industrial Structure.*

A.1.3 Residential - 300

A.1.3.1 Urban Single-family Dwelling - 310

A residential building in Portsmouth (Composite Residential Structure)

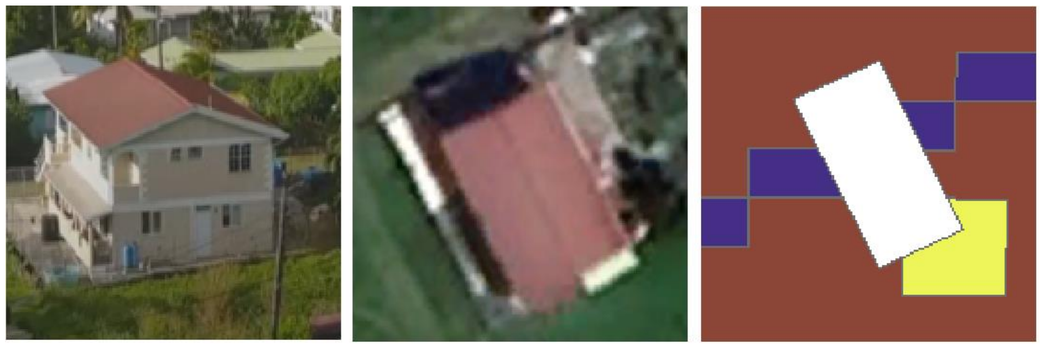

(Aerial video screenshot) (Google Imagery, 2021) (OSM building footprint)

Figure A.12: *An example of the urban single-family dwelling occupancy class (code 310) in composite residential structure.*

A.1.3.2 High-density Apartment Building - 321

An apartment in Roseau (Concrete Structure 2)

(Aerial video screenshot) (Google Imagery, 2021) (OSM building footprint)

Figure A.13: *An example of the high-density apartment building occupancy class (code 321) in Concrete Structure 2.*

A.1.3.3 Low-density Apartment Building - 322

An apartment in Wesley (Concrete Structure 2)

(Aerial video screenshot) (Google Imagery, 2021) (OSM building footprint)

Figure A.14: *An example of the low-density apartment building occupancy class (code 322) in Concrete Structure 2.*

A.1.3.4 Rural Single-family dwelling - 330

A house in Wesley (Composite Residential Structure)

(Aerial video screenshot)   (Google Imagery, 2021)   (OSM building footprint)

Figure A.15: *An example of the rural single-family dwelling building occupancy class (code 330) in composite residential structure.*

A.1.3.5 Residential-area Single-family Dwelling - 340

Bellevue Chopin Housing Project (Composite Residential Structure)

(Google Photo)   (Google Imagery, 2021)   (OSM building footprint)

Figure A.16: *An example of the residential-area single-family dwelling building occupancy class (code 340) in composite residential structure.*

A.1.4 Tourism - 400

A.1.4.1 Large Multi-unit Hotel Building - 411

Cabrits Kempinski Resort (Reinforced Concrete Structure)

(Aerial video screenshot) (Google Imagery, 2021) (OSM building footprint)

Figure A.17: *An example of the large multi-unit hotel building occupancy class (code 411) in the reinforced concrete structure.*

A.1.4.2 Small Hotel/Villa - 412

Oceanview Apartments (Concrete Structure 2)

(Aerial video screenshot) (Google Imagery, 2021) (OSM building footprint)

Figure A.18: *An example of the small hotel/villa building occupancy class (code 412) in Concrete Structure 2.*

A.1.5 Cultural - 500

A.1.5.1 Stadium - 510

Windsor Park Stadium (Reinforced Concrete Structure)

(Aerial video screenshot) (Google Imagery, 2021) (OSM building footprint)

Figure A.19: *An example of the stadium building occupancy class (code 510) in the reinforced concrete structure.*

A.1.5.2 Recreational Center - 520

Portsmouth Youth Centre (Concrete Structure 2)

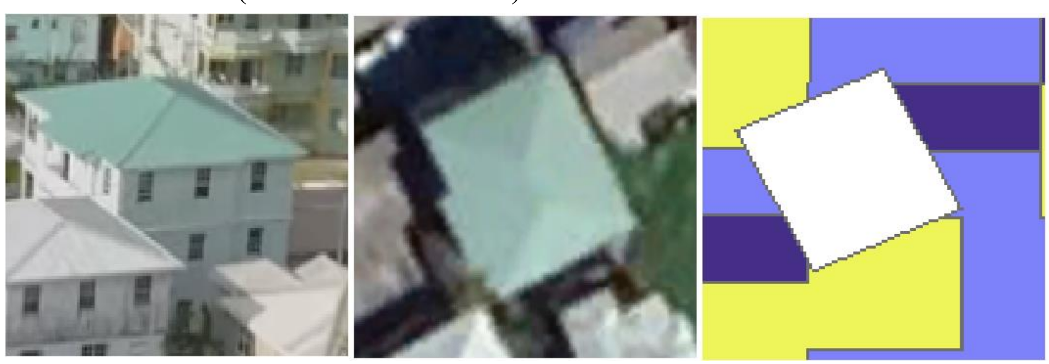

(Aerial video screenshot) (Google Imagery, 2021) (OSM building footprint)

Figure A.20: *An example of the recreational centre building occupancy class (code 520) in Concrete Structure 2.*

A.1.5.3 Historic Building - 530

Fort Shirley (Brick Historical Structure)

(Aerial video screenshot) (Google Imagery, 2021) (OSM building footprint)

Figure A.21: *An example of the historic building occupancy class (code 530) in Brick Historical Structure.*

A.1.6 Transport - 600

A.1.6.1 Seaport - 610

A seaport in Portsmouth (Concrete Structure 2)

(Aerial video screenshot) (Google Imagery, 2021) (OSM building footprint)

Figure A.22: *An example of the seaport building occupancy class (code 610) in Concrete Structure 2.*

A.1.6.2 Airport - 620

Canefield Airport Terminal (Reinforced Concrete Structure)

(Google Photo) (Google Imagery, 2021) (OSM building footprint)

Figure A.23: *An example of the airport building occupancy class (code 620) in the reinforced concrete structure.*

A.2 Material Intensity Typologies Used for MSA

Table A.1: *Adopted material intensity typologies with relevant building construction types (Symmes et al., 2020) and corresponding construction types identified by Cuny (2017) (if applicable). Unit: kg/m^2.*

Material intensity typology	Aggregate	Timber	Concrete	Steel	Concept Sketch (Cuny, 2017)	Relevant occupancy classes (codes)
Concrete Structure 1						310 330 340
Foundation - Pad footings	45	-	45	1		
Foundation - Posts	-	-	300	5		
Floors	-	-	450	10		
Walls	-	-	520	1		
Roof - Frame	-	40	-	-		
Roof - Covering	-	-	-	10		
Total	**45**	**40**	**1315**	**27**		
Concrete Structure 2						112 412 121 520 122 610 132 312 210 322 220 230 (80%) 310 (30.2%) 330 (30.2%) 340 (30.2%)
Foundation -Strip footings	135	-	225	5		
Foundation - Ground slab	24	-	450	10		
Floors	-	-	450	10		
Walls	-	-	520	1		
Roof - Frame	-	40	-	-		
Roof - Covering	-	-	-	10		
Total	**159**	**40**	**1645**	**36**		

Timber Structure						310 (27.6%) 330 (27.6%) 340 (27.6%)
Foundation - Pad footings	45	-	45	1		
Foundation - Posts	-	-	300	5		
Floors	-	-	-	20		
Walls	-	50	-	-		
Roof - Frame	-	40	-	-		
Roof - Covering	-	-	-	10		
Total	**45**	**90**	**345**	**36**		
Concrete/Timber Mix Structure						310 (10.8%) 330 (10.8%) 340 (10.8%)
Foundation -Strip footings	135	-	225	5		
Foundation - Ground slab	24	-	450	10		
Floors	-	-	450	10		
Walls	-	50	-	-		
Roof - Frame	-	40	-	-		
Roof - Covering	-	-	-	10		
Total	**159**	**90**	**1125**	**35**		
Steel Structure					-	230 (20%)
Foundation -Strip footings	135	-	225	5		
Foundation - Ground slab	24	-	450	10		
Floors	-	-	450	10		
Walls	-	-	520	145		
Roof - Frame	-	-	-	145		
Roof - Covering	-	-	-	10		
Total	**159**	**0**	**1645**	**325**		

Brick Historical Structure					-	111 530
Foundation -Strip footings	135	-	225	5		
Foundation - Ground slab	24	-	450	10		
Floors	-	-	-	20		
Walls	-	50	-	-		
Roof - Frame	-	40	-	-		
Roof - Covering	-	-	-	-		
Total	**159**	**90**	**675**	**35**		
Reinforced Concrete Structure					-	131 140 411 510 620
Foundation -Strip footings	135	-	225	5		
Foundation - Ground slab	24	-	450	10		
Floors	-	-	450	10		
Walls	-	-	-	145		
Roof	-	-	-	10		
Total	**159**	**0**	**1125**	**180**		

Note: The percentage in the last column quantifies the allocation of the material intensity typology in the occupancy class. For example, the industrial occupancy class (code 230) is allocated 80% of Concrete Structure 2 and 20% of Steel Structure, so its final material intensities are: 159 kg/m^2 for aggregate, 32kg/m^2 for timber, 1645kg/m^2 for concrete, and 93.8kg/m^2 for steel.

Appendix B. Supplementary Information for Flash Flood Modelling

B.1 Series of Rainfall Intensities for the Design Rainfall Events

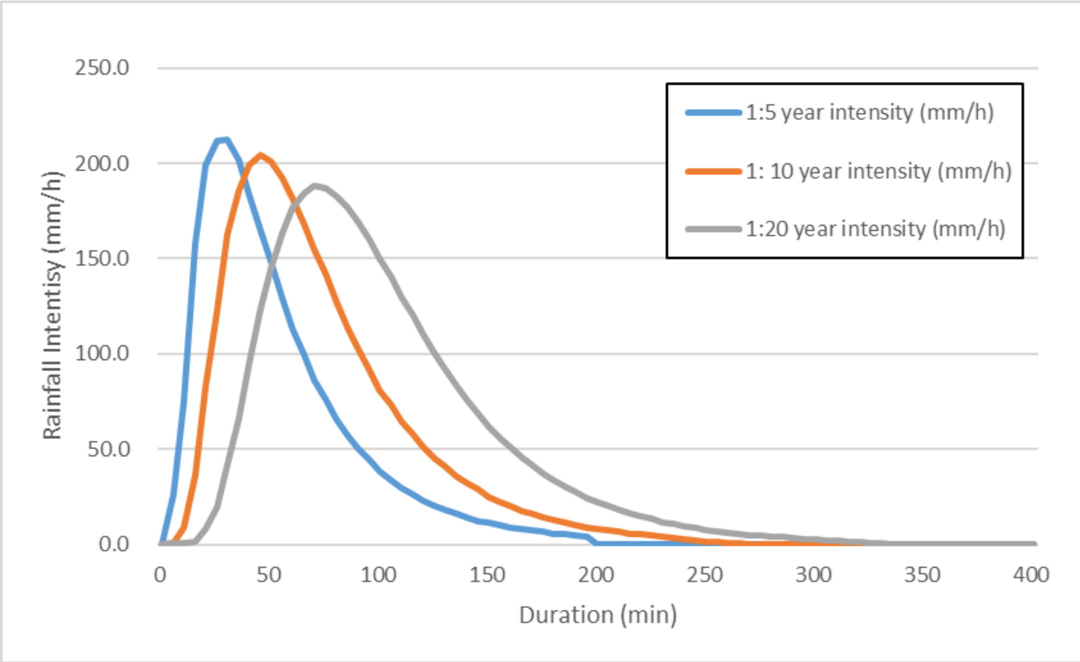

Figure B.1: *The IDF curves for design rainfall events of the three return periods., adopted from Jetten (2016).*

Table B.1: *Five-min rainfall intensities for the design rainfall events of the three return periods.*

Time (min)	Rainfall Intensity (mm/h)		
	1:5 year	**1:10 year**	**1: 20 year**
0	0.0	0.0	0.0
5	26.0	0.4	0.4
10	74.6	9.0	0.8
15	157.8	36.5	1.1
20	198.9	82.5	7.9
25	211.7	122.4	19.6
30	212.4	162.7	41.4
35	201.5	185.3	65.9
40	183.8	199.2	94.9
45	164.6	204.1	123.5
50	148.4	200.8	144.6
55	129.2	192.5	163.1
60	112.6	181.2	176.6
65	99.4	168.0	184.2
70	86.3	154.4	187.9
75	76.1	141.6	187.2
80	65.9	127.7	183.1
85	57.3	113.7	176.6

90	50.5	102.8	169.5
95	44.1	91.5	160.1
100	38.4	81.0	149.9
105	33.9	73.1	140.5
110	29.8	64.8	129.6
115	26.4	58.0	120.5
120	23.0	51.2	110.0
125	20.3	45.2	100.2
130	18.1	40.7	92.3
135	15.8	35.8	83.6
140	14.3	32.0	75.7
145	12.4	28.6	68.9
150	11.3	25.2	62.1
155	9.8	22.2	55.7
160	9.0	20.0	51.2
165	7.9	17.7	46.0
170	7.2	15.8	41.8
175	6.4	14.3	37.3
180	5.6	12.8	33.5
185	5.3	11.3	30.5
190	4.5	10.2	27.5
195	3.8	9.0	24.5
200	0.0	8.3	22.2
205	0.0	7.2	20.0
210	0.0	6.4	18.1
215	0.0	5.6	16.2
220	0.0	5.3	14.7
225	0.0	4.5	13.2
230	0.0	4.1	11.7
235	0.0	3.4	10.5
240	0.0	2.6	9.4
245	0.0	1.9	8.7
250	0.0	1.5	7.5
255	0.0	1.1	6.8
260	0.0	0.8	6.0
265	0.0	0.4	5.3
270	0.0	0.0	4.9
275	0.0	0.0	4.5
280	0.0	0.0	4.1
285	0.0	0.0	3.8
290	0.0	0.0	3.4
295	0.0	0.0	3.0
300	0.0	0.0	2.6
305	0.0	0.0	2.3
310	0.0	0.0	1.9
315	0.0	0.0	1.5
320	0.0	0.0	1.1
325	0.0	0.0	0.8
330	0.0	0.0	0.4

B.2 River Dimension Input Maps

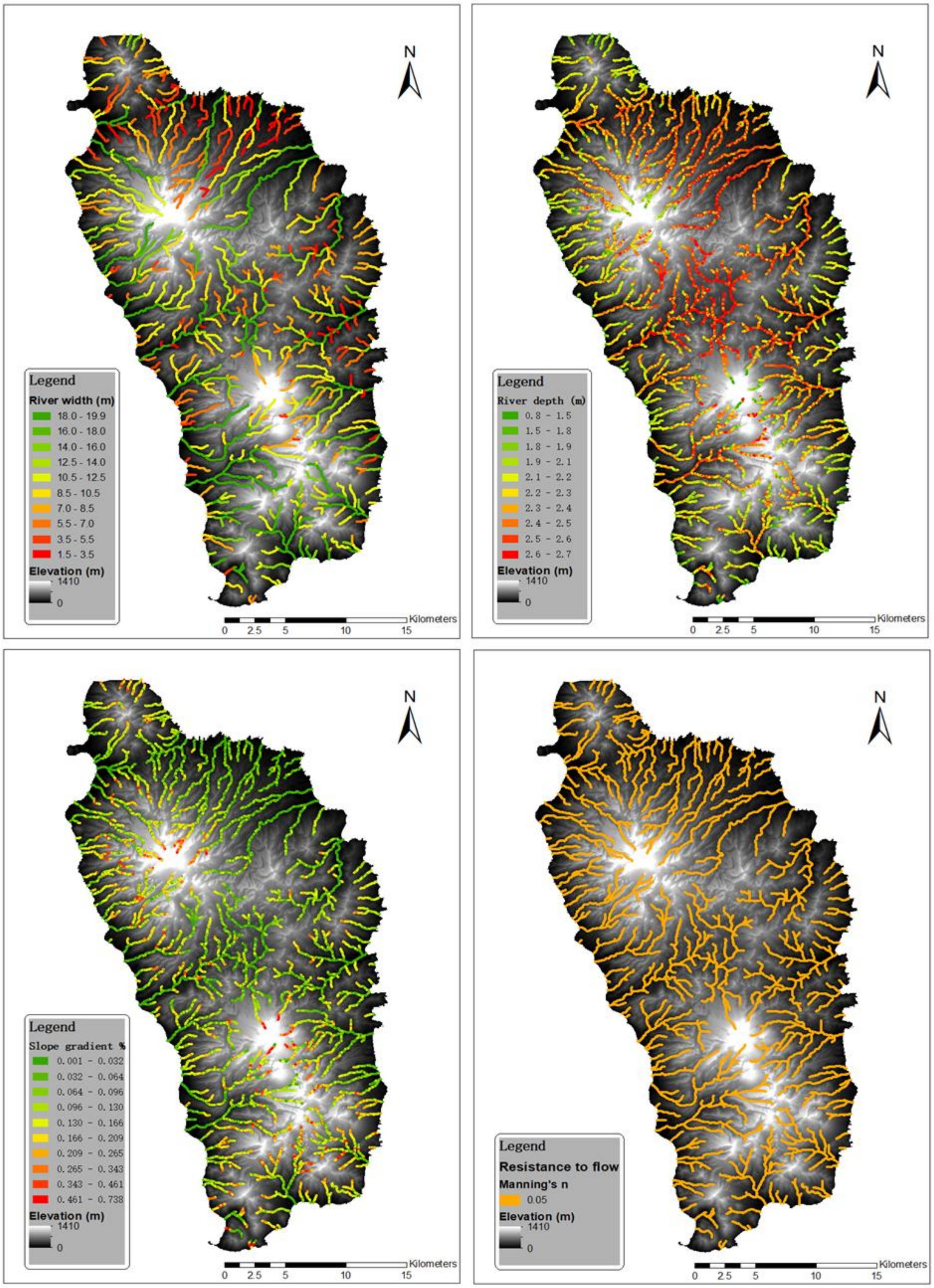

Figure B.2: *Input maps relevant to river channel dimensions and riverbed flow resistance. Top left: river width; Top right: river depth; Bottom left: gradient in percentage; Bottom right: channel resistance to flow as manning's n (assumed to be consistent at 0.05).*

B.3 Soil Physical Parameters Input Maps

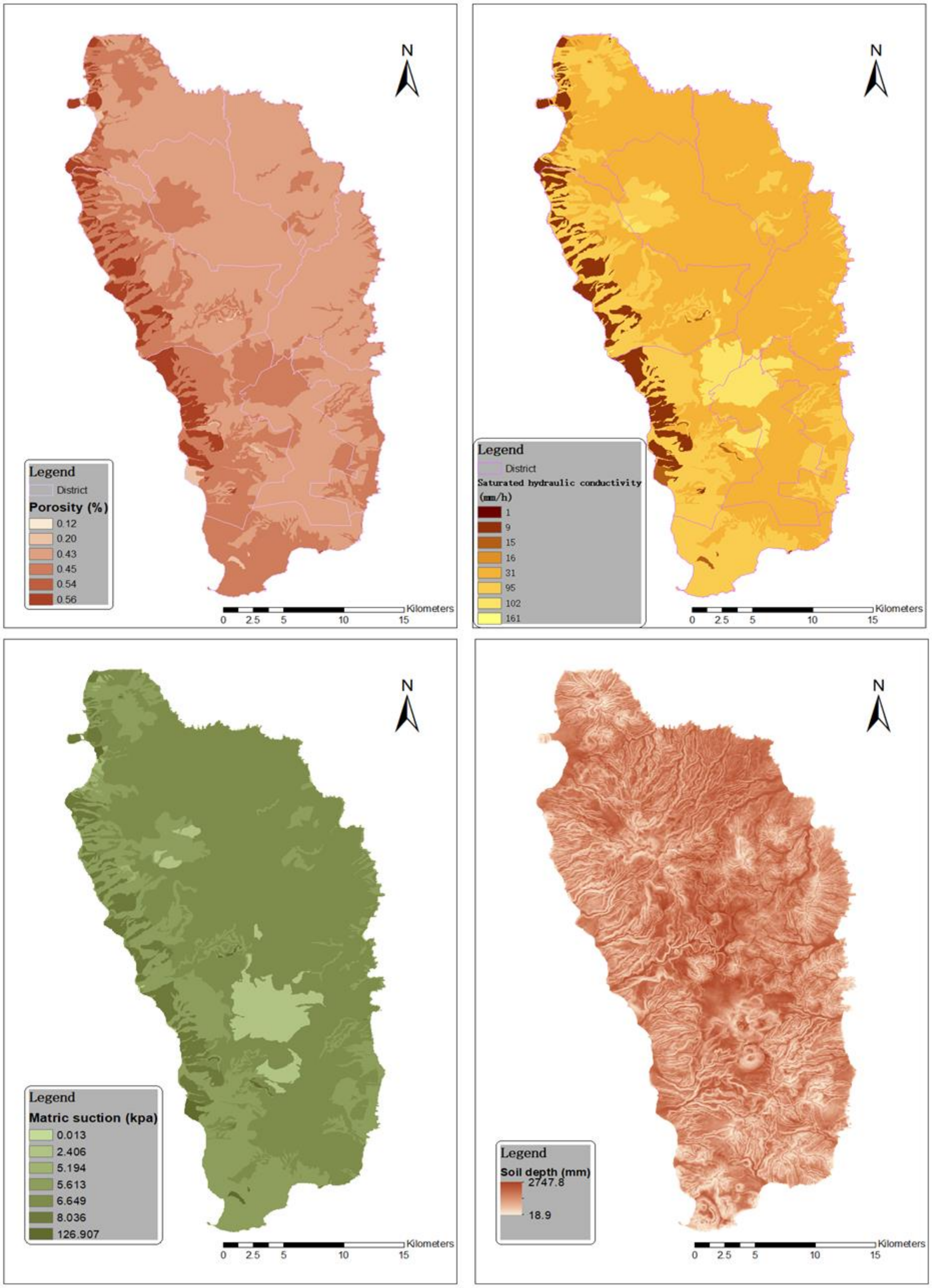

Figure B.3: *The input maps relevant to soil physical properties. Top left: porosity; Top right: saturated hydraulic conductivity; Bottom left: matric suction at the wetting front; Bottom right: soil depth.*

B.4 Buildings and Roads Input Maps

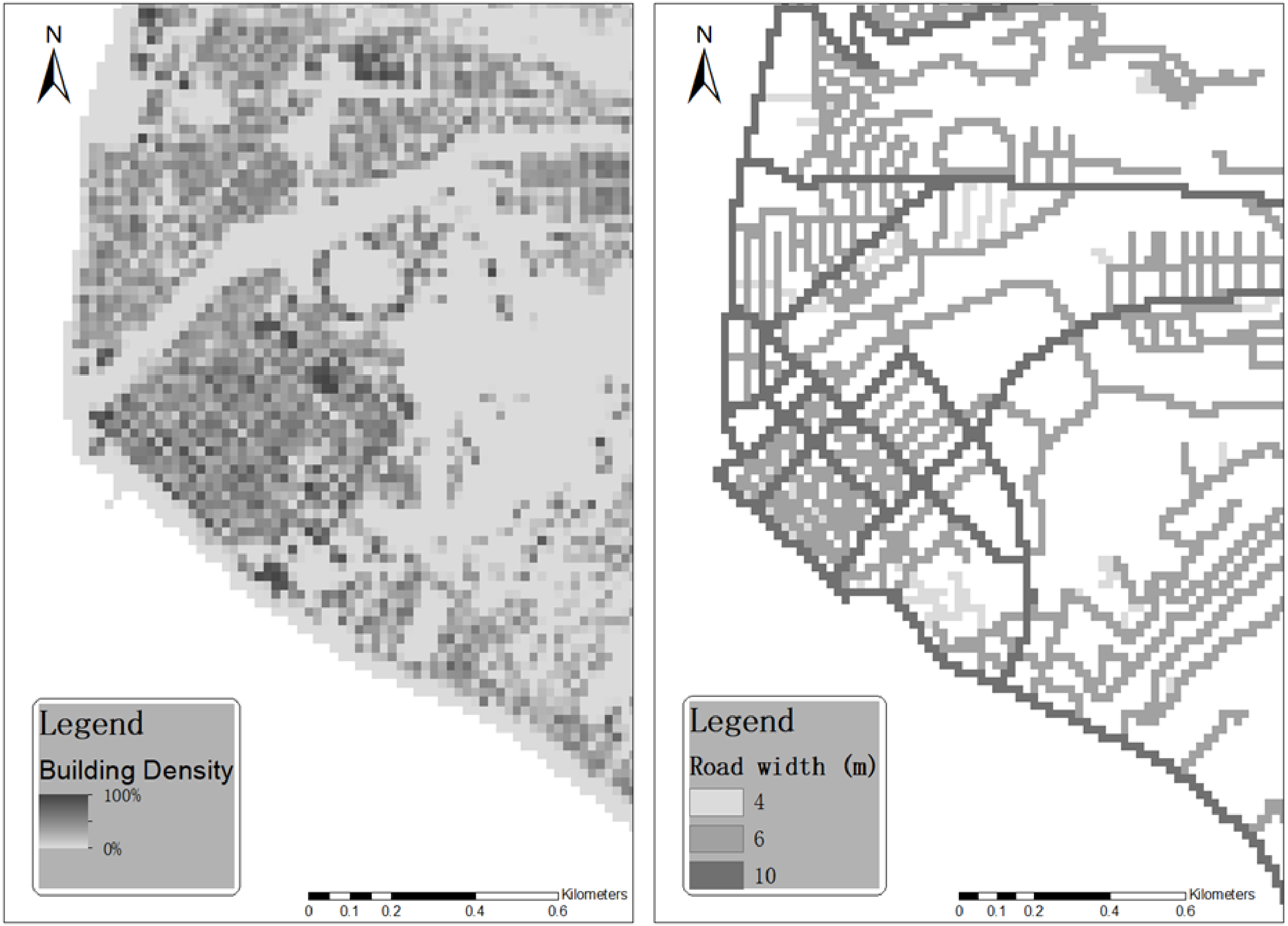

Figure B.4: *Local-scale input maps of building density and road width in the capital city of Roseau. Left: fraction of building occupation as building density; Right: road width.*

B.5 Land Use Input Maps

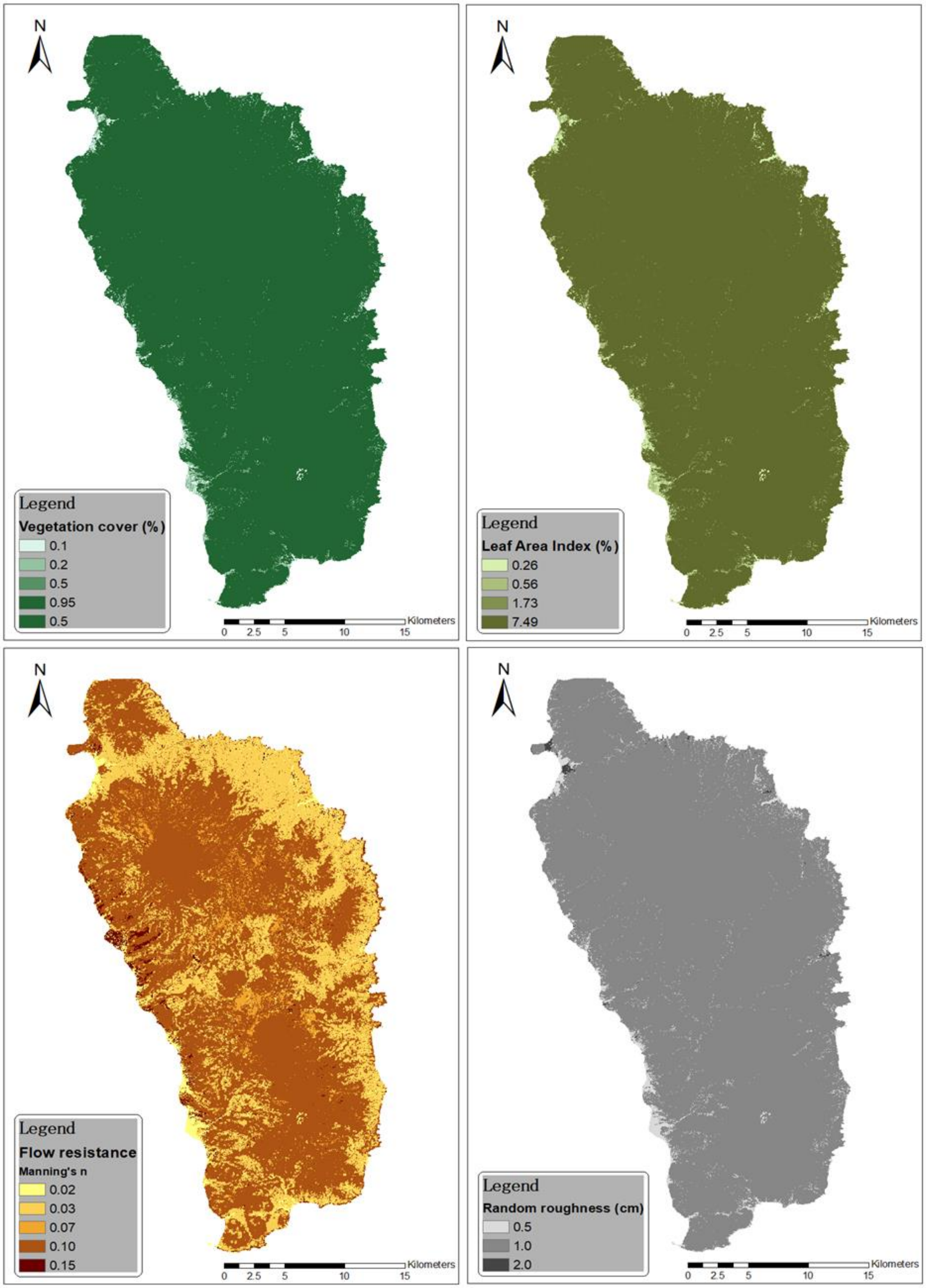

Figure B.5: *The input maps of land use-derived surface properties. Top left: vegetation cover; Top right: leaf area index; Bottom left: flow resistance in manning's n; Bottom right: surface random roughness.*

B.6 LISEM Run Options

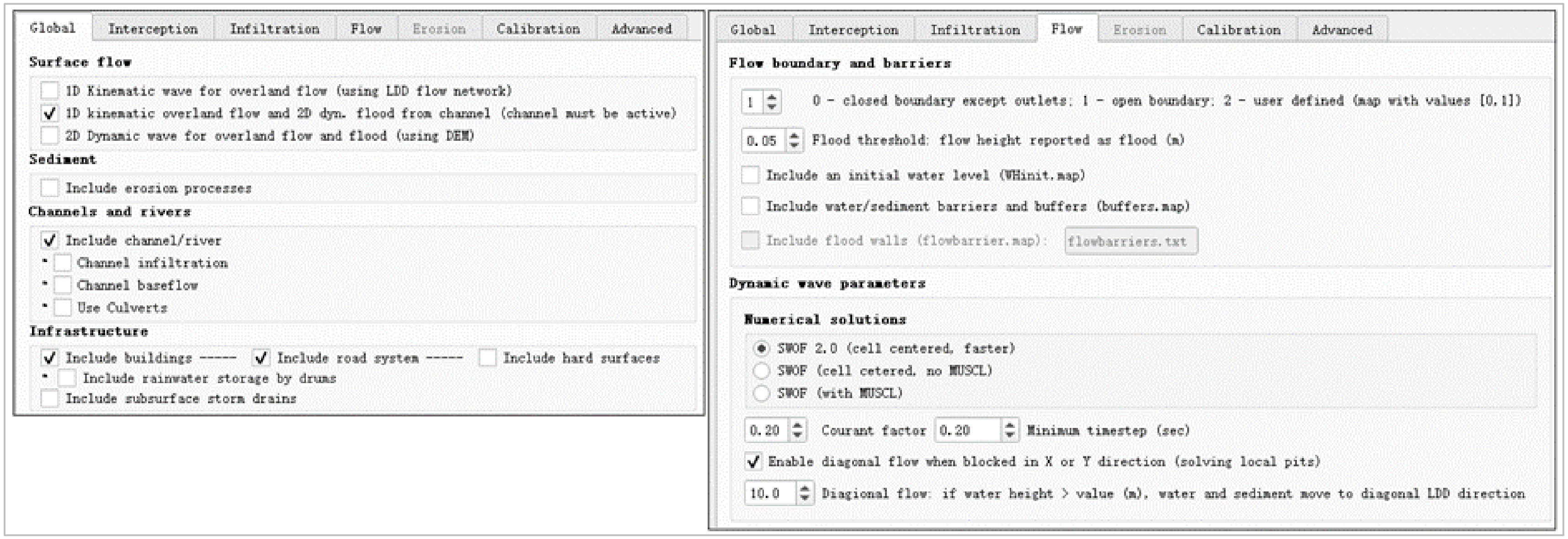

Figure B.6: *LISEM run options with interception and infiltration sections set as default for the lack of relevant datasets to optimize the model.*

B.7 Infiltration Maps for the Simulated Flash Flood Events for the Three Return Periods

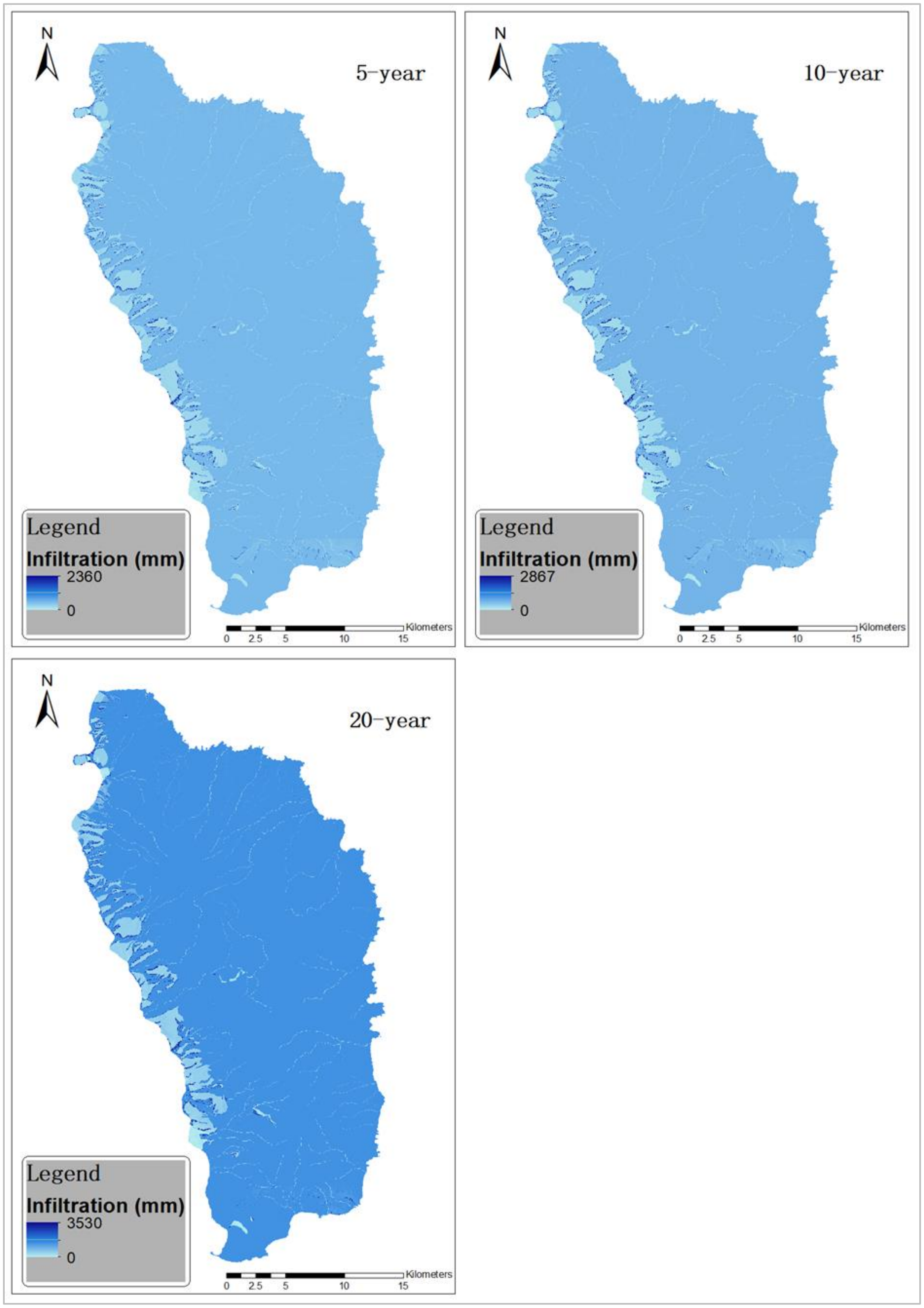

Figure B.7: *Output infiltration maps for the three simulated flash flooding events. Top left: 5-year flood event; Top right: 10-year flood event; Bottom left: 20-year flood event.*

Appendix C. Supplementary Information for Collecting Vulnerability Factors to Flooding in Dominica

C.1 Commonly Used Variables for Vulnerability to Flooding Collected from Literature

Table C.1: *Commonly used variables for vulnerability to flooding and their adaptability to the household level (SIS stands for small island states).*

Concept of Vulnerability	Description	Original Scale(s)	Reference(s)
Age	Percent of population under the age of five	SIS Parish, U.S. County, SIS Enumeration District (ED)	Boruff & Cutter (2007); Cutter, Boruff & Shirley, (2003); Cumberbatch et al., (2020)
	Percentage of population attending primary school	SIS Parish	Boruff & Cutter (2007)
	Percentage of population aged 65 or above	SIS Parish, U.S. County, Orleans Parish	Boruff & Cutter (2007); Cutter, Boruff & Shirley, (2003); Flanagan et al., (2011)
	Median age	U.S. County	Cutter, Boruff & Shirley, (2003)
Population growth	Number of birth per 1,000 population	U.S. County	Cutter, Boruff & Shirley, (2003)
	Number of housing units per area unit	U.S. county SIS parish	Cutter, Boruff & Shirley, (2003); Boruff & Cutter (2007)
	Number of housing units per new residential construction per area unit	U.S. County	Cutter, Boruff & Shirley, (2003)

	Percent population change	U.S. County	Cutter, Boruff & Shirley, (2003)
Commercial and industrial development	Number of manufacturing establishments per area unit	U.S. County	Cutter, Boruff & Shirley, (2003)
	Number of commercial establishments per area unit	U.S. County	Cutter, Boruff & Shirley, (2003)
	Value of property and farm products sold per area unit	U.S. County	Cutter, Boruff & Shirley, (2003)
	Profit in all industries per area unit	U.S. County	Cutter, Boruff & Shirley, (2003)
Education	Percentage of population 25 years or older with no high school diploma	U.S. County, Orleans Parish	Cutter, Boruff & Shirley, (2003); Flanagan et al., (2011)
	Percentage of population 20 years and over with exposure to tertiary level education	SIS Nation	St. Bernard (2007)
	Percentage of population aged 15 years and over with computer literacy	SIS Nation	St. Bernard (2007)
	Literacy rate of population 15 years or older	Chinese County	Chen et al., (2013)
Employment loss	Percent of the population in the labor force	U.S. County	Cutter, Boruff & Shirley, (2003)
	Percent of labor force unemployed	U.S. County, Orleans Parish, SIS ED	Cutter, Boruff & Shirley, (2003); Flanagan et al.,

			(2011), Cumberbatch et al., (2020)
	Percentage of population employed	SIS Parish	Boruff & Cutter (2007)
Socioeconomic status (income, political power, prestige)	Per capita income	U.S. County, Orleans Parish	Cutter, Boruff & Shirley, (2003); Flanagan et al., (2011)
	Percent voting for leading party	U.S. County	Cutter, Boruff & Shirley, (2003)
	Percent of households with an annual income over [certain amount]	U.S. County	Cutter, Boruff & Shirley, (2003)
	Percent living in poverty	U.S. County Orleans Parish	Cutter, Boruff & Shirley, (2003); Flanagan et al., (2011)
Infrastructure and lifelines	General local government debt to revenue ratio	U.S. County	Cutter, Boruff & Shirley, (2003)
Residential property	Median monetary value of owner-occupied housing	U.S. County	Cutter, Boruff & Shirley, (2003)
	Percent mobile homes	U.S. County; Orleans Parish	Cutter, Boruff & Shirley, (2003); Flanagan et al., (2011)
Renters	Percent renter-occupied housing	U.S. County	Cutter, Boruff & Shirley, (2003)
	Median monetary value of renter-occupied housing	U.S. County	Cutter, Boruff & Shirley, (2003)
Gender	Percent female population	SIS Parish,	Boruff & Cutter

		SIS ED, U.S. County	(2007); Cumberbatch et al., (2020); Cutter, Boruff & Shirley, (2003)
	Percent females in labor force	U.S. County	Cutter, Boruff & Shirley, (2003)
Family structure	Average number of people per household	SIS Parish, U.S. County, SIS ED	Boruff & Cutter (2007); Cutter, Boruff & Shirley, (2003); Cumberbatch et al., (2020),
	Percentage of single-parent or elder headed households with children under 18	U.S. County, Orleans Parish	Cutter, Boruff & Shirley, (2003); Flanagan et al., (2011), Mavhura et al., (2017)
	Crowding with more residents than rooms	Household level	Flanagan et al., (2011)
	Population dependency by age distribution	Chinese County	Chen et al., (2013)
Social dependence	Percentage of population retired	SIS Parish, SIS ED	Boruff & Cutter (2007). Cumberbatch et al., (2020)
	Per capita residents in nursing homes	U.S. County, Orleans Parish	Cutter, Boruff & Shirley, (2003); Flanagan et al., (2011)
	Per capita Social Security recipients	U.S. County	Cutter, Boruff & Shirley, (2003)
Special needs	Percentage of population	SIS Parish,	Boruff & Cutter

	disabled	Orleans Parish, SIS ED	(2007). Flanagan et al., (2011), Cumberbatch et al., (2020)
Infrastructure	Percentage of households without piped water	Chinese County	Chen et al., (2013)
	Percentage of housing units possessing radios	SIS Parish	Boruff & Cutter (2007).
	Percentage of housing units possessing television sets	SIS Parish	Boruff & Cutter (2007).
	Percentage of households with no vehicle	Orleans Parish	Flanagan et al., (2011),
	Percentage of housing units cooking with electricity	SIS Parish	Boruff & Cutter (2007).
	Percentage of housing units lighting with electricity	SIS Parish	Boruff & Cutter (2007),
Rural/urban	Percentage of land used for agriculture	SIS Parish, U.S. County	Boruff & Cutter (2007); Cutter, Boruff & Shirley (2003)
	Percent rural population	U.S. County	Cutter, Boruff & Shirley, (2003)
	Percent urban population	U.S. County	Cutter, Boruff & Shirley, (2003)
Medical services	Number of physicians per 100,000 population	U.S. County	Cutter, Boruff & Shirley, (2003)
	Per capita number of	U.S. County	Cutter, Boruff &

	community hospitals		Shirley, (2003)
Race and ethnicity	Net international migration	U.S. County	Cutter, Boruff & Shirley, (2003)
	Percentage of African American population	U.S. County, Orleans Parish	Cutter, Boruff & Shirley, (2003); Flanagan et al., (2011)
	Percentage of native American population	U.S. County, Orleans Parish	Cutter, Boruff & Shirley, (2003); Flanagan et al., (2011)
	Percentage of Asian population	U.S. County	Cutter, Boruff & Shirley, (2003)
	Percentage of Hispanic population	U.S. County	Cutter, Boruff & Shirley, (2003)
Occupation	Percent of population employed in primary extractive industries	U.S. County	Cutter, Boruff & Shirley, (2003)
	Percent of population employed in transportation, communications, and other public utilities	U.S. County	Cutter, Boruff & Shirley, (2003)
	Percent of population employed in the service sector	U.S. County	Cutter, Boruff & Shirley, (2003)

C.2 The Resident Household Survey for Vulnerability Factors Collection

The designed survey instrument and relevant ethics materials are on the next page.

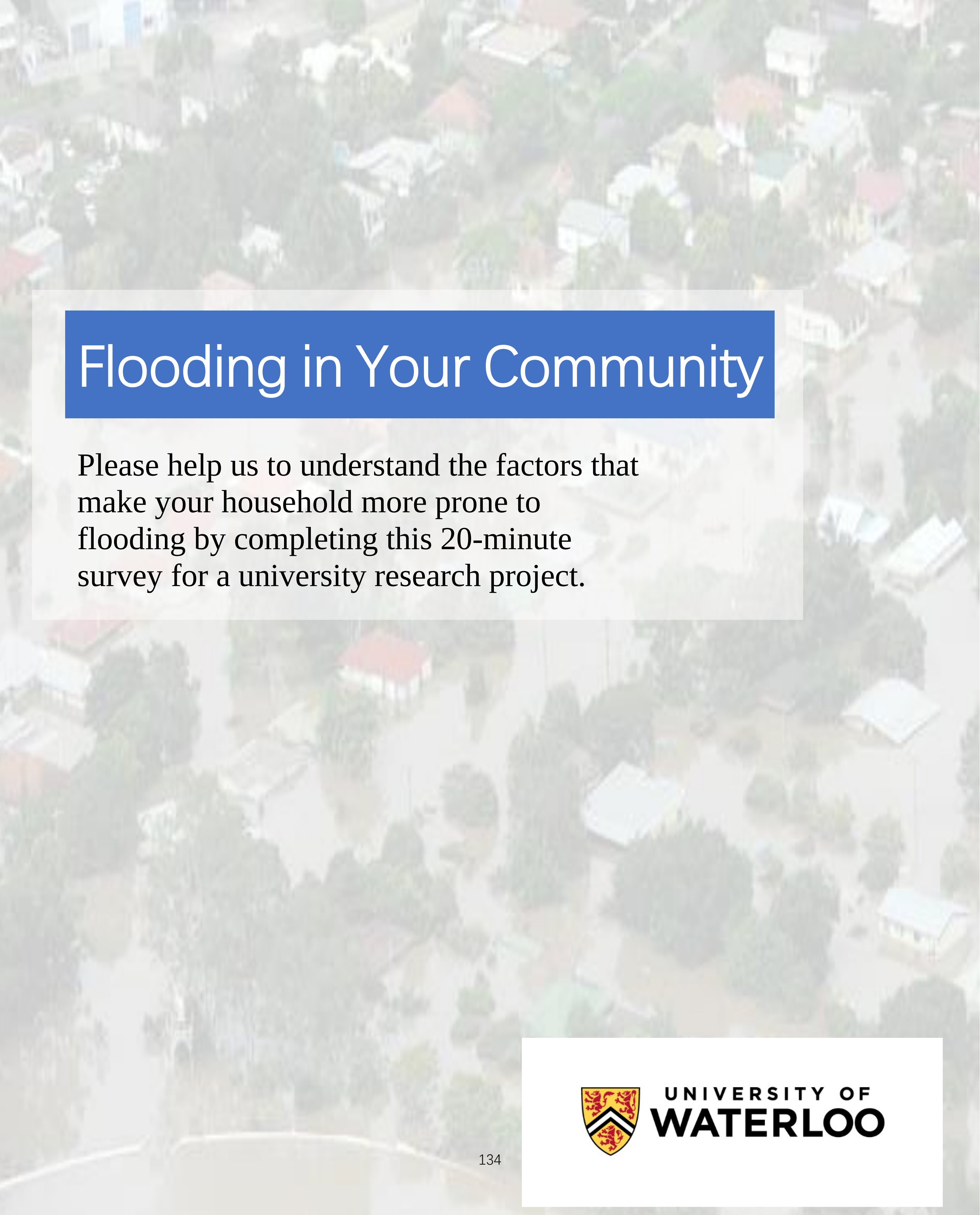

Flooding in Your Community

Please help us to understand the factors that make your household more prone to flooding by completing this 20-minute survey for a university research project.

UNIVERSITY OF WATERLOO

Dear community resident,

I am writing as a master's student from the Department of Geography and Environmental Management at the University of Waterloo, Canada. I would like to ask you for your assistance with a study that I am conducting as a part of my master's degree. The title of my study is "*Quantifying the Impacts of Flash Flooding on Dominica's Material Stocks in Buildings: A GIS-based methodological framework for Small Island States*". I would like to provide you some information about this research project that explores flood risk perceptions involving both flood exposure and vulnerability.

The purpose of this study is to find out how different household socioeconomic characteristics may affect the degree to which a household is susceptible to the impact of flooding. If you are interested in obtaining more information about my research, please contact me by e-mail at t6ren@uwaterloo.ca.

You are invited to participate in my research under the supervision of Dr. Su-Yin Tan from the Department of Geography and Environmental Management of the University of Waterloo, Canada. Participate by completing this resident survey, where different questions about your household will be asked (for example, "*How many of the family members are below five years old?"*).

Your involvement in this survey is entirely voluntary, and the survey should not take more than 20 minutes. You may decline to answer any questions that you do not wish to answer, and you can withdraw your participation at any time by not submitting your responses. The information that you provide will be kept confidential and will be used at an aggregated level indicating the overall vulnerability score of your neighborhood.

This paper copy of the survey will be collected on a door-to-door basis during **[time period of collection]**, and you will be entered in a draw for 1 of 5 EC$60 remuneration after submitting your responses. The remuneration will be paid to you in cash during **[time period of payment].** If you are not available during any of the two time periods, please feel free to contact me at **[phone number]**, or contact me by e-mail at t6ren@uwaterloo.ca.

The results of this study will be useful to practitioners involved in flood risk management and emergency response. Thank you very much in advance for your assistance with this study!

This study has been reviewed and received ethics clearance through the University of Waterloo Research Ethics Committee.

Yours sincerely,

Tianyu Ren
MSc Candidate
Department of Geography & Environmental Management
University of Waterloo

A Resident Survey for Vulnerability to Floods

The impacts of flooding on different households are highly variable. This survey aims to gather information on how different household characteristics may affect their vulnerability levels to the impacts of flooding. Your household social and economic characteristics may play a role in your ability to prepare for an upcoming flood event, cope with it during the event, and recover in the aftermath of flooding.

Guide: For multiple choice questions, please check all the boxes that apply. Example: ☑ Yes

Part A: Basic Information about Your Household

Your family structure may affect how much stress you have when taking care of the dependents (children and elders) for evacuation, and female family members are usually more affected by hazards due to family care responsibilities.

1. Do you own your home? ☐ Yes ☐ No

2. How many people live in your home? (**Sleep at least four nights per week**, please indicate the number of family members below, with regard to their ages.)

   ___________ preschool children (age 0 - 5)

   ___________ children (age 6 - 12)

   ___________ teenagers (age 13 - 17)

   ___________ adults (age 18 - 64)

   ___________ elders (age 65 and over)

3. How many bedrooms are there in your home?

   ☐ One ☐ Two ☐ Three ☐ Four ☐ Five ☐ Six or more

4. How many female family members are there in your home?

   ☐ None ☐ One ☐ Two ☐ Three ☐ Four ☐ Five ☐ Six or more

5. How many family members in your home are native English speakers?

   ☐ None ☐ One ☐ Two ☐ Three ☐ Four ☐ Five or more ☐ Prefer not to answer

6. How many family members in your home were born in Dominica?

   ☐ None ☐ One ☐ Two ☐ Three ☐ Four ☐ Five or more ☐ Prefer not to answer

7. How many family members in your home are disabled?

   ☐ None ☐ One ☐ Two ☐ Three or more ☐ Prefer not to answer

Part B: Your Socioeconomic Status

Improved income level or employment status can help you cope with the impacts of floods. Please tell us more about your socioeconomic status.

8. Which category best describes your total annual household income?

☐ Less than EC$10,000 ☐ EC$10,001 to EC$15,000 ☐ EC$15,001 to EC$25,000

☐ EC$25,001 to EC$40,000 ☐ More than EC$40,000 ☐ Prefer not to answer

9. How many family members in your home are employed?

☐ None ☐ One ☐ Two ☐ Three

☐ Four ☐ Five ☐ Six or more ☐ Prefer not to answer

10. How many vehicles are owned by your family (vehicles that can be accessed anytime when they are needed)?

☐ None ☐ One ☐ Two ☐ Three or more

11. When was your house constructed?

☐ 2022 – 2012

☐ 2011 – 2000

☐ 1999 – 1990

☐ 1989 – 1980

☐ 1979 – 1970

☐ Before 1970

☐ I cannot recall.

12. Which category best describes the amount of money you spent on construction of the house that you are living in? (If you rent your home, please skip this question.)

☐ Less than EC$50,000

☐ EC$50,001 to EC$100,000

☐ EC$100,001 to EC$150,000

☐ EC$150,001 to EC$200,000

☐ More than EC$200,000

☐ Prefer not to answer/I cannot recall

13. If you rent your home, what is the amount of rent that you pay each month? (If you answered Question 10, please skip this question.)

☐ Less than EC$500

☐ EC$501 to EC$750

☐ EC$751 to EC$1,000

☐ EC$1,001 to EC$1,500

☐ More than EC$1,500

☐ Prefer not to answer

Part C: Education Status

A higher level of education and the ability to use a computer or mobile phone may help you to better access hazard warning and recovery information.

14. How many adult family members (18 years or older) in your household have a high school diploma?

☐ None ☐ One ☐ Two ☐ Three ☐ Four ☐ Five or more ☐ Prefer not to answer

15. How many adult family members (18 years or older) in your household have completed university or college education?

☐ None ☐ One ☐ Two ☐ Three ☐ Four ☐ Five or more ☐ Prefer not to answer

16. How many family members in your home are 15 years or older and can use a computer or a mobile phone?

☐ None ☐ One ☐ Two ☐ Three ☐ Four ☐ Five or more ☐ Prefer not to answer

Thank You for participating in this survey.